

34436

National Library  
of CanadaBibliothèque nationale  
du CanadaCANADIAN THESES  
ON MICROFICHETHÈSES CANADIENNES  
SUR MICROFICHENAME OF AUTHOR / NOM DE L'AUTEUR Ben A. MetsonTITLE OF THESIS / TITRE DE LA THÈSE The Effects of Lead Pollution on  
Urban Steel PlantsUNIVERSITY / UNIVERSITÉ University of Alberta, EdmontonDEGREE FOR WHICH THESIS WAS PRESENTED /  
GRADE POUR LEQUEL CETTE THÈSE FUT PRÉSENTÉE M.Sc.YEAR THIS DEGREE CONFERRED / ANNÉE D'OBTENTION DE CE GRADE 1977NAME OF SUPERVISOR / NOM DU DIRECTEUR DE THÈSE Dr. S. H. Summers

Permission is hereby granted to the NATIONAL LIBRARY OF  
CANADA to microfilm this thesis and to lend or sell copies  
of the film.

The author reserves other publication rights, and neither the  
thesis nor extensive extracts from it may be printed or other-  
wise reproduced without the author's written permission.

L'autorisation est, par la présente, accordée à la BIBLIOTHÈ-  
QUE NATIONALE DU CANADA de microfilmer cette thèse et  
de prêter ou de vendre des exemplaires du film.

L'auteur se réserve les autres droits de publication; ni la  
thèse ni de longs extraits de celle-ci ne doivent être imprimés  
ou autrement reproduits sans l'autorisation écrite de l'auteur.

DATED / DATE 6 Aug / 77 SIGNED / SIGNÉ R. MetsonPERMANENT ADDRESS / RÉSIDENCE FIXE #308 1121 82 Ave  
Edmonton  
Alberta



National Library of Canada

Cataloguing Branch  
Canadian Theses Division

Ottawa, Canada  
K1A 0N4

Bibliothèque nationale du Canada

Direction du catalogage  
Division des thèses canadiennes

## NOTICE

The quality of this microfiche is heavily dependent upon the quality of the original thesis submitted for microfilming. Every effort has been made to ensure the highest quality of reproduction possible.

If pages are missing, contact the university which granted the degree.

Some pages may have indistinct print especially if the original pages were typed with a poor typewriter ribbon or if the university sent us a poor photocopy.

Previously copyrighted materials (journal articles, published tests, etc.) are not filmed.

Reproduction in full or in part of this film is governed by the Canadian Copyright Act, R.S.C. 1970, c. C-30. Please read the authorization forms which accompany this thesis.

**THIS DISSERTATION  
HAS BEEN MICROFILMED  
EXACTLY AS RECEIVED**

## AVIS

La qualité de cette microfiche dépend grandement de la qualité de la thèse soumise au microfilmage. Nous avons tout fait pour assurer une qualité supérieure de reproduction.

S'il manque des pages, veuillez communiquer avec l'université qui a conféré le grade.

La qualité d'impression de certaines pages peut laisser à désirer, surtout si les pages originales ont été dactylographiées à l'aide d'un ruban usé ou si l'université nous a fait parvenir une photocopie de mauvaise qualité.

Les documents qui font déjà l'objet d'un droit d'auteur (articles de revue, examens publiés, etc.) ne sont pas microfilmés.

La reproduction, même partielle, de ce microfilm est soumise à la Loi canadienne sur le droit d'auteur, SRC 1970, c. C-30. Veuillez prendre connaissance des formules d'autorisation qui accompagnent cette thèse.

**LA THÈSE A ÉTÉ  
MICROFILMÉE TELLE QUE  
NOUS L'AVONS REÇUE**

THE UNIVERSITY OF ALBERTA



THE EFFECTS OF JOINT ECCENTRICITY IN  
OPEN WEB STEEL JOISTS

by

REIN A. MATIISEN

A THESIS

SUBMITTED TO THE FACULTY OF GRADUATE STUDIES AND RESEARCH  
IN PARTIAL FULFILMENT OF THE REQUIREMENTS FOR THE DEGREE  
OF MASTER OF SCIENCE

DEPARTMENT OF CIVIL ENGINEERING

EDMONTON, ALBERTA

FALL 1977

THE UNIVERSITY OF ALBERTA  
FACULTY OF GRADUATE STUDIES AND RESEARCH

The undersigned certify that they have read, and recommend to the Faculty of Graduate Studies and Research, for acceptance, a thesis entitled "The Effects of Joint Eccentricity in Open Web Steel Joists" submitted by Rein Arnold Matisen in partial fulfilment of the requirements for the degree of Master of Science.

*J. G. Hammond*  
.....  
Supervisor  
*J. R. Colbourne*  
.....  
*R. A. Murray*  
.....  
*A. C. Kuntz*  
.....

Date *March 9, 1977*  
.....

## ABSTRACT

In the manufacture of open web steel joists, hot rolled hat shaped sections are commonly used as chord members in conjunction with tube web members. The relatively small depth of the hat shapes combined with tube shapes as web members may result in joints which have eccentricities that are sufficiently large that they must be taken into account when designing by the present CSA standards. In this study joists with such eccentric joints were investigated to establish the effects of the eccentricities on the behavior of the joist.

Six test specimens were loaded to failure. Member axial forces and bending moments and joint deflections were measured and compared to those obtained from an elastic frame analysis in which the eccentric joints were modelled as individual frame members.

From this study it was concluded that the elastic frame analysis was a reasonable model for the eccentricities, and that the major effect of the eccentricities was to introduce bending moments into the members of the joist. It was also concluded that a strict application of existing beam column interaction formula would not give reliable predictions of member load capacities without further studies into the effective lengths of the individual members.

## ACKNOWLEDGEMENTS

This study is the start of a project to investigate the effects of joint eccentricities on the behavior of open web steel joists. The project is funded by the Canadian Steel Industries Construction Council, and is being carried out at the University of Alberta under the direction of Dr. S.H. Simmonds and Dr. D.W. Murray.

The assistance and comments of H.A. Krentz, Vice-President and General Manager, C.I.S.C. are particularly acknowledged. The cooperation of Dominion Bridge Company Limited and Great West Steel Industries Limited who supplied the test specimens, and the interest and assistance of D.L.T. Oakes and D.G. Calder is gratefully acknowledged.

The author wishes to express his appreciation to Dr. S.H. Simmonds who directed the testing program, and whose guidance and assistance have been invaluable throughout. Also the work of Dr. D.W. Murray, who wrote the computer programs to store and analyze the test data is acknowledged with thanks.

## TABLE OF CONTENTS

| Chapter                                    | Page |
|--|------|
| I      Introduction                        | 1    |
| 1.1    Open-Web Steel Joists               | 1    |
| 1.2    Definition of Joint Eccentricity    | 3    |
| 1.3    Object and Scope of Study           | 4    |
| 1.4    Previous Investigations             | 5    |
| II     The Test Program                    | 12   |
| 2.1    Description of Test Specimens       | 12   |
| 2.2    Description of Testing Arrangements | 16   |
| 2.3    Instrumentation                     | 22   |
| 2.4    Materials Testing                   | 23   |
| III    The Analytical Study                | 35   |
| 3.1    Elastic Frame Analysis              | 35   |
| 3.2    Analysis of Test Joists             | 35   |
| 3.3    Parameter Studies                   | 38   |
| IV    Presentation of Results              | 40   |
| 4.1    Joist Geometry                      | 40   |
| 4.2    Load-Deflection Plots               | 40   |
| 4.3    Axial Forces and Bending Moments    | 41   |
| 4.4    Failure Loads                       | 43   |
| 4.5    Material Properties                 | 44   |

|    |   |     |
|----|---|-----|
| V  | Discussion of Results                           | 81  |
|    | 5.1 Comparison of Measured and Predicted Values | 81  |
|    | 5.2 Failure Modes and Ultimate Strength         | 85  |
|    | 5.3 Design Methods for Eccentricity             | 90  |
| VI | Conclusions                                     | 101 |
|    | 6.1 Conclusions From the Pilot Study            | 101 |
|    | 6.2 Further Research                            | 102 |
|    | List of References                              | 103 |
|    | Appendix A - Calculation of Allowable Loads     | 104 |
|    | Appendix B - Changes in Moments of Inertia      | 106 |

# LIST OF TABLES

| Table | Description  | Page |
|-------|--|------|
| 4.1   | Geometry AX01  | 45   |
| 4.2   | Geometry AX02  | 46   |
| 4.3   | Geometry AX03  | 47   |
| 4.4   | Geometry AX04  | 48   |
| 4.5   | Geometry AY01  | 49   |
| 4.6   | Geometry AY02  | 50   |
| 4.7   | Comparison of analytical and experimental stress resultants - AX01 | 51   |
| 4.8   | Comparison of analytical and experimental stress resultants - AX02 | 52   |
| 4.9   | Comparison of analytical and experimental stress resultants - AX03 | 53   |
| 4.10  | Comparison of analytical and experimental stress resultants - AY01 | 54   |
| 4.11  | Comparison of analytical and experimental stress resultants - AY02 | 55   |
| 4.12  | Summary of failure loads and modes                                 | 56   |
| 5.1   | Interaction equation applied to AX joists                          | 94   |

## LIST OF FIGURES

| Figure |   | Page |
|--------|---|------|
| 1.1    | Positive joint eccentricity-top chord         | 10   |
| 1.2    | Positive joint eccentricity-bottom chord      | 11   |
| 2.1    | Typical X-type joint                          | 26   |
| 2.2    | Typical Y-type joint                          | 27   |
| 2.3    | Longitudinal section of testing arrangement   | 28   |
| 2.4    | Cross section of testing arrangement          | 29   |
| 2.5    | Panel point loading mechanism                 | 30   |
| 2.6    | Two point loading mechanism                   | 31   |
| 2.7    | Comparison of two point and uniform loading   | 32   |
| 2.8    | Location and numbering of gauges              | 33   |
| 2.9    | Data acquisition equipment - schematic        | 34   |
| 3.1    | Chord discontinuity in AX joists              | 39   |
| 4.1    | Geometry of AX joists                         | 57   |
| 4.2    | Geometry of AY joists                         | 58   |
| 4.3    | Load deflection plot AX01                     | 59   |
| 4.4    | Load deflection plot AX02                     | 60   |
| 4.5    | Load deflection plot AX03                     | 61   |
| 4.6    | Load deflection plot AX04                     | 62   |
| 4.7    | Load deflection plot AY01                     | 63   |
| 4.8    | Load deflection plot AY02                     | 64   |
| 4.9    | Analytical and measured moments AX01 - chords | 65   |
| 4.10   | Analytical and measured moments AX01 - web    | 66   |
| 4.11   | Stress strain curve - AX01 & AX02 C chord     | 67   |
| 4.12   | Stress strain curve - AX01 & AX02 1.66" Tube  | 68   |

|      |   |                                     |     |
|------|---|-------------------------------------|-----|
| 4.13 | Stress strain curve - AX01 & AX02                                 | 1.315" Tube                         | 69  |
| 4.14 | Stress strain curve - AX01 & AX02                                 | $\frac{58}{64}$ x $\frac{1}{2}$ Bar | 70  |
| 4.15 | Stress strain curve - AX01 & AX02                                 | 3/4" Rod                            | 71  |
| 4.16 | Stress strain curve - AX03 & AX04                                 | C chord                             | 72  |
| 4.17 | Stress strain curve - AX03 & AX04                                 | B chord                             | 73  |
| 4.18 | Stress strain curve - AX03 & AX04                                 | 1.315" Tube                         | 74  |
| 4.19 | Stress strain curve - AX03 & AX04                                 | $\frac{58}{64}$ x $\frac{1}{2}$ Bar | 75  |
| 4.20 | Stress strain curve - AX03 & AX04                                 | 3/4" Rod                            | 76  |
| 4.21 | Stress strain curve - AY01 & AY02                                 | #4 chord                            | 77  |
| 4.22 | Stress strain curve - AY01 & AY02                                 | #3 chord                            | 78  |
| 4.23 | Stress strain curve - AY01 & AY02                                 | 1 1/2" Tube                         | 79  |
| 4.24 | Stress strain curve - AY01 & AY02                                 | 1/4" x 1 1/2" Bar                   | 80  |
| 5.1  | Variation of joist deflections with increasing eccentricities     |                                     | 95  |
| 5.2  | Variation of chord bending moments with increasing eccentricities |                                     | 96  |
| 5.3  | Variation of chord axial forces with increasing eccentricities    |                                     | 97  |
| 5.4  | Top chord profiles AY joists                                      |                                     | 98  |
| 5.5  | End panel mechanism for AX03 and AX04                             |                                     | 99  |
| 5.6  | Variation of shear force with joist span                          |                                     | 100 |

## LIST OF SYMBOLS

|          |  |
|----------|--|
| $A$      | Area of cross section.   |
| $d$      | Depth of joist measured between centroids of chords.   |
| $e_1$    | Joint eccentricity measured perpendicular to axis of chord.                                  |
| $e_2$    | Joint eccentricity measured along axis of chord.   |
| $E$      | Modulus of elasticity.   |
| $g$      | Gap between web members on inside face of chord.   |
| $I$      | Moment of inertia of cross-section.  |
| $k$      | Effective length factor.   |
| $\ell$   | Length of member.  |
| $L$      | Total clear span of joist.   |
| $M$      | Bending moment.  |
| $M_o$    | Maximum bending moment applied to joist at design load.                                      |
| $M_p$    | Plastic bending moment.  |
| $M_u$    | Maximum bending moment applied to joist at failure load.                                     |
| $M_y$    | Moment causing first yielding of a cross-section, ignoring the effects of residual stresses. |
| $P$      | Axial force.   |
| $P_a$    | Allowable axial force.   |
| $P_{cL}$ | Axial compressive force to right of a joint.   |
| $P_{cR}$ | Axial compressive force to left of a joint.  |
| $P_o$    | Axial load which can be supported by a column when $M = 0$ .                                 |
| $P_y$    | Axial load causing yield of a cross-section ignoring the effects of residual stresses.       |
| $r$      | Radius of gyration of a cross-section.   |
| $w$      | Uniform load on the top chord of a joist.  |

## CHAPTER 1

### INTRODUCTION

#### 1.1 Open-Web Steel Joists

An open-web steel joist is a simply supported steel truss of relatively light weight, with parallel or slightly pitched chords and a triangulated web system. Such members are commonly used in roof and floor construction as secondary framing members carrying loads to primary framing members or masonry walls. The top chord is considered to provide continuous support for floor or roof decking.

The great majority of open-web steel joists are produced by fabricators using an assembly line process geared specifically to their production. The assembly procedure may vary greatly from manufacturer to manufacturer, dependent upon the economics of the operation. Thus the joint and member details of joists from different manufacturers may differ considerably.

Also, within each plant, the joist details and even the assembly process will differ as the loading and span of the joist changes. Three ranges of joists are commonly designated; namely short, intermediate and long span. The code design requirements are identical for all three ranges, however, economics of manufacture leads to different section types and overall geometry for the different ranges.

In general, when mass produced, short span joists are light Warren trusses with continuous bent bar webs which are welded to the chords using either resistance or arc welding. Intermediate joists tend to be of a modified Warren geometry, with verticals supporting the top

chord midway between joints formed by the intersection of web diagonals. (See Figs. 4.1 & 4.2) Normally both short and intermediate span joists have panel lengths of 24 inches or less, which permits the compression chords to be proportioned for axial forces only when designed using CSA Standards. Long span joists are usually of the Pratt configuration with no limitations on panel length.

In this study, all joists tested were of the modified Warren geometry belonging to the intermediate span range.

The design of open-web steel joists is treated separately from other steel members in most building codes. In this study reference to a code refers to CSA Standard S16.1, 1974, (12) unless noted otherwise.

In this standard, tension chords are designed for axial forces only, provided the joint eccentricities are not in excess of those specified in the next section and the chord is not subjected to applied loads between panel points. Compression chords, if they meet the required eccentricity restriction, and the panel lengths do not exceed 24 inches may also be proportioned for axial forces only. When panel lengths exceed 24 inches the compression chord is required to be designed as a continuous beam column. Web members are designed to resist the shears due to the factored loads in which unbalanced loading is considered. For the purposes of determining the axial forces in all members the loads may be replaced by statically equivalent loads applied at the panel points.

When the specified limits of joint eccentricity are exceeded the Standard requires consideration of the total joint eccentricity in the design.

## 1.2 Definition of Joint Eccentricity

CSA Standard S16.1-1974 contains the following clause:

"16.5.11.4. Eccentricity Limits. Members connected at a joint preferably shall have their gravity axes meet at a point. Where this is impractical and eccentricities are introduced such eccentricities may be neglected if they do not exceed:

(a) For continuous web members:

The greater of the two distances measured from the neutral axis of the chord member to the extreme fibres of the chord member;

(b) For non-continuous web members:

The distance measured from the neutral axis to the back (outside face) of the chord member.

When the eccentricity exceeds these limits, provision shall be made for the effects of total eccentricity.

Eccentricities assumed in design shall be those at maximum fabrication tolerances which shall be stated on the shop drawings."

Thus eccentricity is the distance-measured perpendicular to the span of the joist - between the neutral axis of the chord and the intersection of the axes of the web members. This is the distance  $e_1$ , shown on Fig. 1.1 & 1.2 in a positive sense.

In this investigation joint eccentricity is redefined as follows:

"The eccentricity of a joint is the distance between the separate intersections of chord neutral axis with the extensions of the axis of the web members, measured along the axis of the chord."

This is the distance  $e_2$  shown on Figs. 1.1 & 1.2. Unless otherwise stated, it is the dimension  $e_2$  which is referred to as eccentricity in this study.

There were two reasons for redefining joint eccentricity. In the laboratory it is possible to mark the intersections of the member centroidal axes and to measure the distance  $e_2$  directly. In addition, when modelling joint eccentricity for the analytical studies, the length

$e_2$  corresponds to the length of the member inserted into the equivalent elastic frame.

It is to be noted that  $e_1$  and  $e_2$  are related geometrically, and if the geometry of the joist is known, one can be calculated from the other. The eccentricities shown on Figs. 1.1 & 1.2 are of a positive sense. That is, a positive distance  $e_1$  falls outside of the chord neutral axis. For a negative eccentricity, the axis of the web members intersect each other before intersecting the neutral axis of the chord. The eccentricity  $e_2$  is of the same sign or sense as the corresponding eccentricity  $e_1$ .

In the design of intermediate span joists, the use of round hollow structural sections for web members is common. These sections are very economical because they have a large moment of inertia to area ratio, allowing utilizations of higher strength steels. However, when combined with hat sections as chords a problem of joint detail arises. Since hat sections are relatively shallow when compared with the width of the tubes, it becomes increasingly difficult to meet the requirements of Clause 16.5.11.4. Positive joint eccentricity as shown in Figs. 1.1 & 1.2 may exist. Depending upon the joint detail, magnitude of the eccentricity and overall joist geometry, these eccentricities may influence joist behavior.

### 1.3 Object and Scope of Study

CSA Standard S16.1 limits joint eccentricity in joists to small values, dependent upon chord depth and web continuity. Since little research had been conducted to verify these limits a research program was initiated to study this problem, with the object of confirm-

ing or revising the code requirements, and also to give design guidance when allowable limits of eccentricity are exceeded.

Since many factors influence joist behavior, it was decided to undertake a pilot study to isolate the important parameters, and to determine procedures for a more detailed study of the problem. This report contains the results of this pilot study.

#### 1.3.1 Scope of pilot study

Six joists of similar geometry and capacity were instrumented and tested to failure. Deflections were measured at all panel points and sufficient strain readings were taken to establish experimental axial force and bending moment distributions for all members on one half of all test joists. Materials tests were carried out for the different sections involved to establish actual yield points and axial stiffness values.

An elastic analysis was made for each joist utilizing a computer program based on the direct stiffness matrix procedure. Both published and measured values of section properties were used in the analysis. The results for the stiffness analysis were compared to test results. Further analytical studies were carried out to establish theoretical elastic joist response when the joint eccentricity was increased.

The results of both testing and analysis were evaluated by present code criteria to establish their applicability to stresses resulting from eccentricities.

#### 1.4 Previous investigations

A literature search was conducted to determine the extent of

previous investigations. This search included use of an automated retrieval system, CANOLE, and contact of people known to have done previous work in the field of open-web steel joists. Although no work on joint eccentricity in joists was found, several studies of compression chord behavior have been carried out, and are summarized below.

An investigation sponsored by the Canadian Institute of Steel Construction was conducted by W.H.D. Rowan and D.J.L. Kennedy at the University of Toronto in 1963. The purpose of this research was to resolve conflicts existing in design requirements for the continuous compression chords of open-web steel joists, the intent being to establish proper effective length factors for design. The authors conducted an investigation of existing literature but found no previous studies on the compression chords of joists.

They then tested a total of eight joists, all with spans of 24 feet. Joist depths were 12 and 20 inches. All test joists were typical industry products with the exception that bottom chords and web members were oversized to assure a failure of the top chord. Six joists were loaded at panel points, two were loaded at mid-panels. Deflections, joint rotations and member curvatures were recorded. From these tests the following conclusions were drawn.

1. The deflection of a joist (regardless of the loading method) can be calculated by simple truss theory. These deflections can be approximated by applying a 10% increase to the simple beam deflections computed using a moment of inertia based on chord areas alone.
2. The effective length of a top chord member depends on the initial profile along the top chord. When all initial

deformations between panel points (due to welding stresses) are in the same direction, buckling will occur in double curvature and  $k$  may approach 0.65. However, if initial deformations are random,  $k$  may be as high as 0.90.

3. Ultimate strength when bending is present, can be conservatively predicted by the interaction

$$P/P_o + M/M_p = 1.0$$

where the terms are defined in the nomenclature.

4. When the top chord is loaded by a uniform load, the drop in capacity from the panel point load case should be no more than 10% if the panel length is 24 inches or less.

The authors also noted that further investigation was needed

to:

1. Verify their results experimentally.
2. Establish the interaction between various deck and top chord stiffness.
3. To verify the assumption that compression chords can be designed for axial loads alone for certain limited panel lengths.

At the University of Kansas several series of tests of open-web steel joist have been carried out under the direction of K.H. Lenzen. The first of these by Omhart (1) investigated the effects of uniform loading on the bending moments in the compression chord, with the intent of establishing a method by which a true uniform load could be applied to the top chord. Test joists were loaded by means of an air bag device. Moments in the top chord were measured and compared to analytical results. Agreement was considered good.

From these tests, the author concluded that a uniform load is

more severe than panel point loads of corresponding magnitude, and established a viable method for testing joists under a uniform top chord loading.

The buckling of top chords under uniform loading conditions was investigated by W. Scott McDonald Jr. (3). This report treated the top chord of the joists as a beam column. Actual stress-strain relationships of the top chord sections were used to evaluate the buckling load of 51 test joists, including those tested by Omhart as discussed previously. The analytical study agreed well with the test results, and both indicated that the design formulas of AISC, AISI, and SJI will give adequate factors of safety. However an analytical parameter study indicated that the factor of safety could be reduced if the ratio of uniform load to axial design force in the top chord was increased.

The results obtained from the University of Kansas studies are summarized by K.H. Lenzen. He concluded that design techniques which use only  $\ell/r$  ratios and axial forces to proportion compression members are not rational. An interaction formula of the form

$$\frac{\text{Axial stress}}{\text{Tangent Modulus Stress}} + \frac{\text{Bending stress}}{\text{Yield stress}} = 0.92$$

was proposed. In the above investigations eccentricities were present in some of the test joists, and it was noted that under concentrated loading these eccentricities could affect joist behavior.

It was concluded, however, that uniform loading is a more severe testing criteria than concentrated loading, and that under uniform loading eccentricities would not affect the critical chord members.

A series of joist tests were conducted by J.A. Hribar and W.P. Laughlin (7), to determine lateral bracing requirements. Joists tested had a Warren truss configuration, and were loaded at third points. Based on the test results and analytical procedures, the authors made recommendations for bridging requirements for light trusses and open web steel joists.

Eccentric web to chord joints also occur in trusses of hollow structural steel shapes. Research on the effects of these eccentricities is well documented. In particular, work conducted by W. Eastwood and A.A. Wood (10) forms the basis of a design procedure of trusses in a Stelco publication, (9), "Hollow Structural Sections - Design Manual for Connections". The applicability of the design rules given in this publication to the open-web steel joists investigated in this study is discussed in Chapter 5.

In general, there is a lack of published material on open-web steel joists. This may be attributed to the proprietary nature of the joist industry. Different joist design and manufacturing systems have evolved through the experience and research of private industry rather than publicly funded institutions.

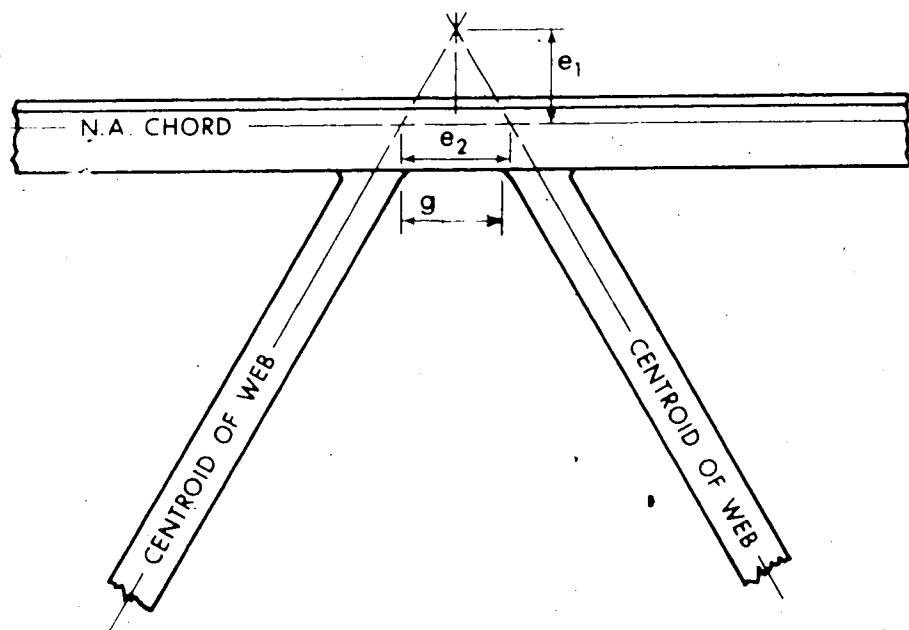


Fig. 1.1 Positive Joint Eccentricity - Top Chord

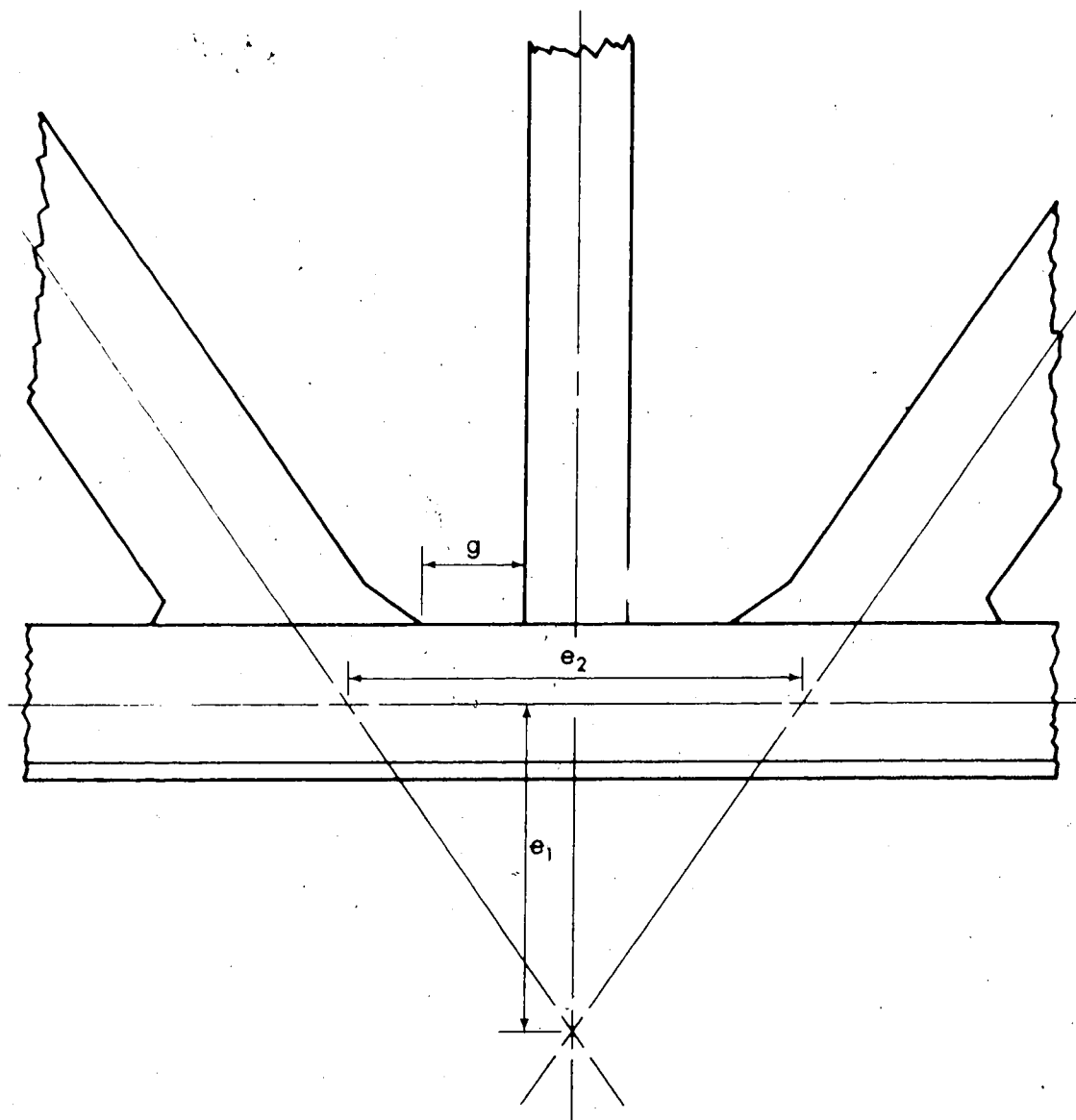


Fig. 1.2 Positive Joint Eccentricity - Bottom Chord

## CHAPTER II

### THE TEST PROGRAM

#### 2.1 Description of Test Specimens

##### 2.1.1 Joist designation

The major variable in the design of the test specimens was the value of joint eccentricity. Differing assembly procedures of the two manufacturers involved produced another important variable; namely the web to chord joint detail. This difference was used to group joists as one of two types, which were coded as either X or Y.

The X-type joists had discontinuous hollow tube diagonal web members. The ends of these members were flattened during the cutting to length process and arc-welded to the inside face of the chords such that the major axis of the end of the flattened web member was parallel to the chord direction. This results in a stiff web to chord joint, with the moment of inertia of the web member in the plane of the joist increasing at the joint as shown in Fig. 2.1.

The Y-type joists had continuous web tubes flattened at connections such that the major axis of the ends of web members were perpendicular to the chord direction. The bottom of the flattened part was welded to the chord, resulting in a much more flexible joint, with the moment of inertia of the web members approaching zero at the joint as shown in Fig. 2.2.

Since the web configuration for the Y-type joists was formed using a press with a head of fixed dimension, it was not possible to

vary the eccentricity in these joists. Also, for the combinations of chord and web tube sizes used in the test specimens, the resulting eccentricities were very small.

The designation of a test specimen consists of two letters followed by a sequence number. The first letter distinguishes the test series; all joists discussed herein belong to the "A" pilot series. The second letter designates the manufacturer or joint detail, which is followed by the sequential number assigned to each test specimen. These designations are used to refer to the test itself as well as the test specimen.

For example the designation AX03 indicates the joist was part of the pilot study, had X-type web to chord fabrication details and was the third joist of this type.

#### 2.1.2 Design of test specimens

In keeping with the objectives of the test series, the joists were designed to accentuate the effects of shear forces and joint eccentricities. This was achieved by utilizing a much lower span to depth ratio than is normally used in industry. With the exception of the limits on joint eccentricity, calculations for the allowable uniform load for the test joists were based on the design procedures of CSA Standard S16-1969, Section 20, (14) which was the latest available standard at the time the joists were designed. However, it must be noted that the low span to depth ratio resulted in a top chord that was of much smaller section than would normally be used for the calculated uniform load. Thus the allowable uniform load,  $w$ , is a reference to a strict application of code design procedure only.

The specific geometry for the test joists was chosen as follows:

1. The total span was set at 22 feet, to provide eight 2 foot interior panels and two 3 foot end panels. The web configuration was set to correspond to that for intermediate span joists.
2. In order to assure load capacities large enough to accentuate problems associated with eccentricity, a depth of 36 inches was chosen, giving a span to depth ratio of 7.3.
3. The lightest available hat sections were chosen as chords.
4. The provisions of CSA Standard S16-1969 were used to calculate allowable axial loads for the chord members. Thus an allowable uniform load for the joist was established.
5. The web members were designed in accordance with the code to carry the uniform load calculated in 4.
6. Normal shop details were altered in X-type joists to achieve differing values of eccentricity.

The detailed calculations are given for both X and Y-type joists in Appendix A.

### 2.1.3 Measured joist geometry

All test joists were measured in the laboratory to determine their actual as-built centerline geometries.

All X-type joists were placed on a flat portion of floor and held down by steel weights. A spirit level was attached to a short section cut from a pipe whose inner radius conformed roughly to the outer radius of the web members. This pipe section had a notch at the top center such that when levelled, the top of the web members could be

marked out by the position of the notch. The centerlines of all web members were marked out in this manner. The centroids of the chords were marked from the bottom flange using a milled steel marker of the right thickness. The centerlines of the members were then drawn until they intersected, and small punch marks made at the points of intersection. The distances between the points of intersection were then measured to obtain the actual geometry of the joist. The punch marks were later used to determine accurately the position of the strain gauges.

This procedure was carried out on both sides of AX01, and the results were found to agree with sufficient closeness that thereafter only one side of the joists were measured. For AX01 the two sets of values were averaged.

The geometry for joist AX03 was also obtained by a second method. The joist was laid on a piece of smooth papered wall board 4 feet high and 24 feet long. The entire outline of the joist was then traced onto the board. After the joist was removed, the member centerlines were drawn, and the member lengths measured from intersection point to intersection point. The results of these measurements checked well with those of the previous method.

The dimensions of the Y joists were found to agree with the specified dimensions given on the shop drawings. Thus for these joists these dimensions were used. The results of the measured geometry along with other joist details are given in Tables 4.1 to 4.6. See also Figs. 4.1 & 4.2.

## 2.2 Description of Testing Arrangements

The joists were tested in the vertical position, with the top chords uppermost, corresponding to actual joist position in most structures. All lateral bracing, instrumentation, and data acquisition equipment was kept to one side of the test bed. This facilitated observation of the test specimens, qualitative assessment of failure mechanisms and total joist behavior.

### 2.2.1 Description of loading facility

With the joist in the vertical position, loads were applied to the top chord by 9 hydraulic jacks located beneath the test floor. Lateral support was provided by adjustable arms extending from beams running parallel with the test joist. The ends of the joists rested on rocker supports, one of which was attached to a ball-bearing roller assembly. Figs. 2.3 and 2.4 show cross-sections of the test setup.

The 9 jacks were all identical O.T.C. Model B 10 Ton rams as manufactured by the Owatona Tool Company. These jacks have a piston area of 2.6739 in.<sup>2</sup> and a maximum operating pressure of 9,700 psi. System pressure was supplied and regulated by an Amsler 27.5 in. Hg. Dynamometer which was located on the test floor. A pipe manifold located in the test vault distributed the hydraulic fluid to the individual jacks.

The ends of the jack piston rods were threaded into the center of the lower load arms, which were 4 x 4 x 0.25 H.S.S. Two 3/4" diameter rods passing through the load bed transferred the jack force to an identical upper load arm. The upper load arm either bore directly on the top chord either through a 1" x 1" steel bar, or a load cell, or

was supported by a load distributing beam, dependent upon the chord loading conditions desired. (See Figs. 2.5 & 2.6).

Two point load distributing beams were used to simulate a uniform loading condition for joists AX01, AX02 and AY01. Joists AX03, AX04, and AY02 were tested with panel point loading. Comparisons of the bending moments resulting from the two point loading and uniform loading on a continuous beam on simple supports are shown on Fig. 2.7. Since the top chord is supported at panel points by the web members, the comparative effects of these two loading cases varies with the eccentricity at the panel point. Thus as joint eccentricities increase the two point loading system with a constant distance between points of load application becomes less severe than a uniform load system.

The eccentricity at the end support for the X-type joists was approximately 2 inches, this being one-half of the bearing surface length provided on the joists. The actual eccentricity was calculated by measuring from the centreline of the support pivot to the intersection of the end diagonal with the centroid of the chord in the end panel.

For AY01 it was apparent early in the loading sequence that member 1T was not designed to take such a large eccentricity, and subsequently was remounted with as small an end eccentricity as possible. Since AY02 was similar, it was also tested with a very small value of eccentricity at the supports. The resulting reduction in span was considered when comparing test results with analytical studies. The actual values of these eccentricities at the supports are shown in Tables 4.1 to 4.6, following the notation of Fig. 4.1.

Lateral support was provided to the top chord at panel points 3T through 9T by adjustable arms which extended from a frame work running parallel to the test bed. See Figs. 2.3 & 2.4. These arms could swing freely in both the horizontal and vertical direction, and were adjustable in the vertical direction. A spirit level was mounted on each arm, allowing them to be kept level at each load point during the test. The ends of the arms had short extensions bolted to them, which were tack welded to the top chord. These extensions were to accommodate any out-of-plane sweep in the test specimens without forcing the specimen into a straight configuration in the test assembly. Some sweep was visually apparent in the joists, but all were well within the specified limits, which would allow a variation of 0.55 inches for a 22 foot span.. Thus this quantity was not recorded.

For the first test, AX01, only the top chord was laterally supported. During the test the bottom chord showed a tendency to deflect out-of-plane, which made recording of deflections difficult. For all subsequent tests, the bottom chords were supported at points 2B and 4B by arms identical to those used for the top chord. No further difficulties were then encountered.

#### 2.2.2 Load measurement and jack calibration

Two methods of load measurement were used during the testing. First the jacks were calibrated separately in a static test against a load cell, and jack load versus system pressure curves were obtained. During this calibration the hydraulic system was similar to that used during tests, with the exception that only one jack was attached to the pressure distribution manifold. All jacks had similar curves, and in

the load range in which the load tests were conducted, these curves were linear. Thus the system pressure to applied load relationship was reduced to a single valued linear response, and this used as a measure of applied load.

W.H.D. Rowan (2) reported a problem with friction losses due to piston seals in the jacks, causing a force drop as the jacks worked against a deflecting joist rather than a static calibration unit. These friction losses were reported to have been reduced to negligible values when the seals were replaced by mechanical O-Rings.

The O.T.C. jacks used in this test set-up were equipped with rubber O-ring seals. However, it was decided to check for changes in jacking forces during actual testing. To this end, three load cells were placed between the bottom of the test bed and the jacks for AX01. The load cell used in jack calibration was placed under the centerline jack, J6. The load was regulated by using this load cell reading rather than the system pressure. The pressure was also recorded, so that a check against previous calibration could be made.

While loading AX01 the three jacks with the load cells proved to be unstable. The load arms tended to twist and misalign and thus this method of load measurement was discontinued. From the load cell readings of AX01 no loss in jack force due to deflections could be detected. There were, however, small random departures from the pressure-load relationship previously established. Since the twisting of the load arms could have altered the load cell readings a further test was conducted.

The three jacks were dismantled and recalibrated, this time working against an H.S.S. beam. The span of the beam was chosen to

give deflections equal to the calculated centreline deflection of AX01 at working load. This calibration showed that changes in jack force with piston extension were in the order of 0.2%, and were neglected. AX02, AY01 and AY02 were then tested with no load cells, and loads were established from the original static calibration curve.

Before the actual testing of AX03 and AX04 commenced, data reduction had begun for the other joists. Some inconsistencies in results suggested that:

1. In the actual tests, the applied jack loads differed from each other by amounts larger than the static or deflecting calibrations indicated.
2. The jack force applied by a jack at a given pressure could vary, depending whether that pressure was obtained by loading or unloading. In general, the force at a given pressure which was obtained by loading was consistent, while the force at a given pressure which was obtained by unloading varied randomly.

For this reason AX03 and AX04 were again tested with the three load cells. This time the load cells were mounted on the top chord of the joist, replacing the 1" x 1" steel bar. A ball and socket joint was threaded into the load arm to avoid placing a moment on the load cells. The bottom of the load cells were bolted to a flat base plate which was carefully shimmed to be level with the upper load arm. This arrangement proved to be stable throughout the test.

One load cell remained at the centerline panel point T6 for both AX03 and AX04. The other two were changed to different positions in the two tests. Thus calibrations were obtained under actual conditions for five jacks. The conclusions from these readings were:

1. Any force drop due to friction as the rams extended was negligible.
2. Jacking forces varied between jacks. This variation was a function of the system pressure, the percentage difference becoming smaller as the load increased, but the absolute difference becoming larger. The actual relationship between jack loads was random.
3. At ultimate specimen loads, the percentage difference between the average assumed load per jack and the actual load from any given jack was approximately 2%. Thus while the actual jack load for any given jack could not be accurately known ( $\pm 50$  pounds at 0.5 kips to a maximum of  $\pm 180$  pounds at 3 kips) the bending moment and shear force applied to the total span was not likely to vary much from that assumed.

It was concluded that the problem of load variations was largely due to the use of equipment at a very small percentage of its rated capacity. The jack capacities were 20 kips each. At joist design loads they exerted approximately 1 1/2 kips each. To measure elastic response, readings were taken well below design load. Thus the jacks were operating at 2 to 5 percent capacity. The same is true for the Amsler pressure system and the load cells. At these small loads, the variations, though small in absolute value, could be a significant portion of the load. While the variation increased as applied load increased, the percentage deviation from the assumed loads became smaller, and would have a small effect on calculations of ultimate load.

## 2.3 Instrumentation

Quantitative measurements were taken of joist deflections and member strains at selected points. Full sets of readings were taken at all load points. Loading sequences varied from test to test.

All joints and critical members were whitewashed to obtain a qualitative measure of behavior. Any visual member distress was recorded and photographed.

### 2.3.1 Deflection measurements

Joint deflections were measured to the nearest one thousandth of an inch by Mercer Dial Gauges. Readings were manually recorded at every load point. Placement of the gauges was similar in every test, with a gauge at each bottom chord panel point, and one monitoring lateral movement at the roller support. A plot of the load centreline deflection curve was drawn to a large scale as the test progressed. This plot served to indicate any abnormalities in the test, and was useful in selecting unloading sequences for each joist.

### 2.3.2 Strain measurements

The strain gauges used in the tests were type EA-06-25BG 120 ohm gauges as supplied by Micro Measurements Limited, and installed as per manufacturer's instructions. These gauges have a resistance of  $120 \text{ ohms} \pm .15\%$ , and a gauge factor of  $2.095 \pm .5\%$ . The strain limit of the gauges is 3 to 5%, allowing measurements well into the yield range for the steel.

Each gauge used on the joists was wired to a dummy gauge with

a similar gauge factor to compensate for any temperature effects.

Seventy-nine of these gauges were placed on that half of the specimen which had the largest web-to-chord joint eccentricities. This allowed the establishment of in-plane bending moments and axial forces at two points on each member for the gauged half of the joist. Gauge placement and numbering is shown on Fig. 2.8.

The points on each member at which the strain gauges were placed were six inches from the ends of the member. This was done on the web members to ensure that the sections at which strains were measured were sufficiently removed from the effects of end flattening so that the strains would be linear across the section. For the top chord loading simulating uniform load the jack was located four inches from the joint. The six inch length in this case was to avoid local stresses caused by the presence of the jack. For uniformity the six inch length was used for all members.

At each load point the strain gauge readings were sequentially scanned and recorded automatically. The unit used was a Digitec system from United Systems Corporation. A scanning unit sequentially reads voltage values from a digital voltmeter (the unit used was a Hewlett Packard 3400 B Digital Voltmeter) and punched the information in ANSI code on a paper tape. Along with the 79 strain gauges, the input voltage was also recorded at each load set, as a control on both input voltage and the recording unit. A rough schematic of the gauge wiring and data acquisition equipment is shown on Fig. 2.9.

## 2.4 Materials Testing

Materials tests were made on the various component sections of

the test joists after the tests were completed. Specimens for these tests were cut from the joists. The strain gauge readings from the joist tests were used to assure that the sections being tested had not been stressed to their proportional limit during the joist test.

The true area of each section was established experimentally. This was done by weighing a specimen of known length, after brushing off all paint, white wash and millscale. For the purpose of calculating the areas, the density of steel was taken as 495 pounds per cubic foot. If the area thus established agreed with the published value to within 5%, then the published value of area and moment of inertia was used and the value of Young's modulus was computed. If a difference of more than 5% was observed, then the measured area was taken as correct, and the value of the moment of inertia was adjusted accordingly.

All circular and flat bar shapes were tested in tension in a Baldwin Universal Testing Machine. Tension specimens were a minimum of 24 inches between the jaws of the machine, with the gauged section centered. The hat shaped chord sections were tested in compression in an Amsler testing unit. Compression specimens were 6 inches long, with the resultant  $\ell/r$  ratio being approximately 14. This was found to be the maximum length which could be used to minimize platten restraint while still assuring full yield before buckling.

The criteria for acceptance of a specimen test was that no one gauge could differ by more than 3% from the average strain measured. To achieve this level of uniformity in the compression tests the specimens were milled flat to a tolerance of one one-thousandth of an inch, and then hand polished against very fine emery cloth which was glued to a milled surface. Plattens of the testing machine were similarly prepared.

The strain gauges used in the materials tests were identical to those used in the joist tests. The section properties and stress-strain relationships thus measured were used to reduce joist test data to axial forces and bending moments. It is to be noted that this procedure gives a direct measure of the axial stiffness of a cross-section ( $AE$ ), but only an approximation of the value of the bending stiffness ( $EI$ ). The results of these materials tests are given in Chapter 4.



Fig. 2.1 Typical X-type Joint



Fig. 2.2 Typical Y-type Joint

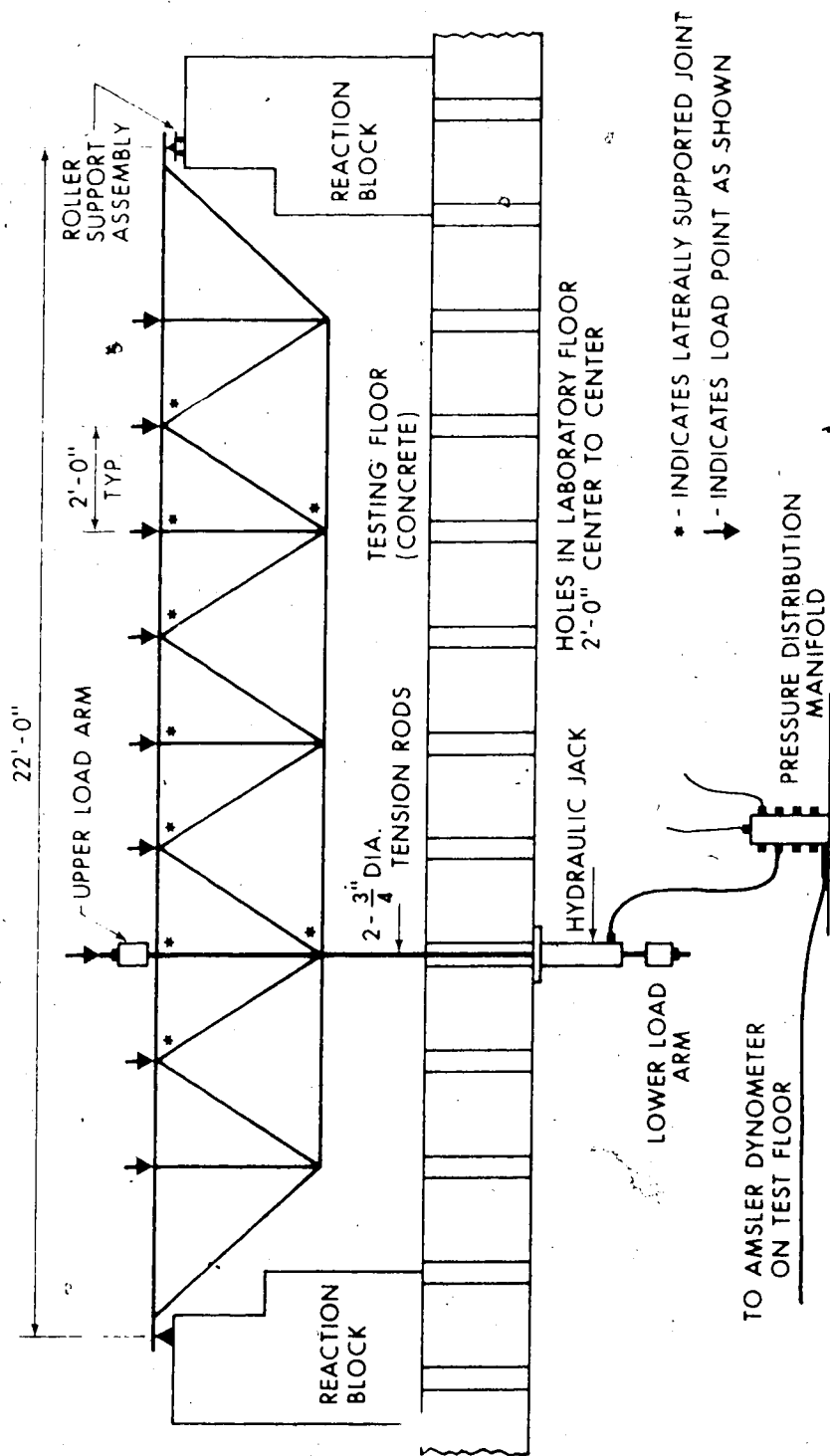


Fig. 2.3 Longitudinal Section of Testing Arrangement

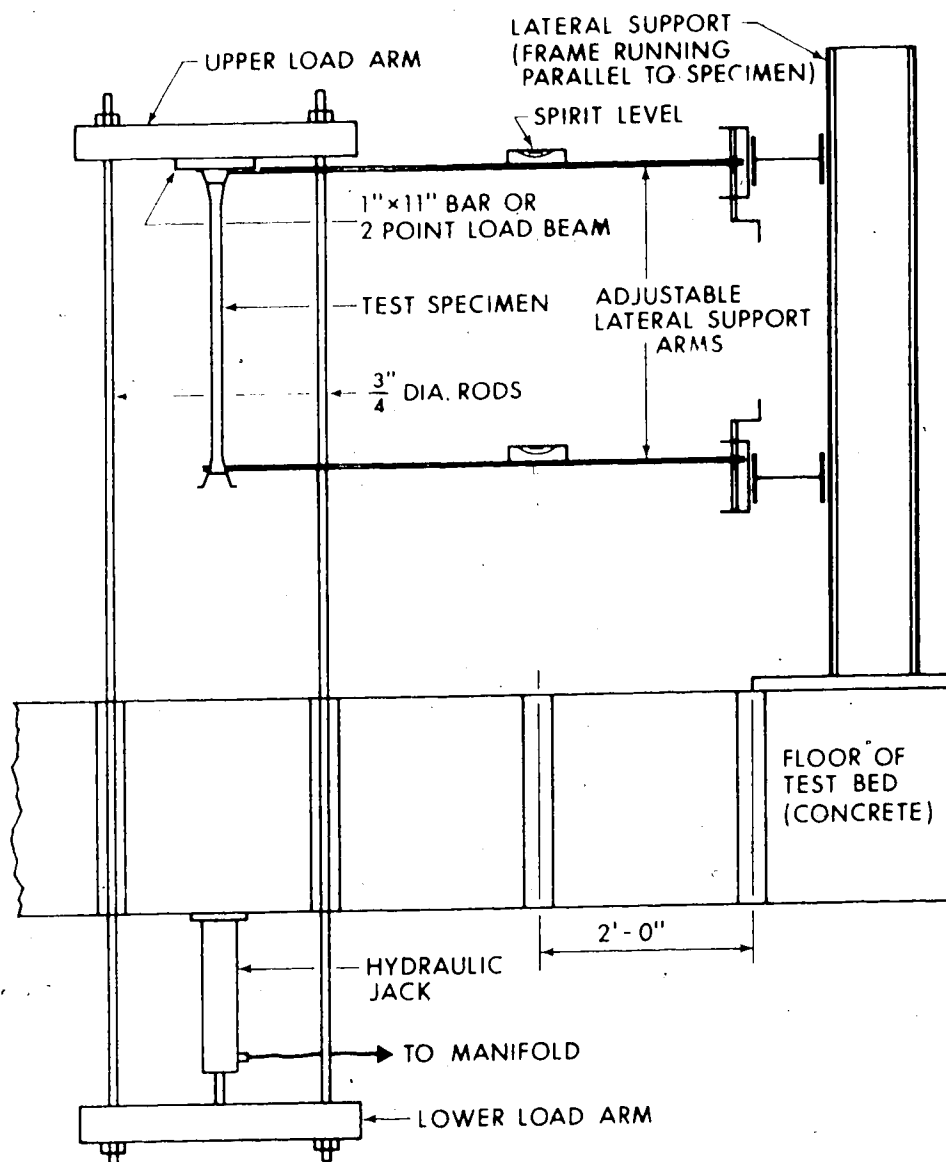


Fig. 2.4 Cross Section of Testing Arrangement

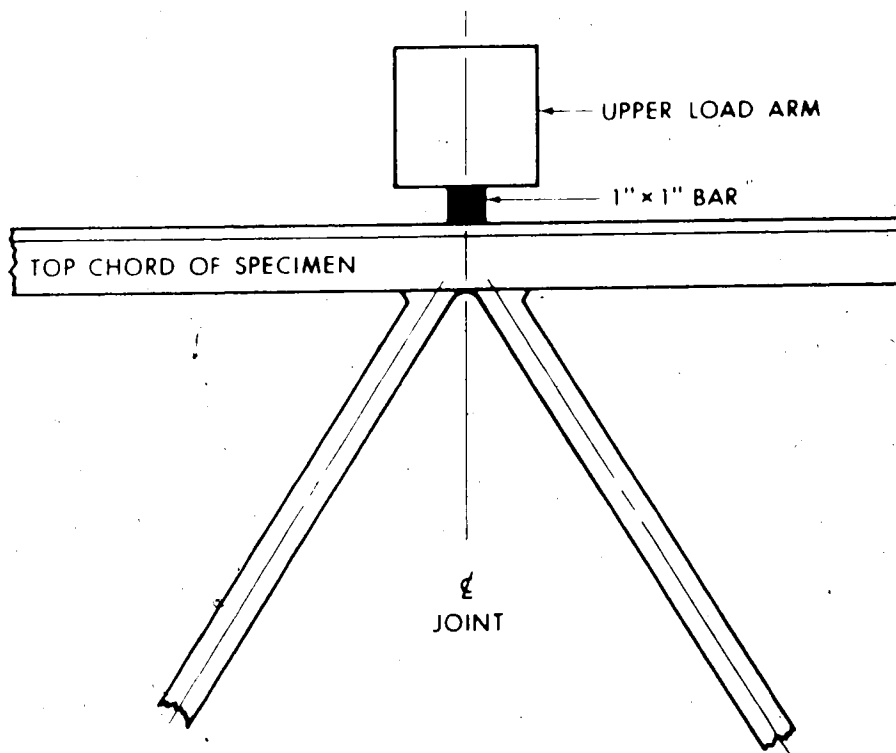


Fig. 2.5 Panel Point Loading Mechanism

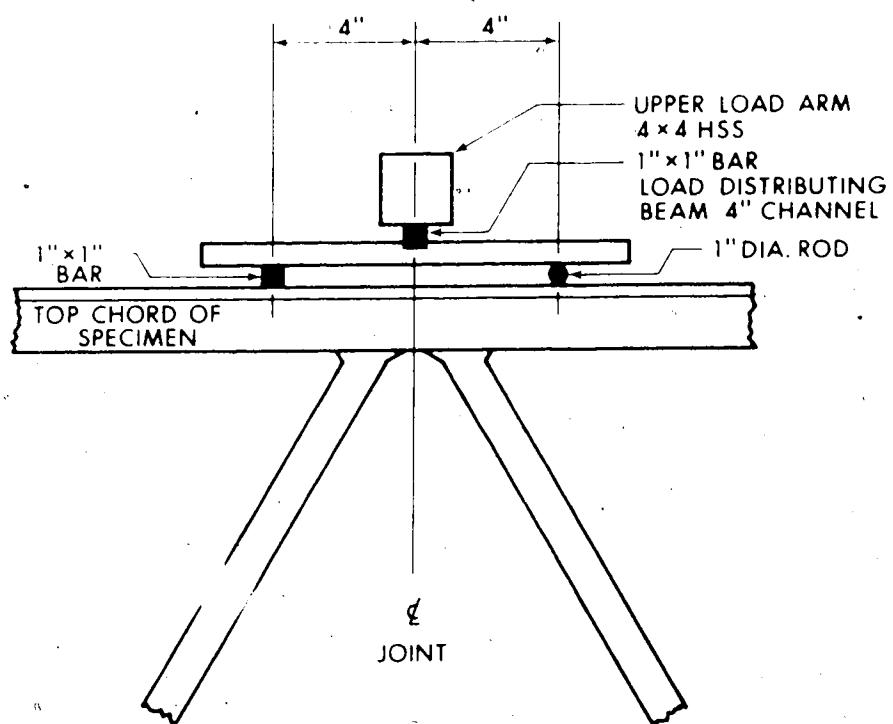


Fig. 2.6 Two Point Loading Mechanism

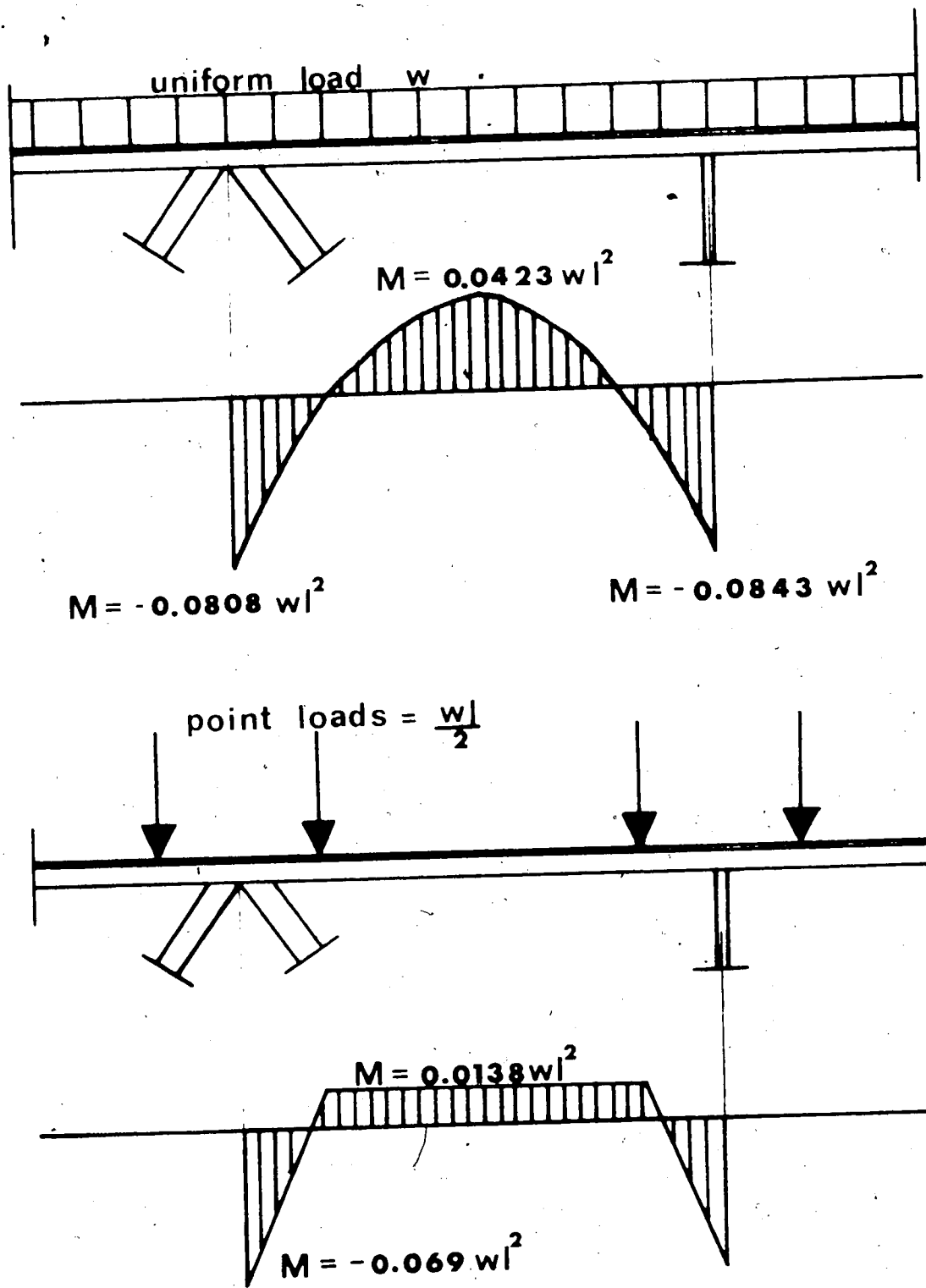


Fig. 2.7 Comparison of Two Point and Uniform Loading

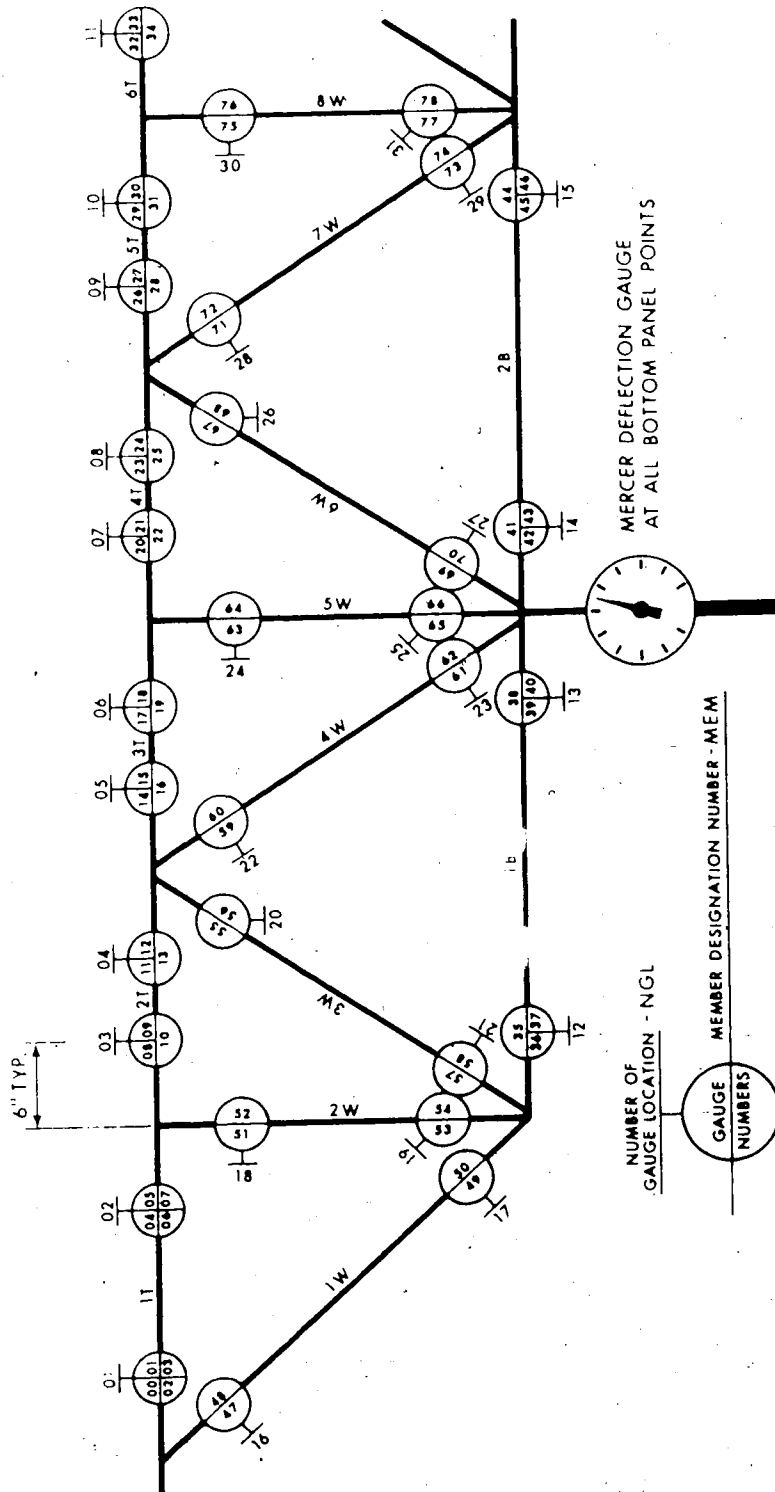


Fig. 2.8 Location and Numbering of Gauges

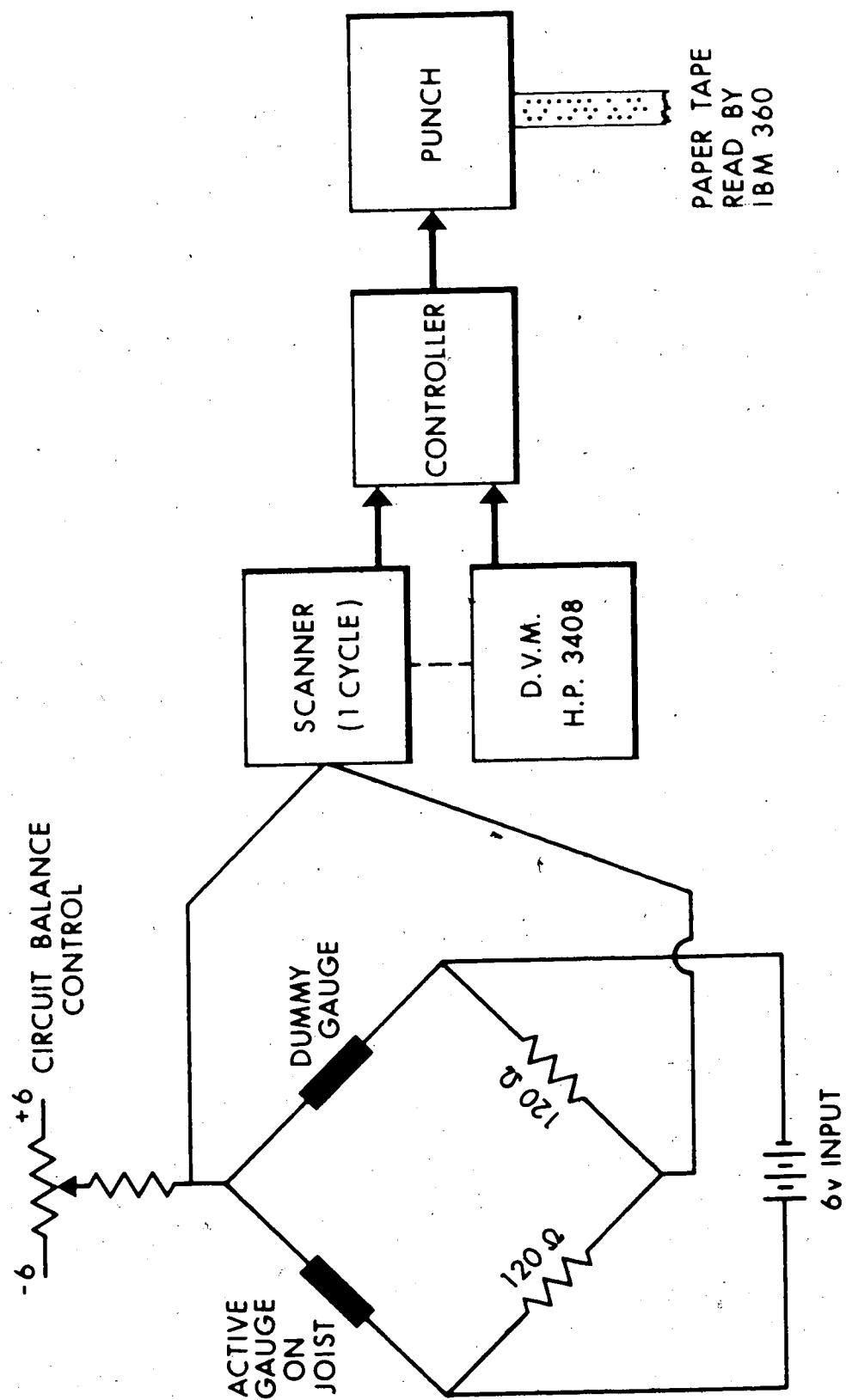


Fig. 2.9 Data Acquisition Equipment - Schematic

## CHAPTER III

### THE ANALYTICAL STUDY

#### 3.1 Elastic Frame Analysis

Each joist in the pilot test series was analysed as an elastic frame using the direct stiffness matrix procedure. The computed deflections and member stress resultants were compared with those obtained experimentally to determine whether such an analysis could be used to predict joist behavior under design load conditions. In addition, using the geometry of the X-type joists, the joist eccentricity was varied to demonstrate quantitatively the effects of increasing the joint eccentricity.

The analyses were performed on the IBM 360/67 digital computer in the Computer Services Department, The University of Alberta, using a modified "Planar Frame and Truss Program" obtained from "Computer Methods of Structural Analysis" (11). The modifications included changing all length units to inches for convenience and performing all numerical calculations in double precision. With these modifications it was possible to obtain an excellent statics check at each joint.

#### 3.2 Analysis of Test Joists

The length of each member of the joist used in the analysis was obtained from the measured centerline geometries. Both published and measured values of member sectional properties were used.

### 3.2.1 Modelling of Joints

In X-type joists all joints were manually arc welded. The joint was made by a fillet weld all around the web member. This resulted in a very stiff web to chord joint, thus these joints were considered fixed in the analysis. In the manufacturing process the ends of the web tubes were flattened, resulting in an increase in the moment of inertia in the plane of the joist at the ends of the web members. Although this increase in moment of inertia was quite large, approximately 63% at the face of the chord, it occurs over a very short distance. In a trial analysis this variation in the moment of inertia was modelled by representing the web member as three separate members with appropriate moments of inertia. Since only an insignificant change in the results was observed this variation in the moment of inertia near the joint was ignored in later analyses.

In the Y-type joists the web tubes were flattened in the perpendicular plane, such that the moment of inertia of the web tube at the joint was greatly reduced. This in effect provided a hinge with little resistance to bending. However for analysis these joints were modelled as being both pinned and fixed. As in the X-type joists, the short tapering section between the surface of the chord and the fully round web member was ignored in the analysis. See Appendix B for calculations in changes of moments of inertia.

### 3.2.2 Modelling of Eccentricities

The length of chord shown as  $e_2$  in Fig. 1.2 was input as a separate chord member, with the two distinct intersections of web and chord axis input as two joints with independent rotations. Thus a top

chord eccentric joint in the test joist was analyzed as two separate joints and a connecting member. The bottom chord joints were modelled in a similar manner except that the vertical web member necessitates the use of 3 joints and two connecting members to model the actual joint. By this procedure all eccentricities which were parallel to the axis of the chords were accounted for in the analysis.

The eccentricity in the plane of the joist due to the change in size of the top chord in the end panel in the X-type joists was ignored in the analysis, see Fig. 3.1. A discussion on the effect of ignoring this eccentricity in the analysis is given in Chapter 5.

The effect of extra stiffness in the eccentric chord member due to the finite width of the web members of the X-type joists or due to the added material of the flattened portion of the continuous web tubes of the Y-type joists was also ignored. The area and moment of inertia of the eccentric chord member was taken as that of one adjoining chords. Thus the stiffness of the joint was under estimated.

Another method of modelling the effect of eccentric joints in trusses is described in "Hollow Structural Sections - Design Manual for Connections" (9). By this method eccentricities are modelled as moments, applied to a joint that is assumed concentric. This technique was not used in this study but the difference between the two is described in Chapter 5.

### 3.2.3 Modelling of Loads

All test specimens were analysed for the actual loading method by which they were tested. As the program accepts point loads on continuous members, the modelling of the two point loading system was straight

forward. For panel point loading, the input load at eccentric top chord panel points was equally applied to the two joints used to model the actual joint. In the actual testing the load was applied through a 1 inch wide bar to the centre point of the eccentric member  $e_2$ . In this manner the load input was simplified, and any errors caused would be insignificant in relation to assumptions made in modelling the geometry of the joint.

### 3.3 Parameter Studies

A parameter study was carried out to determine the analytical effects of varying joint eccentricities. The joist analysed was modelled after X-type joists with the same span to depth ratio. The chord sections used were a "B" hat section for the bottom chord and a "C" section for the top chord which corresponded to the chord section for joists AX03 and AX04. With these joists the joint eccentricity near the ends of the joist are approximately 1.1 times the eccentricity of joints near the midspan reflecting the differences in sizes of web tubes. This ratio of eccentricities was also used in the analytical study when the size of the joist eccentricities were varied.

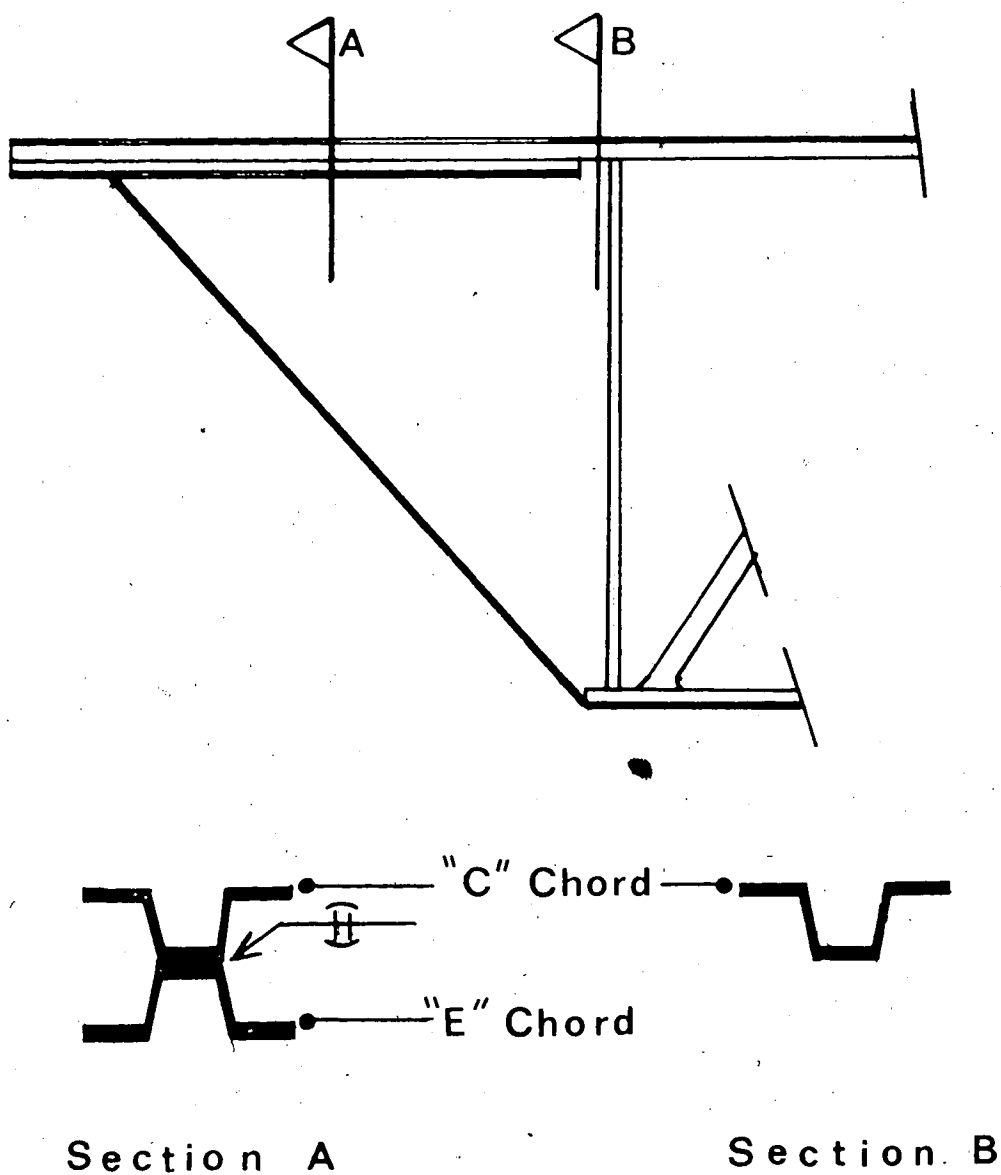


Fig. 3.1 Chord Discontinuity in AX Joists

## CHAPTER IV

### PRESENTATION OF RESULTS

#### 4.1 Joist Geometry

The measured length and material properties for each member of the X-type joists are tabulated in Tables 4.1 to 4.6. To facilitate tabulation use was made of the fact that the test joists were essentially symmetrical about the midspan. This permitted using the same member designation for each half and listing measured lengths under "north" and "south" halves. The member designation consisted of a sequence number plus a letter indicating member type for primary members and a lower case letter for members representing effects of joint eccentricity as shown in Fig. 4.1.

The measured properties of Y-type joists are given in Fig. 4.2 and Tables 4.5 and 4.6. However, since the joint eccentricities for these joists were very small and the panel points along the chords occurred at regular spacing, the individual member lengths are not tabulated.

#### 4.2 Load-Deflection Plots

The measured load-deflection response as indicated by the applied panel point loading-midspan deflection of the bottom chord relation for the test joists are shown in Figs. 4.3 to 4.8. Also shown are the corresponding predicted load-deflection curves obtained by considering the joist to act as a pin-jointed truss, an elastic frame, and as a prismatic beam with modified stiffness. This latter method of

prediction corresponds to the method recommended in the CSA Standard which considers the joist as a simply supported beam having a moment of inertia based on the chord areas and then increasing the calculated midspan deflection by 10% to account for axial deformations in the web members.

For the Y-type joists, the computed deflections considering the joist as a pin-jointed truss and as an elastic frame gave virtually the same results; hence only the results from the frame analysis are plotted.

It must be noted that the indicated applied load in Fig. 4.3 to 4.8 corresponds to the actual applied jack loads and does not include the weight of the loading yoke and jack which was 152 pounds per panel point.

During testing several loading and unloading sequences were included. In many instances these portions of the load-deflection curve were either very close to the initial curve or to each other and so have been omitted from the plotting for sake of clarity.

#### 4.3 Axial Forces and Bending Moments

From the recorded strain readings and the measured material properties at given sections the axial force and bending moment at those sections were determined. The values of these quantities at design load are tabulated in Tables 4.5 to 4.9.

For points on the chord hat sections the computations are based on the readings from three gauges and for points on flats and tubes on two gauges. In certain cases one gauge at a section would become defective during the test which prevented reducing the data for

that point. In such cases the entry under the measured axial force or bending moment in Tables 4.5 to 4.9 is left blank.

The bending moments tabulated are for the gauge locations which are six inches from the ends of the members. The bending moments obtained from the elastic frame analysis at the ends of the members have been modified to correspond to the moment at the gauge location. For this reason the moments tabulated are not the maximum moments in the member.

Under each tabulated value of axial force and bending moment obtained from measured strains in Table 4.5 to 4.9 is a value corresponding to the coefficient of variation expressed as a percentage. In a single test a large number of load and strain readings were taken during the different loading and unloading sequences. It was felt that rather than use one set of strain readings taken at the design load, a more reliable value would be obtained by considering all readings in the elastic range obtained during the test. Since the test of each joist took several hours there was a drift in the gauge readings with time. To compensate for this drift and to minimize the effects of random errors in the applied loads it was decided to divide each load increment by the corresponding strain increment and then to extrapolate this slope linearly so as to obtain a strain difference corresponding to a load difference equal to the design load. In this manner, for each load increment, in the range in which the load-deflection plot indicated that the joist was behaving linearly, a strain reading corresponding to the application of the design load was obtained. The arithmetic means and standard deviations of the stress resultants based on these strains were computed. The mean value of the axial force or bending moment is tabulated above

the coefficient of variation which is the standard deviation divided by the mean, then multiplied by 100.

Under each tabulated value of axial force and bending moment obtained from elastic frame analysis is a decimal fraction which corresponds to the ratio of the mean of the measured quantity to the predicted quantity.

It will be noted that measured values of the axial forces and bending moments are not presented for joist AX04. Values for these quantities computed from the recorded strains have no consistent correlation with calculated values. Since the load-deflection plot for this joist is in reasonable agreement with the calculated predicted response it would appear that the recorded applied loads from the jacks are satisfactory. The problem seems to be with the recorded strains.

Strains were recorded using a digital volt meter that punched the readings on a paper tape. This piece of apparatus was used in other laboratories for other purposes between tests. It is suspected that the settings on several of the channels were altered and not correctly reset prior to the testing of this joist. Since this apparatus was taken to another laboratory immediately following the test and before the discrepancies in the values on the paper tape were discovered, it was not possible to determine the actual settings at the time of the test and so make the corresponding corrections.

#### 4.4 Failure Loads

Table 4.12 summarizes the loading on the test joists at failure and the mode of failure. These failure loads are compared to the design loads as given in Chapter 2, to obtain the load factors provided by the

joists. This has been done by two methods. In line 6, the applied load per panel point at failure is divided by design load per panel point. In line 7, the maximum moment at failure computed from measured loads and geometry is divided by the maximum moment based on a uniform design load placed on the entire 22 foot span. Thus the comparison in line 7 is based on the actual span of the joist as tested, and also the fact that no increase in load was applied at the ends of the joists to account for the 3 foot end panels.

#### 4.5 Material Properties

The section properties for each member are summarized in Tables 4.1 to 4.6. Values for the cross-sectional area and moment of inertia were obtained using the procedures described in Chapter 2. Values of Young's modulus were obtained from the stress-strain plots for each member type. These plots are presented in Fig. 4.10 to 4.23.

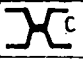

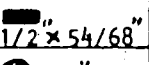
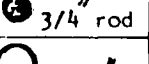
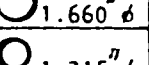
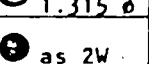
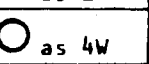
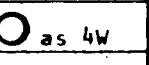
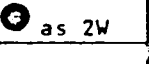

| Geometry - AX01 |           |       |                   |                   |        | Table 4-1   |
|-----------------|-----------|-------|-------------------|-------------------|--------|---|
| Member          | Length in |       | A in <sup>2</sup> | I in <sup>4</sup> | E ksi  | Sect  |
|                 | north     | south |                   |                   |        |   |
| a               | 2.00      | 2.00  | 1.530             | 1.024             | 29,580 |  C & E         |
| 1T              | 34.03     | 34.04 | "                 | "                 | "      | "   |
| 2T              | 22.77     | 22.54 | 0.638             | 0.109             | "      |  C             |
| b               | 2.17      | 2.13  | "                 | "                 | "      | "   |
| 3T              | 23.17     | 23.31 | "                 | "                 | "      | "   |
| 4T              | 23.02     | 22.77 | "                 | "                 | "      | "   |
| c               | 1.96      | 1.98  | "                 | "                 | "      | "   |
| 5T              | 22.88     | 23.23 | "                 | "                 | "      | "   |
| d               | 0.50      | 0.50  | "                 | "                 | "      | "   |
| e               | 1.92      | 1.89  | "                 | "                 | "      | "   |
| 1B              | 44.75     | 44.73 | "                 | "                 | "      | "   |
| f               | 1.44      | 1.36  | "                 | "                 | "      | "   |
| g               | 1.47      | 1.49  | "                 | "                 | "      | "   |
| 2B              | 44.85     | 44.95 | "                 | "                 | "      | "   |
| h               | 1.54      | 1.54  | "                 | "                 | "      | "   |
| 1W              | 48.56     | 48.57 | 0.4531            | 0.009             | 29,500 |  1/2 x 54/68 |
| 2W              | 35.12     | 35.12 | 0.4418            | 0.016             | 29,370 |  3/4 rod     |
| 3W              | 40.85     | 40.75 | 0.4448            | 0.138             | 30,200 |  1.660 d     |
| 4W              | 41.30     | 41.42 | 0.3570            | 0.067             | 29,200 |  1.315 d     |
| 5W              | 35.12     | 35.12 | 0.4418            | 0.016             | 29,370 |  as 2W       |
| 6W              | 41.21     | 41.07 | 0.3570            | 0.067             | 29,200 |  as 4W       |
| 7W              | 41.10     | 41.28 | "                 | "                 | "      |  as 4W       |
| 8W              | 35.12     | 35.12 | 0.4418            | 0.016             | 29,370 |  as 2W       |

Table 4.1 Geometry AX01











| Geometry - AX02 |            |       |                   |                   |        | Table 4.2   |
|-----------------|------------|-------|-------------------|-------------------|--------|---|
| Member          | Length in. |       | A in <sup>2</sup> | I in <sup>4</sup> | E ksi  | Section   |
|                 | north      | south |                   |                   |        |   |
| a               | 2.00       | 2.00  | 1.530             | 1.024             | 29,580 |  C & E       |
| 1T              | 34.16      | 34.16 | "                 | "                 | "      | "   |
| 2T              | 22.35      | 22.24 | 0.638             | 0.109             | "      |  C           |
| b               | 2.97       | 2.60  | "                 | "                 | "      | "   |
| 3T              | 22.57      | 22.93 | "                 | "                 | "      | "   |
| 4T              | 22.85      | 22.64 | "                 | "                 | "      | "   |
| c               | 2.59       | 2.60  | "                 | "                 | "      | "   |
| 5T              | 22.53      | 22.81 | "                 | "                 | "      | "   |
| d               | 1.00       | 1.00  | "                 | "                 | "      | "   |
| e               | 2.45       | 2.41  | "                 | "                 | "      | "   |
| 1B              | 43.51      | 43.50 | "                 | "                 | "      | "   |
| f               | 1.93       | 1.86  | "                 | "                 | "      | "   |
| g               | 2.08       | 2.00  | "                 | "                 | "      | "   |
| 2B              | 43.96      | 44.08 | "                 | "                 | "      | "   |
| h               | 1.93       | 1.97  | "                 | "                 | "      | "   |
| 1W              | 48.30      | 48.30 | 0.4531            | 0.009             | 29,500 |  1/2 54/68 |
| 2W              | 35.12      | 35.12 | 0.4418            | 0.016             | 29,370 |  3/4 rod   |
| 3W              | 40.37      | 40.34 | 0.4448            | 0.138             | 30,200 |  1.660 Ø   |
| 4W              | 40.74      | 40.96 | 0.3570            | 0.067             | 29,200 |  1.315 Ø   |
| 5W              | 35.12      | 35.12 | 0.4418            | 0.016             | 29,370 |  as 2W     |
| 6W              | 40.81      | 40.74 | 0.3570            | 0.067             | 29,200 |  as 4W     |
| 7W              | 40.72      |       | "                 | "                 | "      |  as 4W     |
| 8W              | 35.12      |       | 0.4418            | 0.016             | 29,370 |  as 2W     |

Table 4.2 Geometry AX02



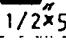
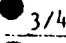
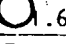
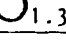
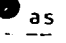
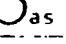
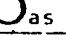

| Geometry - AX03 |            |       |                   |                   |        | Table 43  |
|-----------------|------------|-------|-------------------|-------------------|--------|---|
| Member          | Length in. |       | A in <sup>2</sup> | I in <sup>4</sup> | E ksi  | Section   |
|                 | north      | south |                   |                   |        |   |
| a               | 1.92       | 1.63  | 1.530             | 1.024             | 29,590 |  C & E           |
| 1T              | 34.35      | 34.35 | "                 | "                 | "      | "   |
| 2T              | 22.64      | 22.57 | 0.638             | 0.109             | "      |  C               |
| b               | 2.36       | 2.25  | "                 | "                 | "      | "   |
| 3T              | 22.96      | 23.13 | "                 | "                 | "      | "   |
| 4T              | 23.23      | 22.77 | "                 | "                 | "      | "   |
| c               | 1.81       | 2.17  | "                 | "                 | "      | "   |
| 5T              | 22.97      | 23.14 | "                 | "                 | "      | "   |
| d               | 0.90       | 0.96  | 0.530             | 0.098             | 29,620 | B   |
| e               | 1.93       | 1.74  | "                 | "                 | "      | "   |
| 1B              | 44.42      | 44.58 | "                 | "                 | "      | "   |
| f               | 1.48       | 1.48  | "                 | "                 | "      | "   |
| g               | 1.74       | 1.41  | "                 | "                 | "      | "   |
| 2B              | 44.79      | 45.13 | "                 | "                 | "      | "   |
| h               | 1.65       | 1.65  | "                 | "                 | "      | "   |
| 1W              | 48.44      | 48.40 | 0.4531            | 0.009             | 28,000 |  1/2 x 5/16"   |
| 2W              | 35.04      | 35.04 | 0.4418            | 0.016             | 29,690 |  3/4" rod      |
| 3W              | 40.70      | 40.76 | 0.4450            | 0.138             | 30,200 |  1.660" $\phi$ |
| 4W              | 41.03      | 41.11 | 0.3336            | 0.064             | 29,130 |  1.315" $\phi$ |
| 5W              | 35.04      | 35.04 | 0.4418            | 0.016             | 29,690 |  as 2W         |
| 6W              | 41.17      | 41.11 | 0.3336            | 0.064             | 29,130 |  as 4W         |
| 7W              | 41.03      | 41.08 | "                 | "                 | "      |  as 4W         |
| 8W              | 35.04      | 35.04 | 0.4418            | 0.016             | 29,690 |  as 2W         |

Table 4.3 Geometry AX03



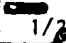


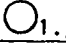




| Geometry - AX04 |            |       |                   |                   |        |   |
|-----------------|------------|-------|-------------------|-------------------|--------|---|
| Table 4.4       |            |       |                   |                   |        |   |
| Member          | Length in. |       | A in <sup>2</sup> | I in <sup>4</sup> | E ksi  | Section   |
|                 | north      | south |                   |                   |        |   |
| a               | 2.00       | 2.00  | 1.530             | 1.024             | 29,590 |  C & E           |
| 1T              | 34.10      | 34.10 | "                 | "                 | "      | "   |
| 2T              | 22.34      | 22.23 | 0.638             | 0.109             | "      |  C               |
| b               | 2.92       | 2.87  | "                 | "                 | "      | "   |
| 3T              | 22.72      | 22.84 | "                 | "                 | "      | "   |
| 4T              | 23.03      | 22.55 | "                 | "                 | "      | "   |
| c               | 2.64       | 2.64  | "                 | "                 | "      | "   |
| 5T              | 22.32      | 22.70 | "                 | "                 | "      | "   |
| d               | 1.12       | 1.14  | 0.530             | 0.098             | 29,620 | B   |
| e               | 2.20       | 2.20  | "                 | "                 | "      | "   |
| 1B              | 44.00      | 43.96 | "                 | "                 | "      | "   |
| f               | 1.73       | 1.75  | "                 | "                 | "      | "   |
| g               | 1.79       | 2.01  | "                 | "                 | "      | "   |
| 2B              | 44.32      | 43.99 | "                 | "                 | "      | "   |
| h               | 1.93       | 1.92  | "                 | "                 | "      | "   |
| 1W              | 48.12      | 48.10 | 0.4531            | 0.009             | 28,000 |  1/2" 54/68    |
| 2W              | 35.04      | 35.04 | 0.4418            | 0.016             | 29,690 |  3/4" $\phi$   |
| 3W              | 40.41      | 40.36 | 0.4450            | 0.138             | 30,200 |  1.66" $\phi$  |
| 4W              | 40.82      | 40.88 | 0.3336            | 0.064             | 29,130 |  1.315" $\phi$ |
| 5W              | 35.04      | 35.04 | 0.4418            | 0.016             | 29,690 |  as 2W         |
| 6W              | 40.00      | 40.63 | 0.3336            | 0.064             | 29,130 |  as 4W         |
| 7W              | 40.54      | 40.73 | "                 | "                 | "      |  as 4W         |
| 8W              | 35.04      | 35.04 | 0.4418            | 0.016             | 29,690 |  as 2W         |

Table 4.4 Geometry AX04

| Geometry - AY01 |                   |         |                   |                   |        |                  |
|-----------------|-------------------|---------|-------------------|-------------------|--------|------------------|
| Table 4.5       |                   |         |                   |                   |        |                  |
| Member          | Length in.        |         | A in <sup>2</sup> | I in <sup>4</sup> | E ksi  | Section          |
|                 | north             | south   |                   |                   |        |                  |
| a               |                   |         | 0.6439            | 0.0864            | 30,090 | #4               |
| 1T              | 36" nominal panel | end     | "                 | "                 | "      | "                |
| 2T              | 24" panel         | typical | "                 | "                 | "      | "                |
| b               |                   |         | "                 | "                 | "      | "                |
| 3T              |                   |         | "                 | "                 | "      | "                |
| 4T              |                   |         | "                 | "                 | "      | "                |
| c               |                   |         | "                 | "                 | "      | "                |
| 5T              |                   |         | "                 | "                 | "      | "                |
| d               |                   |         | 0.5400            | 0.0702            | 29,700 | #3               |
| e               |                   |         | "                 | "                 | "      | "                |
| 1B              |                   |         | "                 | "                 | "      | "                |
| f               |                   |         | "                 | "                 | "      | "                |
| g               |                   |         | "                 | "                 | "      | "                |
| 2B              |                   |         | "                 | "                 | "      | "                |
| h               |                   |         | "                 | "                 | "      | "                |
| 1W              |                   |         | 0.3750            | 0.002             | 29,100 | 1" x 1"          |
| 2W              |                   |         | 0.23              | 0.022             | *      | 1" x 1" x 1/8" L |
| 3W              |                   |         | 0.4193            | 0.1039            | *      | 1 1/2" 13ga.     |
| 4W              |                   |         | "                 | "                 | *      | as 3W            |
| 5W              |                   |         | 0.23              | 0.022             | *      | 1" x 1" x 1/8" L |
| 6W              |                   |         | 0.4193            | 0.1039            | *      | as 3W            |
| 7W              |                   |         | "                 | "                 | *      | as 3W            |
| 8W              |                   |         | 0.23              | 0.022             | *      | 1" x 1" x 1/8" L |

Table 4.5 Geometry AY01

| Geometry - AY02 |                   |         |                   |                   |        | Table 4.6        |
|-----------------|-------------------|---------|-------------------|-------------------|--------|------------------|
| Member          | Length in.        |         | A in <sup>2</sup> | I in <sup>4</sup> | E ksi  | Section          |
|                 | north             | south   |                   |                   |        |                  |
| a               |                   |         | 0.6439            | 0.0864            | 30,090 | #4               |
| 1T              | 36" nominal panel | end     | "                 | "                 | "      | "                |
| 2T              | 24" panel         | typical | "                 | "                 | "      | "                |
| b               |                   |         | "                 | "                 | "      | "                |
| 3T              |                   |         | "                 | "                 | "      | "                |
| 4T              |                   |         | "                 | "                 | "      | "                |
| c               |                   |         | "                 | "                 | "      | "                |
| 5T              |                   |         | "                 | "                 | "      | "                |
| d               |                   |         | 0.5400            | 0.0702            | 29,700 | #3               |
| e               |                   |         | "                 | "                 | "      | "                |
| 1B              |                   |         | "                 | "                 | "      | "                |
| f               |                   |         | "                 | "                 | "      | "                |
| g               |                   |         | "                 | "                 | "      | "                |
| 2B              |                   |         | "                 | "                 | "      | "                |
| h               |                   |         | "                 | "                 | "      | "                |
| 1W              |                   |         | 0.3750            | 0.002             | 29,100 | 1 1/2" x 1/4"    |
| 2W              |                   |         | 0.23              | 0.022             | *      | 1" x 1" x 1/8" L |
| 3W              |                   |         | 0.4193            | 0.1039            | *      | 1 1/2" x 13ga.   |
| 4W              |                   |         | "                 | "                 | *      | as 3W            |
| 5W              |                   |         | 0.23              | 0.022             | *      | 1" x 1" x 1/8" L |
| 6W              |                   |         | 0.3043            | 0.0521            | *      | 1 1/4" x 14ga.   |
| 7W              |                   |         | "                 | "                 | *      | as 6W            |
| 8W              |                   |         | 0.23              | 0.022             | *      | 1" x 1" x 1/8" L |

Table 4.6 Geometry AY02

| Mem.<br>No. | Axial Force - kips |                 |        |                   | Bending Moment - in.kips |                  |                 |                  |
|-------------|--------------------|-----------------|--------|-------------------|--------------------------|------------------|-----------------|------------------|
|             | gauge<br>loc. i    | gauge<br>loc. j | ave.   | frame<br>analysis | gauge<br>loc. i          | analysis<br>at i | gauge<br>loc. j | analysis<br>at j |
| 1T          |                    | -6.88<br>0.8%   | -6.88  | -7.66<br>0.90     |                          | 12.26            | +7.95<br>2.6%   | +3.07<br>2.56    |
| 2T          | -7.23<br>1.0%      | -7.62<br>0.7%   | -7.46  | -7.71<br>0.97     | -0.37<br>30.0%           | -0.15<br>2.47    | -1.05<br>34.1%  | -0.48<br>2.19    |
| 3T          | -14.43<br>2.6%     | -14.40<br>0.7%  | -14.41 | -14.66<br>0.98    | +2.12<br>17.9%           | +2.27<br>0.93    | +1.31<br>9.0%   | +1.18<br>1.11    |
| 4T          | -14.30<br>1.6%     | -14.73<br>1.2%  | -14.55 | -14.68<br>0.99    | +0.06<br>165.1%          | +0.31<br>0.19    | -0.22<br>29.8%  | +0.16<br>-1.38   |
| 5T          | -16.85<br>2.1%     | -16.81<br>2.4%  | -16.83 | -16.96<br>0.99    | +1.48<br>3.5%            | +1.40<br>1.06    | +0.65<br>3.0%   | +0.75<br>0.87    |
| 1B          | +11.66<br>1.7%     | +11.66<br>4.8%  | +11.66 | +11.75<br>0.99    | +3.94<br>13.8%           | +4.14<br>0.95    | -2.46<br>6.5%   | -2.49<br>0.99    |
| 2B          | +16.42<br>2.9%     | +16.32<br>4.2%  | +16.38 | +16.35<br>1.00    | +1.32<br>6.4%            | +1.68<br>0.79    | -0.48<br>16.8%  | -0.26<br>1.85    |
| 1W          | +11.03<br>2.8%     | +12.62<br>18.7% | +11.24 | +11.08<br>1.01    | -0.52<br>3.9%            | -0.28<br>1.86    | +0.51<br>3.7%   | +0.40<br>1.28    |
| 2W          | -1.48<br>15.9%     | -1.79<br>11.8%  | -1.66  | -2.08<br>0.80     | -0.23<br>31.7%           | -0.26<br>0.88    | +0.73<br>20.5%  | +0.84<br>0.87    |
| 3W          | -7.00<br>6.8%      | -7.25<br>1.9%   | -7.20  | -7.33<br>0.98     | -3.99<br>4.4%            | -3.67<br>1.09    | +6.19<br>2.2%   | +6.28<br>0.99    |
| 4W          | +4.95<br>7.4%      | .09<br>3.1%     | +5.05  | +5.37<br>0.94     | -1.58<br>11.2%           | -1.59<br>0.99    | +1.45<br>4.6%   | +1.44<br>1.01    |
| 5W          | -1.62<br>2.2%      | -1.68<br>2.3%   | -1.65  | -1.77<br>0.93     | -0.06<br>15.9%           | -0.09<br>0.67    | +0.34<br>8.3%   | +0.32<br>1.06    |
| 6W          | -3.17<br>1.4%      |                 | 3.17   | -3.09<br>1.03     | -0.63<br>12.6%           | -0.66<br>0.95    |                 |                  |
| 7W          | +0.89<br>20.5%     | +1.05<br>3.7%   | +1.03  | +1.13<br>0.91     | -0.69<br>5.2%            | -0.54<br>1.28    | +0.29<br>8.5%   | +0.08<br>3.63    |
| 8W          | -1.69<br>4.1%      |                 | -1.69  | -1.81<br>0.93     | 0.00                     | 0.00<br>1.00     |                 |                  |

Table 4.7 Comparison of Analytical and Experimental Stress Resultants - AX01

| Mem.<br>No.<br>Z | Axial Force - kips |                 |        |                   | Bending Moment - in.kips |                  |                 |                  |
|------------------|--------------------|-----------------|--------|-------------------|--------------------------|------------------|-----------------|------------------|
|                  | gauge<br>loc. i    | gauge<br>loc. j | ave.   | frame<br>analysis | gauge<br>loc. i          | analysis<br>at i | gauge<br>loc. j | analysis<br>at j |
| 1T               | -6.87<br>4.1%      | -6.34<br>9.4%   | -6.71  | -7.59<br>0.88     | +12.21<br>2.5%           | +12.16<br>1.00   | +6.98<br>4.0%   | +4.88<br>1.43    |
| 2T               | -6.58<br>4.3%      | -6.40<br>1.8%   | -6.45  | -7.66<br>0.84     | -0.89<br>9.8%            |                  | -1.54<br>16.5%  | -1.61<br>0.96    |
| 3T               | -13.47<br>1.7%     | -13.11<br>1.4%  | -13.27 | -14.67<br>0.90    | +3.16<br>7.5%            | +2.97<br>1.06    | +1.27<br>8.5%   | +1.33<br>0.95    |
| 4T               | -13.69<br>2.8%     | -13.06<br>1.1%  | -13.81 | -14.69<br>0.94    | -0.33<br>33.8%           | +0.11<br>-3.00   | -0.48<br>17.5%  | +0.01<br>48.0    |
| 5T               | -16.10<br>2.0%     | -16.00<br>1.3%  | -16.04 | -16.97<br>0.95    | +1.71<br>5.4%            | +1.66<br>1.03    | +0.59<br>3.0%   | +0.74<br>0.80    |
| 1B               | +12.06<br>1.7%     | +11.97<br>3.3%  | +12.03 | +11.76<br>1.02    | +5.90<br>5.7%            | +5.98<br>0.99    | -4.10<br>10.6%  | -3.49<br>1.17    |
| 2B               | +16.51<br>1.8%     | +16.34<br>2.1%  | +16.43 | +16.35<br>1.00    | +1.94<br>8.6%            | +2.22<br>0.87    | -0.91<br>21.6%  | -0.40<br>2.28    |
| 1W               | +8.63<br>0.9%      | +8.69<br>15.5%  | +8.68  | +11.02<br>0.79    | -0.51<br>7.7%            | -0.36<br>1.42    | +1.02<br>12.7%  | +0.64<br>1.59    |
| 2W               | -2.27<br>23.8%     |                 | -2.27  | -2.08<br>1.09     | -0.46<br>8.0%            | -0.44<br>1.05    |                 |                  |
| 3W               | -6.50<br>9.7%      | -7.00<br>30.8%  | -6.62  | -7.43<br>0.89     | -5.14<br>3.9%            | -5.24<br>0.98    | +8.86<br>11.0%  | +9.07<br>0.98    |
| 4W               | +5.26<br>2.5%      | +5.26<br>3.7%   | +5.26  | +5.50<br>0.96     | -2.16<br>2.8%            | -2.16<br>1.00    | +1.68<br>6.4%   | +1.92<br>0.88    |
| 5W               | -2.04<br>10.9%     | -1.71<br>6.7%   | -1.84  | -1.83<br>1.01     | -0.11<br>19.3%           | -0.11<br>1.00    | +0.51<br>7.7%   | +0.44<br>1.16    |
| 6W               | -3.04<br>2.4%      |                 | -3.04  | -3.09<br>0.98     | -1.05<br>4.6%            | -0.93<br>1.13    |                 |                  |
| 7W               | +1.05<br>6.7%      | +1.07<br>6.0%   | +1.06  | +1.19<br>0.89     | -0.78<br>10.5%           | -0.69<br>1.13    | +0.17%<br>9.9%  | +0.11<br>1.55    |
| 8W               | -1.52<br>6.6%      | -1.70<br>4.6%   | -1.63  | -1.86<br>0.88     | 0.00                     | 0.00<br>1.00     | +8.04<br>19.4%  | +0.01<br>4.00    |

Table 4.8 Comparison of Analytical and Experimental Stress Resultants - AX02

| Σ Z | Axial Force - kips |                |        |                | Bending Moment - in.kips |                |                |               |
|-----|--------------------|----------------|--------|----------------|--------------------------|----------------|----------------|---------------|
|     | gauge loc. i       | gauge loc. j   | ave.   | frame analysis | gauge loc. i             | analysis at i  | gauge loc. j   | analysis at j |
| 1T  | -6.65<br>3.7%      | -7.40<br>2.6%  | -7.09  | -7.66<br>0.93  | +11.04<br>2.0%           | +11.60<br>0.95 | +0.68<br>2.7%  | +2.45<br>0.28 |
| 2T  | -7.37<br>1.7%      | -6.95<br>16.0% | -7.33  | -7.72<br>0.95  | -0.98<br>7.1%            | -0.75<br>1.31  | -1.14<br>23.6% | -0.75<br>1.52 |
| 3T  | -13.87<br>6.0%     | -14.19<br>1.5% | -14.12 | -14.73<br>0.96 | +1.60<br>15.3%           | +1.36<br>1.18  | +0.75<br>5.8%  | +0.58<br>1.29 |
| 4T  | -14.46<br>1.6%     | -14.30<br>1.5% | -14.38 | -14.76<br>0.97 | -0.24<br>30.0%           | -0.29<br>0.83  | -0.68<br>15.5% | -0.19<br>3.58 |
| 5T  | -16.75<br>2.5%     | -16.77<br>1.5% | -16.76 | -17.02<br>0.98 | +1.09<br>6.1%            | +0.87<br>1.25  | +0.20<br>35.4% | +0.15<br>1.33 |
| 1B  | +12.17<br>1.4%     | +11.83<br>1.0% | +11.97 | +11.83<br>1.01 | +4.03<br>8.5%            | +4.66<br>0.86  | -2.99<br>7.9%  | -2.70<br>1.11 |
| 2B  | +16.73<br>1.1%     | +16.63<br>1.0% | +16.68 | +16.43<br>1.02 | +0.86<br>4.3%            | +1.72<br>0.50  | -0.85<br>10.2% | -0.29<br>2.93 |
| 1W  | +10.84<br>1.4%     | +10.56<br>9.6% | +10.81 | +11.07<br>0.98 | -0.54<br>16.5%           | -0.33<br>1.64  | +0.39<br>22.7% | +0.58<br>0.67 |
| 2W  |                    |                |        |                |                          |                |                |               |
| 3W  | -6.70<br>23.3%     | -6.57<br>21.4% | -6.64  | -7.36<br>0.90  | -4.57<br>6.5%            | -4.36<br>1.05  | +6.81<br>15.2% | +7.78<br>0.88 |
| 4W  | +4.60<br>1.1%      | +4.71<br>2.7%  | +4.63  | +5.39<br>0.86  | -1.39<br>5.3%            | -1.58<br>0.88  | +1.43<br>4.1%  | +1.54<br>0.93 |
| 5W  | -1.69<br>4.0%      | -1.73<br>3.9%  | -1.71  | -1.81<br>0.94  | -0.10<br>15.8%           | -0.10<br>1.00  | +0.35<br>4.4%  | +0.36<br>0.97 |
| 6W  | -2.99<br>27.6%     | +3.48<br>41.6% | -3.19  | -3.07<br>1.04  | -0.89<br>9.0%            | -0.76<br>1.17  | +1.23<br>12.4% | +1.48<br>0.83 |
| 7W  | +1.11<br>6.9%      | +1.15<br>4.8%  | +1.14  | +1.13<br>1.01  | -0.52<br>4.3%            | -0.43<br>1.21  | +0.24<br>16.5% | +0.04<br>6.00 |
| 8W  | -1.70<br>2.2%      | -1.77<br>4.5%  | -1.72  | -1.82<br>0.95  | +0.02<br>12.8%           | 0.00           | +0.01<br>36.5% | 0.00          |

Table 4.9 Comparison of Analytical and Experimental Stress Resultants - AX03

| Mem.<br>No. | Axial Force - kips |                 |        |                   | Bending Moment - in.kips |                  |                 |                  |
|-------------|--------------------|-----------------|--------|-------------------|--------------------------|------------------|-----------------|------------------|
|             | gauge<br>loc. i    | gauge<br>loc. j | ave.   | frame<br>analysis | gauge<br>loc. i          | analysis<br>at i | gauge<br>loc. j | analysis<br>at j |
| 1T          | -6.69<br>2.2%      | -6.58<br>1.8%   | -6.63  | -6.61<br>1.00     | +1.78<br>11.2%           | +1.50<br>1.19    | +0.33<br>33.0%  | +0.64<br>0.52    |
| 2T          | -6.65<br>4.9%      | -6.43<br>26.7%  | -6.62  | -6.63<br>1.00     | +0.53<br>26.8%           | +0.27<br>1.96    | -0.45<br>57.3%  | +0.60<br>-0.75   |
| 3T          | -13.16<br>3.6%     |                 | -13.16 | -13.21<br>1.00    | +1.17<br>5.6%            | +0.65<br>1.80    |                 |                  |
| 4T          | -13.21<br>2.8%     | -13.35<br>2.3%  | -13.29 | -13.22<br>1.01    | +0.47<br>10.8%           | +0.66<br>1.34    | +0.01           | +0.64<br>0.02    |
| 5T          | -15.68<br>4.6%     | -15.63<br>1.6%  | -15.65 | -15.41<br>1.02    | +0.89<br>17.5%           | +0.66<br>1.34    | +1.58<br>5.1%   | +0.75<br>2.11    |
| 1B          | +10.93<br>1.8%     | +10.98<br>1.3%  | +10.96 | +10.48<br>1.05    | -0.58<br>12.2%           | -0.19<br>3.05    | -0.31<br>13.4%  | +0.10<br>-3.10   |
| 2B          | +15.84<br>1.6%     | +15.64<br>7.9%  | +15.81 | +14.87<br>1.06    | -0.18<br>11.3%           | -0.10<br>1.80    | +0.20<br>14.6%  | +0.15<br>1.33    |
| 1W          | +8.19<br>1.3%      |                 | +8.19  | +9.73<br>0.84     | -0.00                    | -0.03            |                 |                  |
| 2W          | -1.60<br>11.7%     |                 | -1.60  | -1.66<br>0.96     |                          |                  |                 |                  |
| 3W          | -7.96<br>1.5%      | -8.10<br>1.7%   | -8.02  | -6.74<br>1.19     | +0.44<br>15.1%           | -0.26<br>1.69    | -0.48<br>7.8%   | -0.50<br>0.96    |
| 4W          | +5.67<br>1.4%      |                 | +5.67  | +4.81<br>1.18     | +0.29<br>20.2%           | -0.33<br>0.88    |                 |                  |
| 5W          | -1.70<br>7.2%      | -1.32<br>76.6%  | -1.67  | -1.57<br>1.06     |                          |                  |                 |                  |
| 6W          | -3.11<br>49.1%     | -3.06<br>84.3%  | -3.09  | -2.89<br>1.07     | +0.06<br>84.0%           | +0.04<br>1.50    | -0.01           | -0.14<br>0.07    |
| 7W          | +1.09<br>19.7%     | +1.15<br>10.2%  | +1.13  | +0.96<br>1.18     | -0.06<br>47.9%           | -0.19<br>0.32    | -0.05<br>61.9%  | +0.05<br>-1.00   |
| 8W          | -1.83<br>14.1%     | -1.47<br>56.0%  | -1.76  | -1.57<br>1.12     |                          |                  |                 |                  |

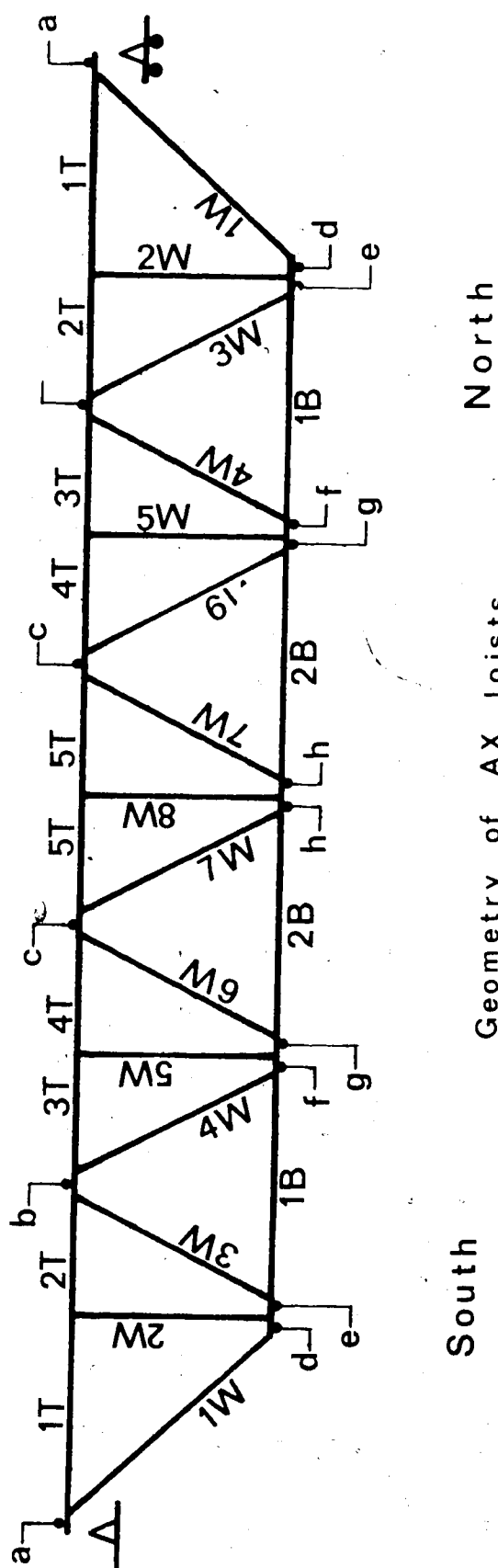
Table 4.10 Comparison of Analytical and Experimental Stress Resultants - AY01

| Mem.<br>No. | Axial Force - kips |                 |        |                   | Bending Moment - in.kips |                  |                 |                  |
|-------------|--------------------|-----------------|--------|-------------------|--------------------------|------------------|-----------------|------------------|
|             | gauge<br>loc. i    | gauge<br>loc. j | ave.   | frame<br>analysis | gauge<br>loc. i          | analysis<br>at i | gauge<br>loc. j | analysis<br>at j |
| 1T          | -6.47<br>3.3%      | -6.32<br>2.5%   | -6.39  | -6.62<br>0.97     | +2.72<br>12.6%           | +1.50<br>1.81    | +0.52<br>35.8%  | +0.64<br>0.81    |
| 2T          | -6.26<br>3.6%      | -6.30<br>2.9%   | -6.28  | -6.64<br>0.95     | -1.16<br>11.9%           | +0.27<br>-4.30   | -0.46<br>10.2%  | +0.60<br>-0.77   |
| 3T          | -12.84<br>1.5%     | -12.77<br>5.2%  | -12.82 | -13.23<br>0.97    | +0.68<br>4.0%            | +0.65<br>1.05    | +0.52<br>59.5%  | +0.79<br>0.66    |
| 4T          | -12.93<br>2.9%     | -12.86<br>1.3%  | -12.88 | -13.24<br>0.97    | +0.06<br>85.5%           | +0.66<br>0.09    | +0.25<br>14.4%  | +0.64<br>0.39    |
| 5T          | -14.91<br>2.0%     | -15.14<br>2.7%  | -15.00 | -15.43<br>0.97    | +0.08<br>51.8%           | +0.66<br>0.12    | +0.83<br>10.4%  | +0.75<br>1.11    |
| 1B          |                    | +10.47<br>2.0%  | +10.47 | +10.49<br>1.00    | -0.29<br>29.6%           | -0.19<br>1.53    | -0.06<br>67.0%  | +0.10<br>-0.60   |
| 2B          | +14.78<br>2.8%     | +14.75<br>3.3%  | +14.76 | +14.88<br>0.99    | -0.32<br>26.4%           | -0.10<br>3.20    | -0.05<br>78.3%  | +0.15<br>-0.33   |
| 1W          | +7.90<br>3.0%      | +7.95<br>4.2%   | +7.92  | +9.79<br>0.81     | -0.38<br>13.8%           |                  | +0.16<br>28.8%  | -0.01<br>-16.0   |
| 2W          | -1.88<br>55.5%     | -1.19<br>7.0%   | -1.26  | -1.68<br>0.75     |                          |                  |                 |                  |
| 3W          | -7.47<br>2.5%      | -7.56<br>2.6%   | -7.51  | -6.74<br>1.11     | +0.29<br>16.0%           | -0.26<br>-1.12   | -0.41<br>13.7%  | -0.50<br>0.82    |
| 4W          | +5.53<br>3.5%      | +5.37<br>4.2%   | +5.46  | 4.82<br>1.13      | +0.19<br>17.2%           | -0.33<br>-0.58   | -0.09<br>27.0%  |                  |
| 5W          | -1.66<br>8.6%      | -1.75<br>7.2%   | -1.71  | -1.58<br>1.08     |                          |                  |                 |                  |
| 6W          | -4.01<br>4.8%      | -3.77<br>5.1%   | -3.90  | -2.89<br>1.35     | 0.00                     | +0.04            | -0.20<br>29.2%  | -0.14<br>1.43    |
| 7W          | +1.22<br>11.1%     | +1.24<br>9.8%   | +1.23  | +0.95<br>1.29     | +0.07<br>22.8%           | -0.19<br>-0.36   | +0.02<br>150.0% | +0.05<br>0.40    |
| 8W          | -1.55<br>4.5%      | -1.43<br>4.5%   | -1.49  | -1.58<br>0.94     |                          |                  |                 |                  |

Table 4.11 Comparison of Analytical and Experimental Stress Resultants - AY02

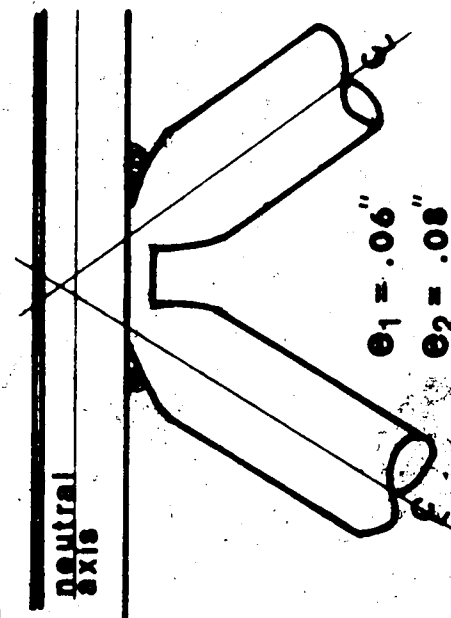
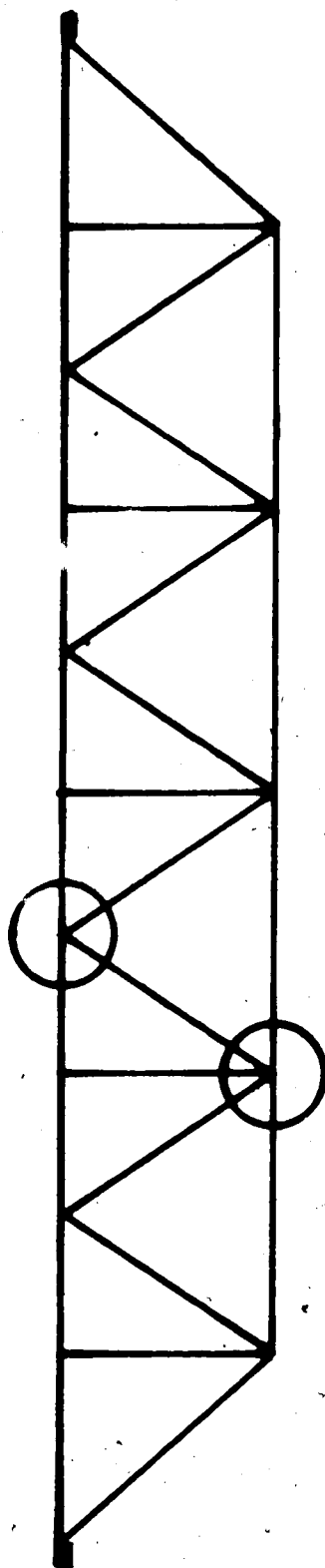
| JOIST  | AX01                  | AX02                  | AX03                   | AX04                   | AY01                  | AY02                  |
|--|-----------------------|-----------------------|------------------------|------------------------|-----------------------|-----------------------|
| DESIGN LOAD<br>K/FT BASED ON<br>22 FT SPAN   | .843                  | .843                  | .843                   | .843                   | .794                  | .794                  |
| DESIGN LOAD<br>K/PANEL POINT                 | 1.686                 | 1.686                 | 1.686                  | 1.686                  | 1.588                 | 1.588                 |
| DESIGN MOMENT<br>FT-K BASED ON<br>22 FT SPAN | 51.00                 | 51.00                 | 51.00                  | 51.00                  | 48.04                 | 48.04                 |
| LOAD/PANEL POINT<br>AT FAILURE<br>KIPS       | 2.759                 | 2.620                 | 2.754                  | 2.506                  | 2.620                 | 2.830                 |
| MOMENT AT<br>FAILURE<br>FT-KIPS              | 81.85                 | 77.79                 | 81.90                  | 74.54                  | 74.10                 | 80.00                 |
| 4 / 2  | 1.64                  | 1.55                  | 1.63                   | 1.49                   | 1.65                  | 1.74                  |
| 5 / 3  | 1.60                  | 1.53                  | 1.61                   | 1.46                   | 1.53                  | 1.67                  |
| FAILURE<br>MECHANISM                         | BUCKLING<br>MEMBER ST | BUCKLING<br>MEMBER ST | END PANEL<br>MECHANISM | END PANEL<br>MECHANISM | BUCKLING<br>MEMBER ST | BUCKLING<br>MEMBER ST |

SUMMARY OF JOIST TESTS      TABLE 4.12

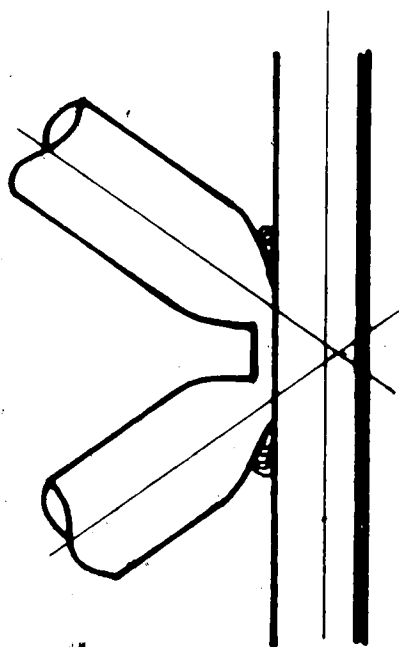


Geometry of AX Joists  
See Tables 4.1 to 4.4

Fig. 4.1 Geometry of AX Joists



Typical Top Chord Joint



Typical Bottom Chord Joint

Fig 4.2 Geometry of AY Joists

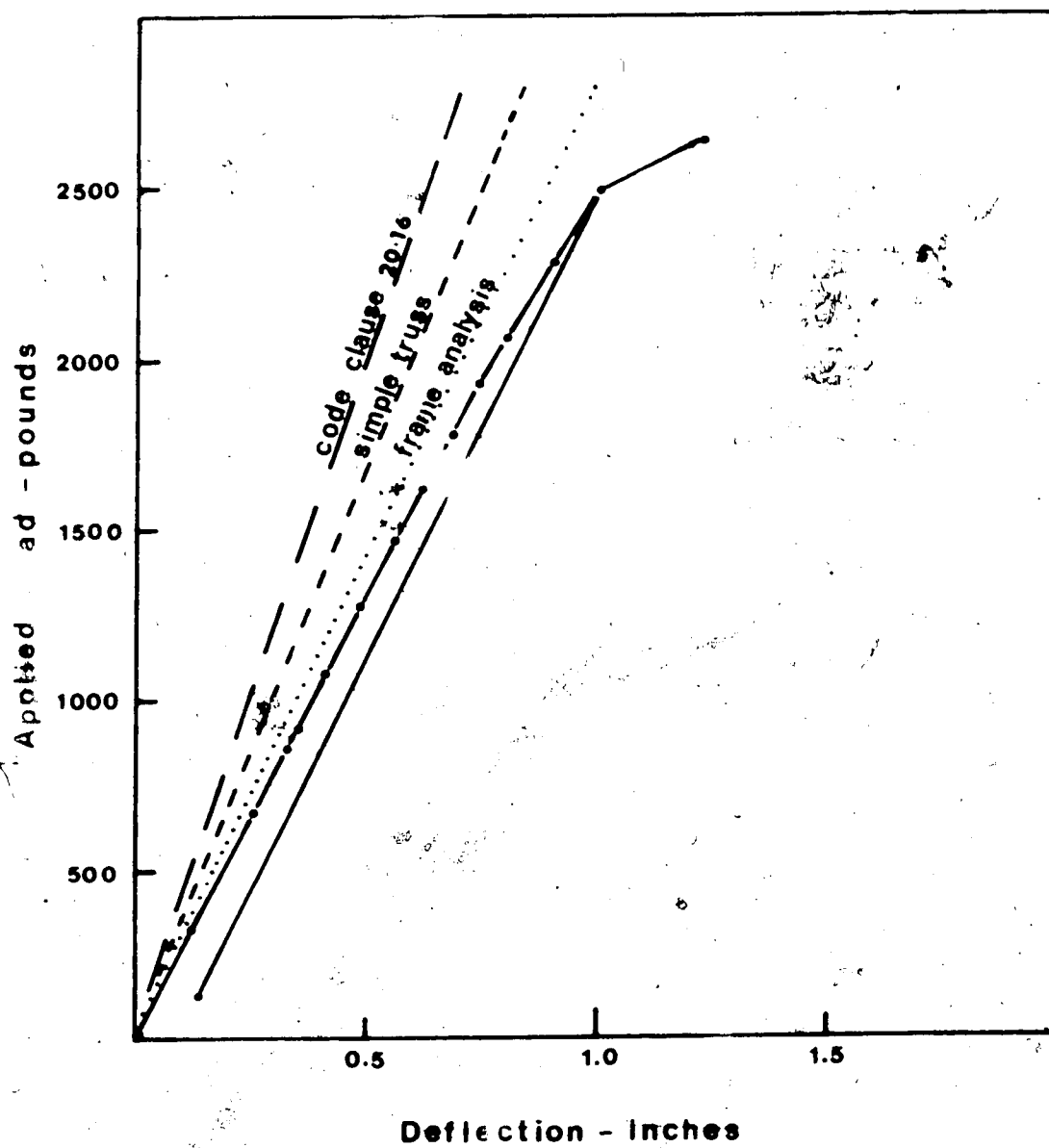


Fig. 4.3 Load Deflection Plot AX01

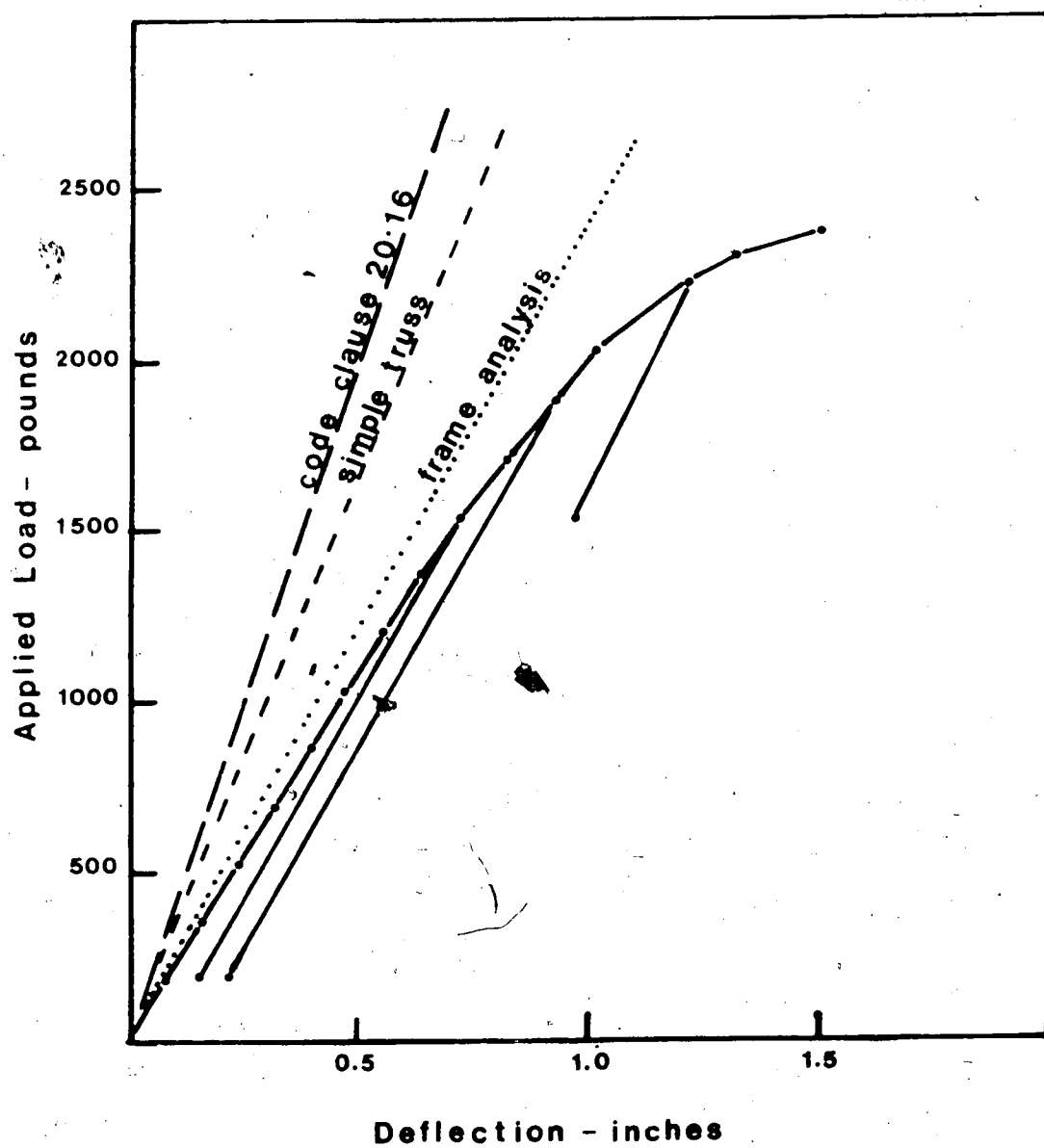


Fig. 4.4 Load Deflection Plot AX02

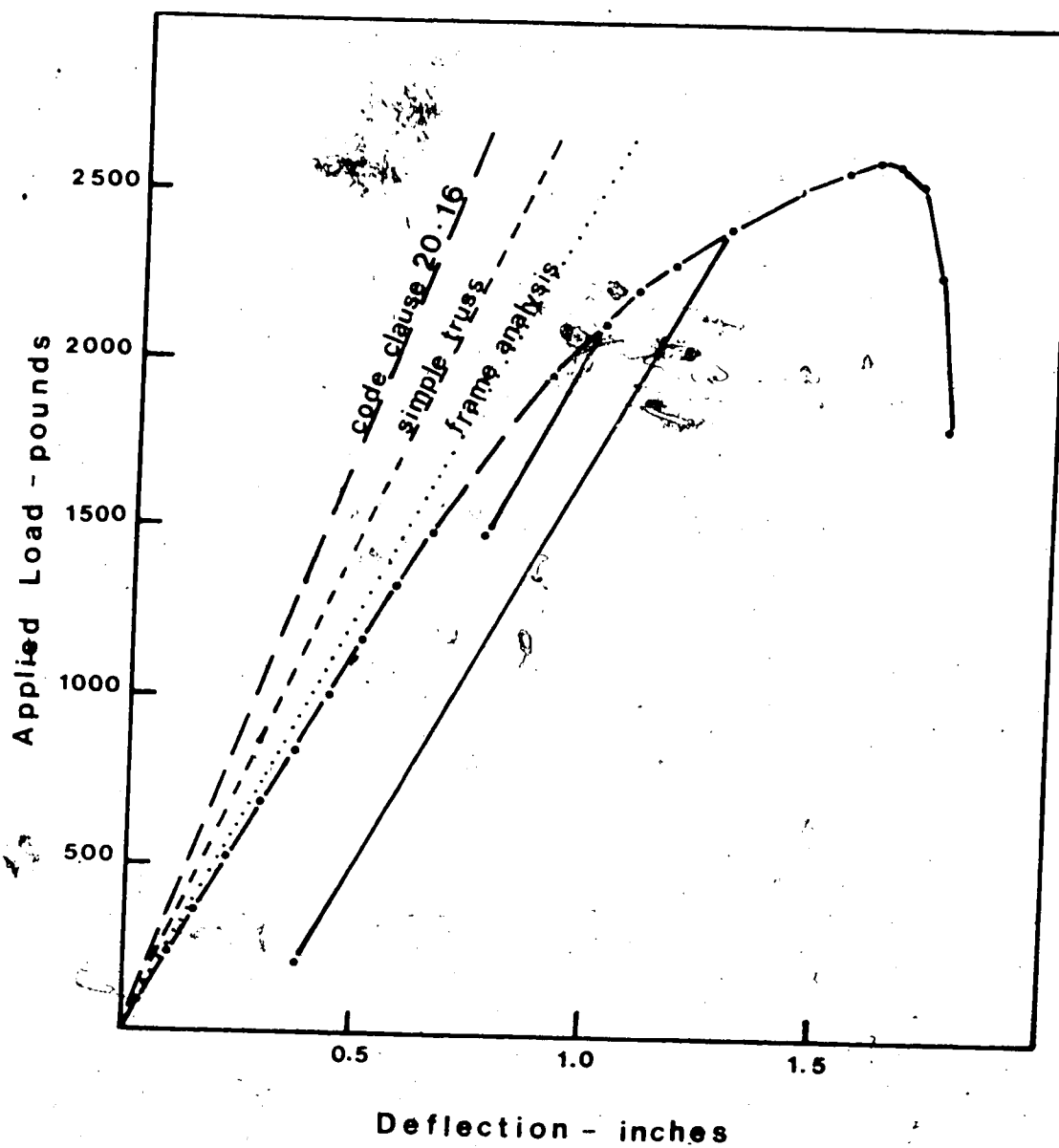


Fig. 4.5 Load Deflection Plot AX03

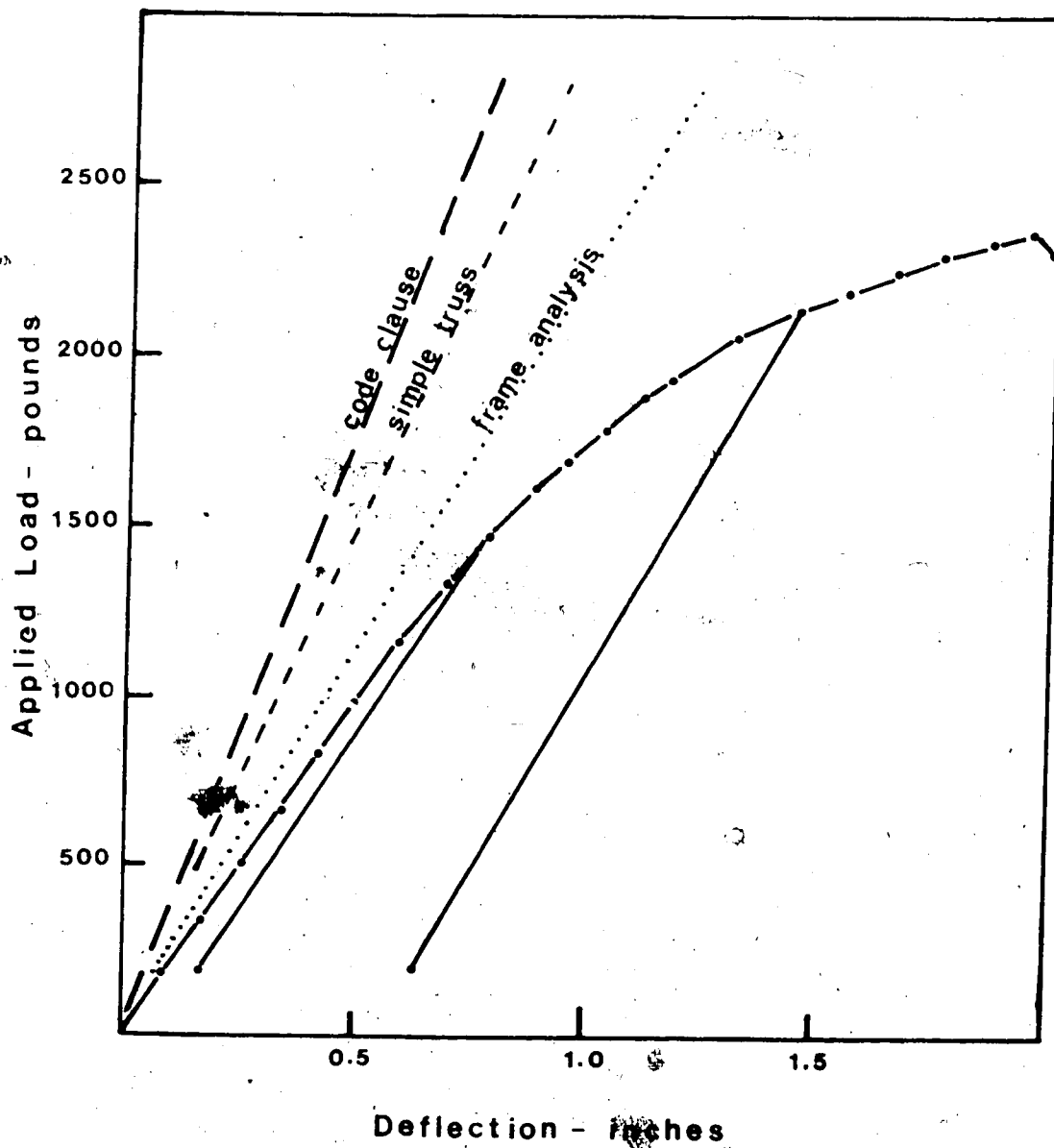


Fig. 4.6 Load Deflection Plot AX04

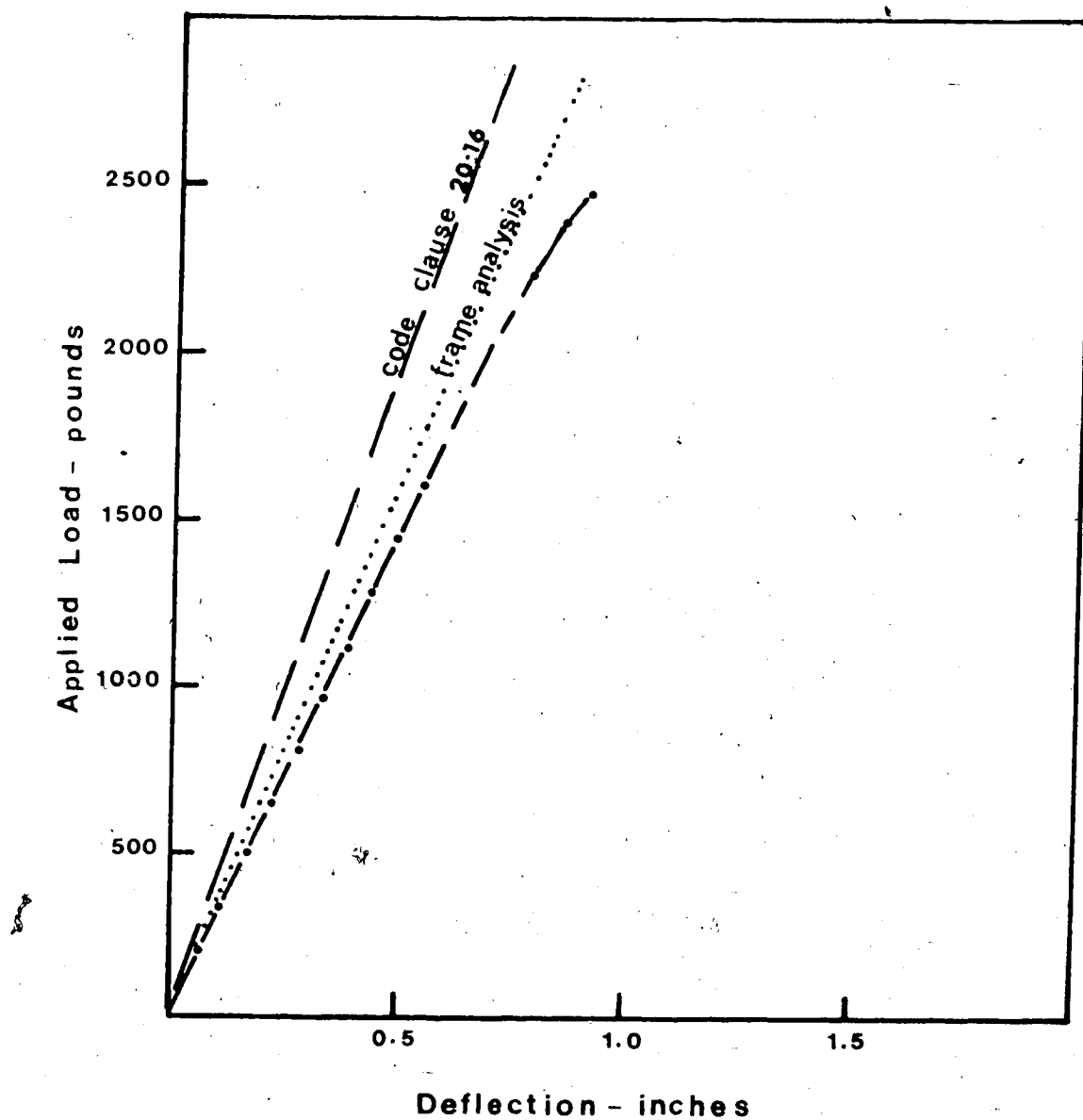


Fig. 4.7 Load Deflection Plot AY01

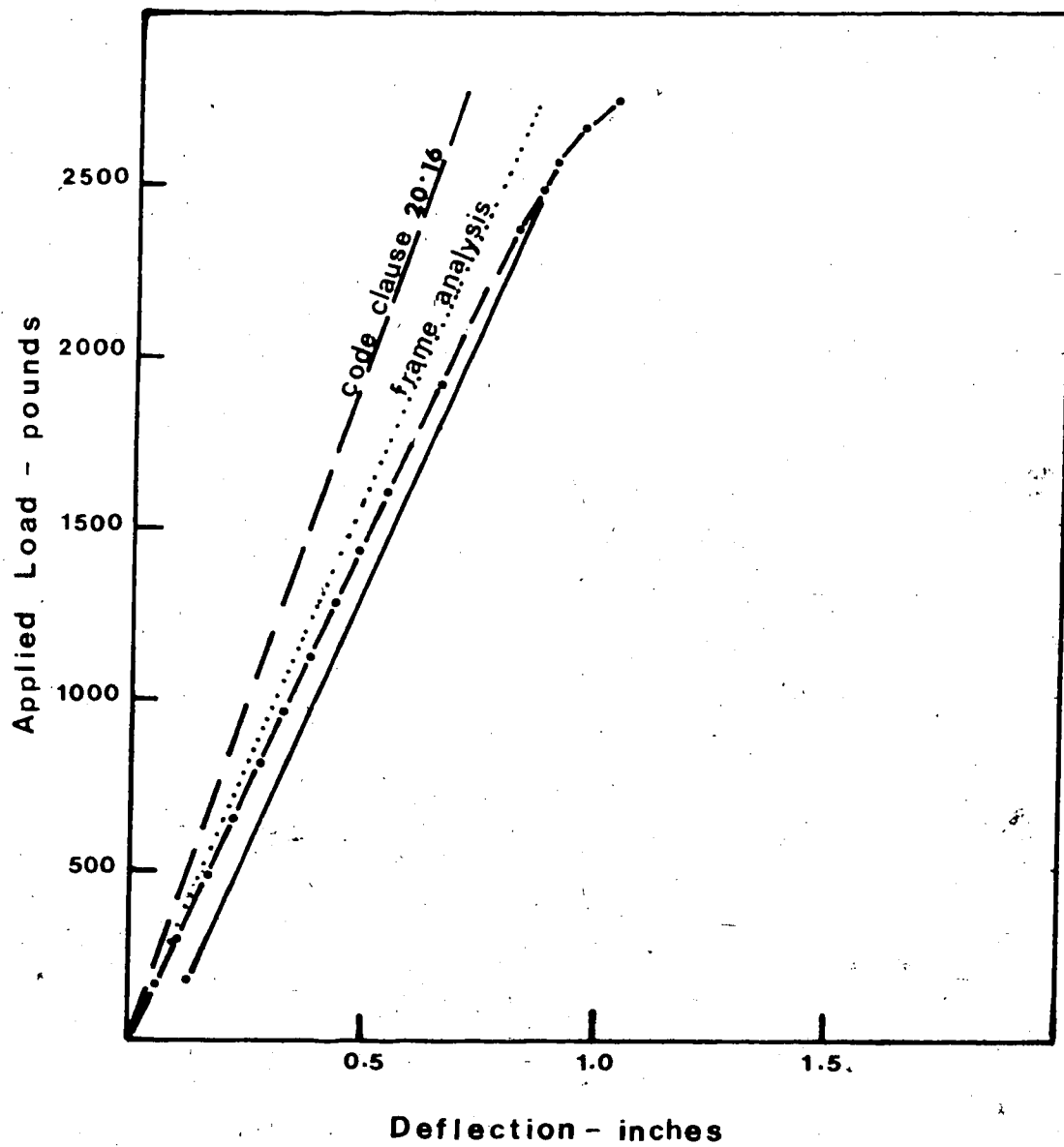


Fig. 4.8 Load Deflection Plot AY02

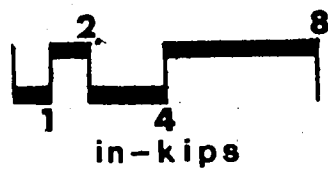
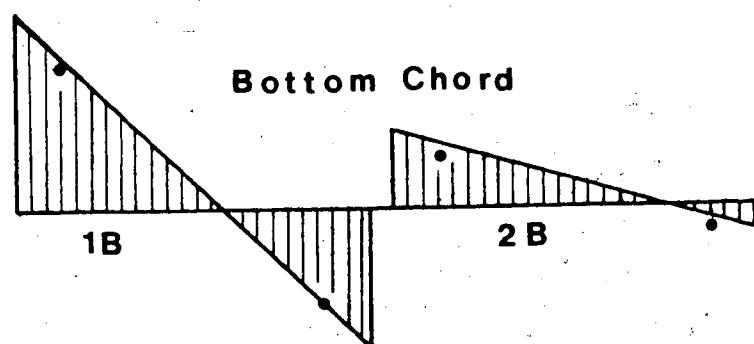
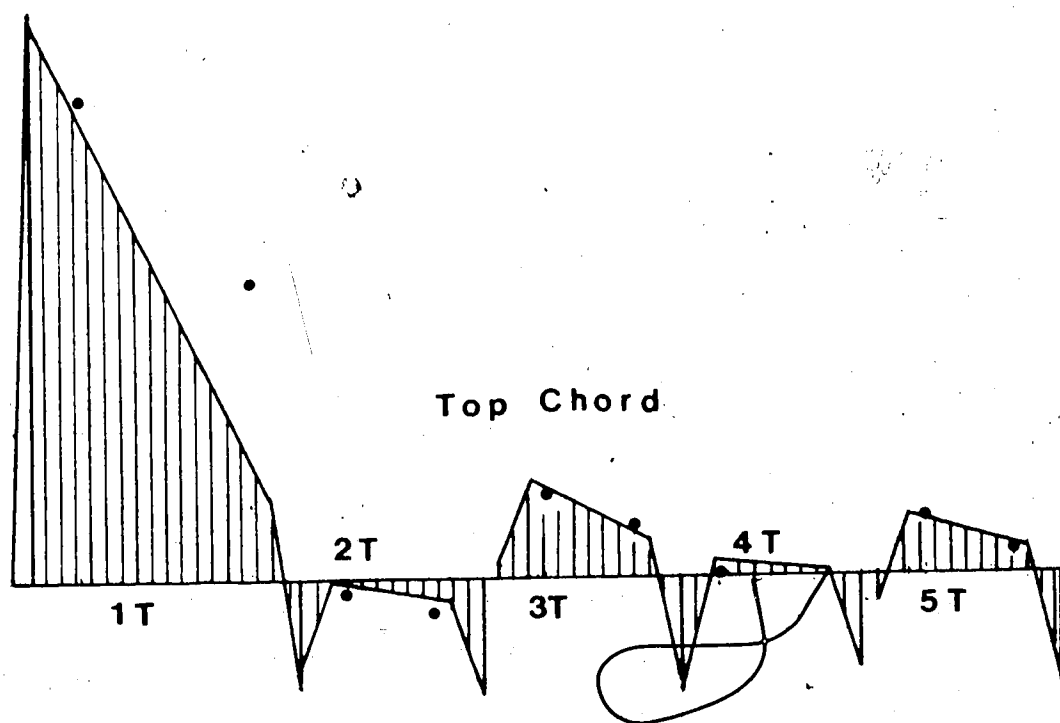


Fig. 4.9 Analytical and Measured Moments AX01 - Chords

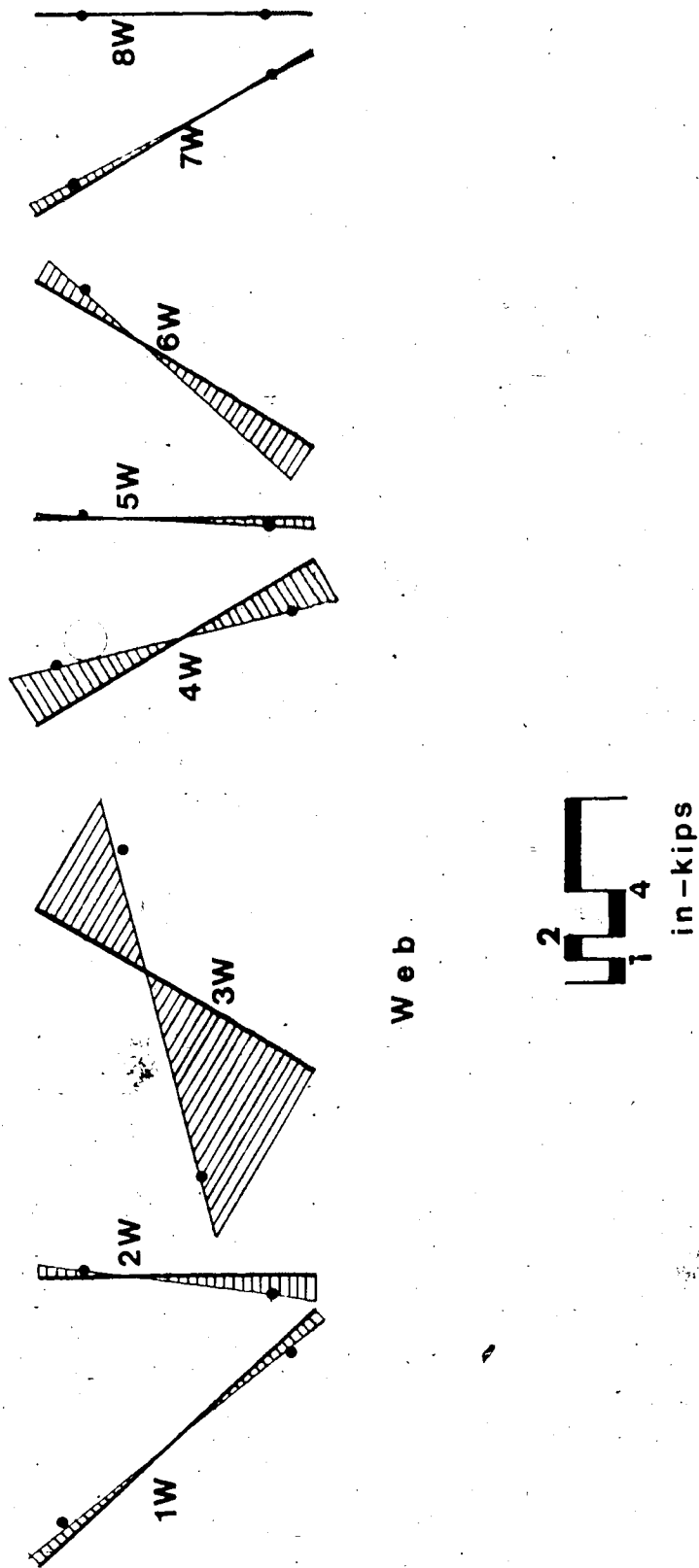


Fig. 4.10 Analytical and Measured Moments AX01 - Web

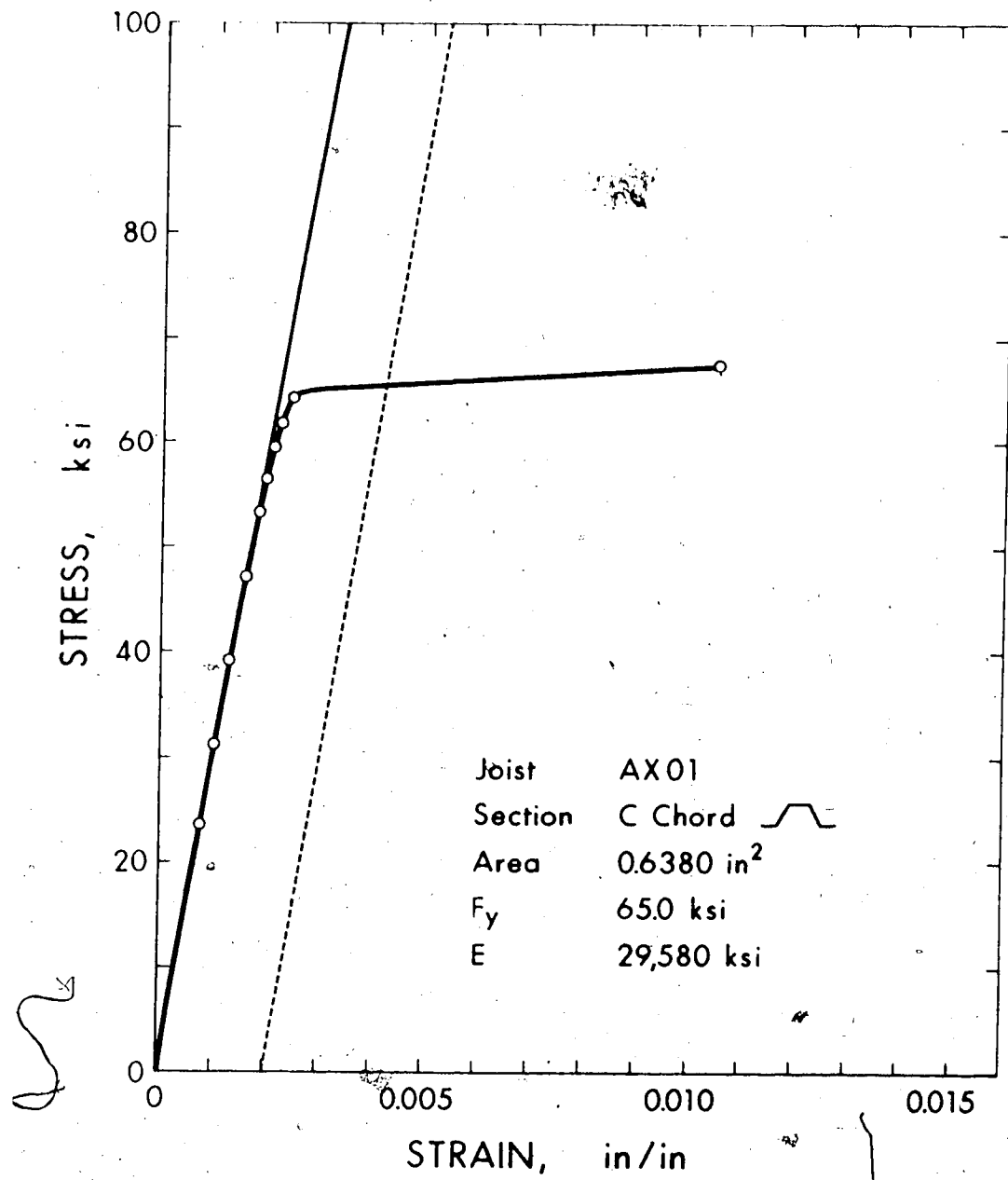


Fig. 4.11 Stress Strain Curve - AX01 &amp; AX02 C Chord

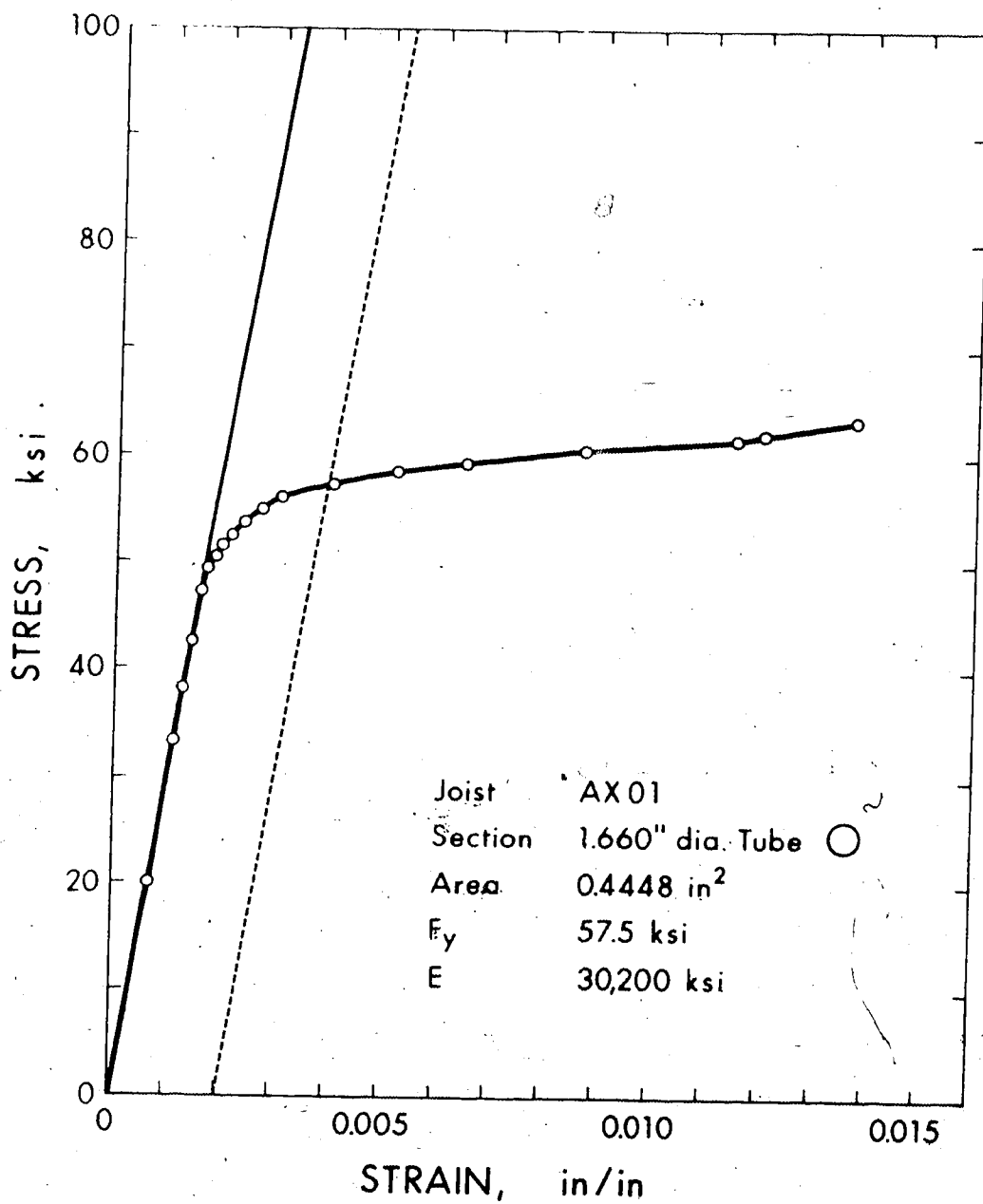


Fig. 4.12 Stress Strain Curve - AX01 & AX02 1.66" Tube

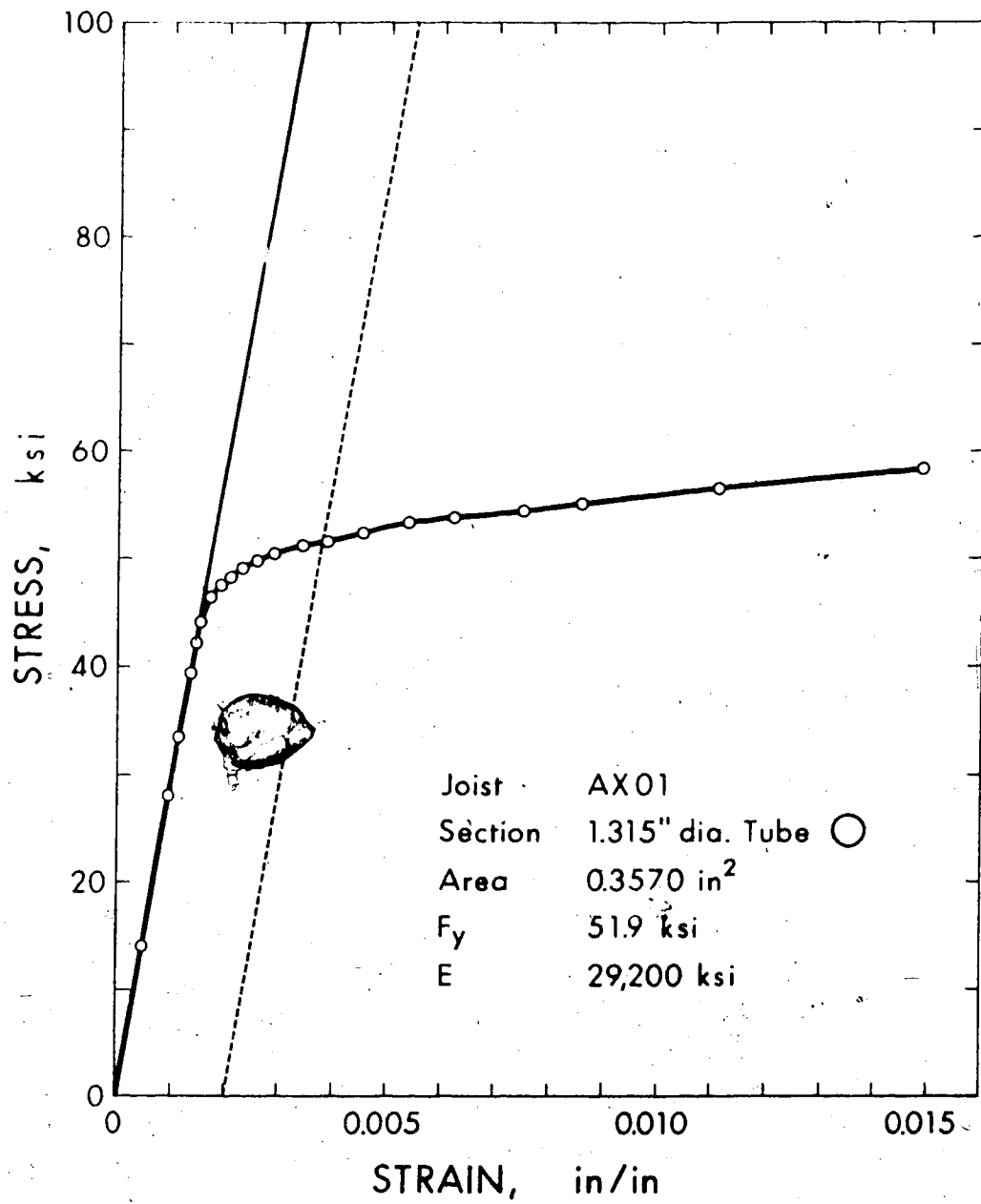


Fig. 4.13 Stress Strain Curve - AX01 & AX02 1.315" Tube

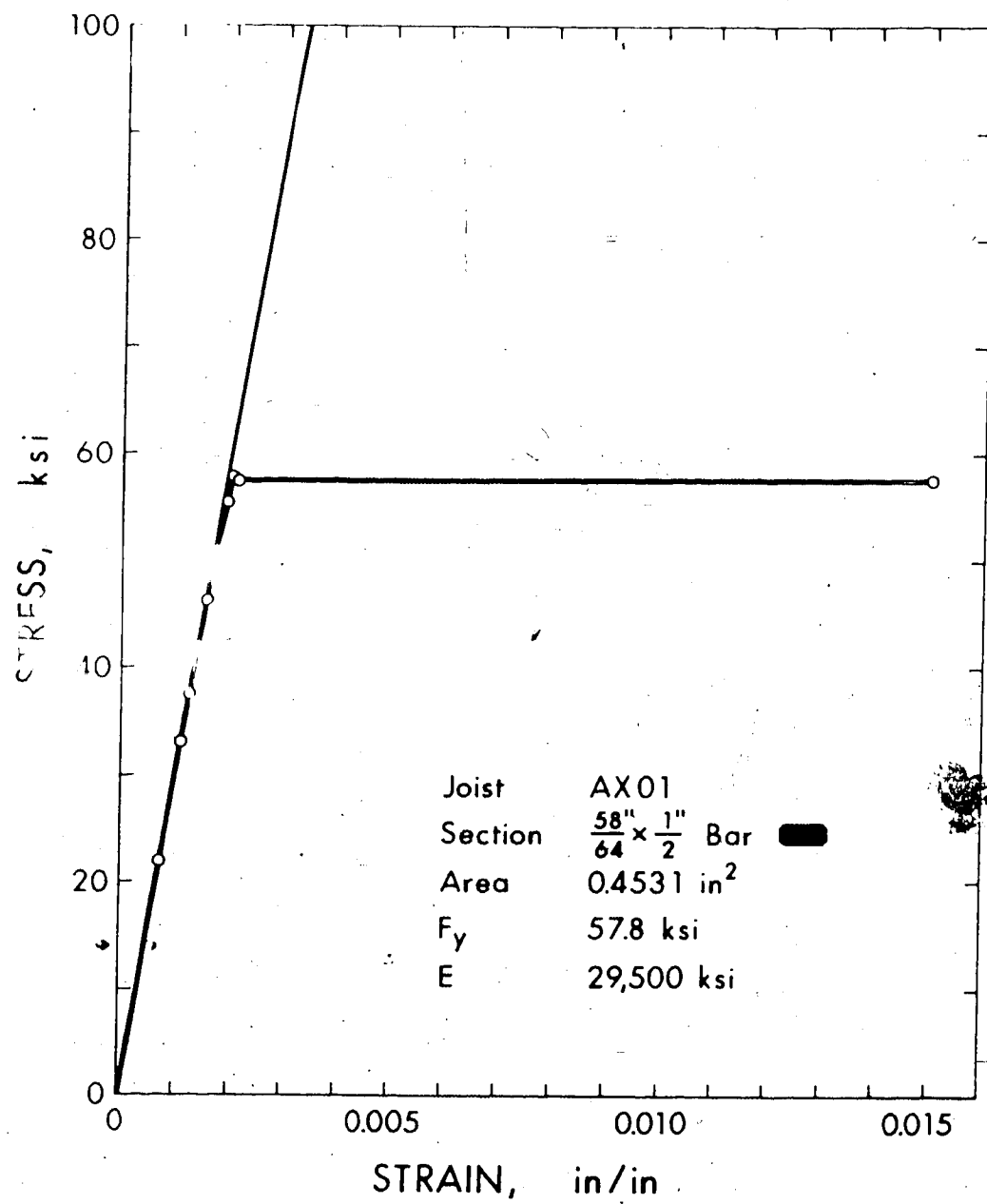


Fig. 4.14 Stress Strain Curve - AX01

 $\frac{58''}{64} \times \frac{1''}{2}$  Bar

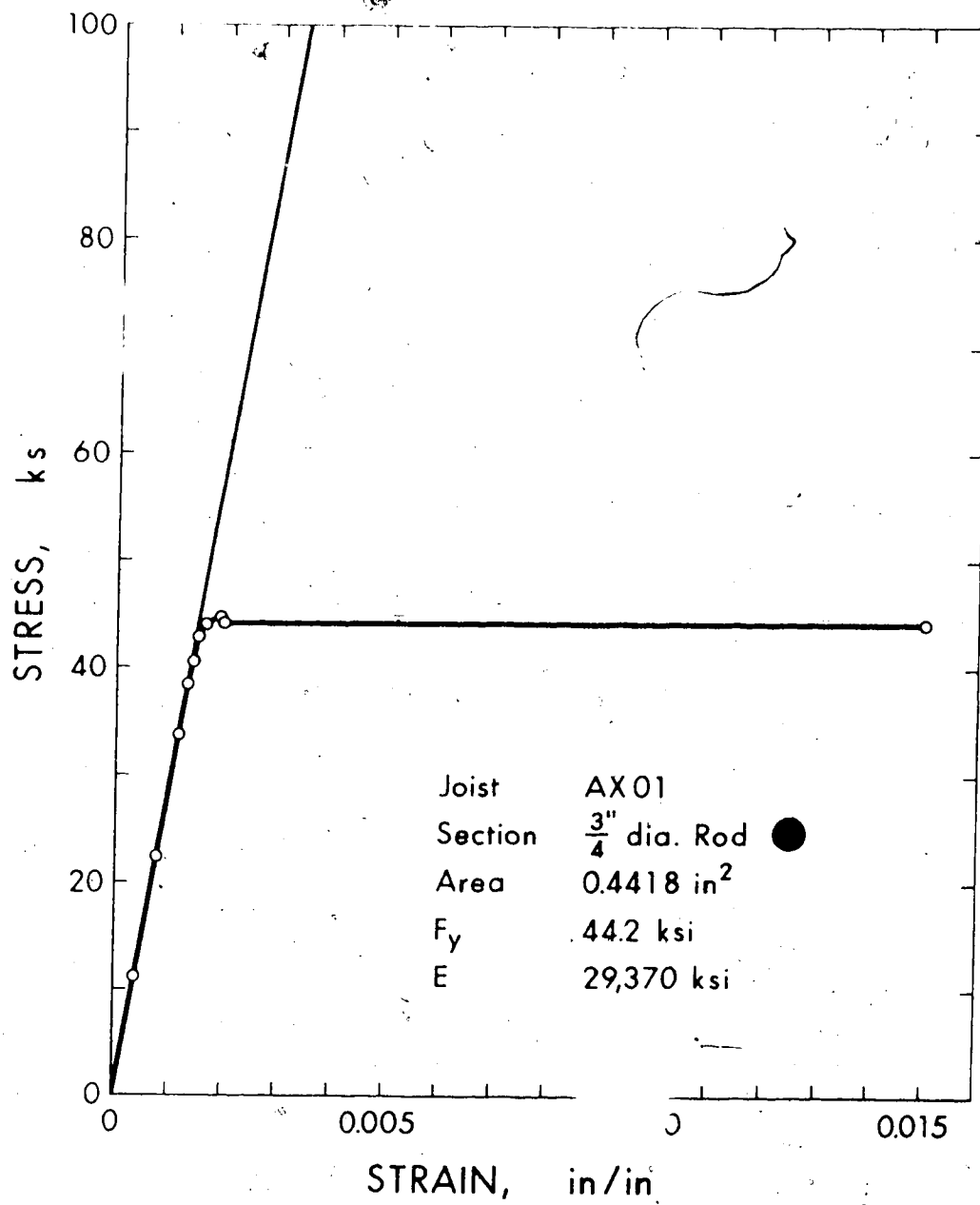


Fig. 4.15 Stress Strain Curve - AX01 & AX02 3/4" Rod

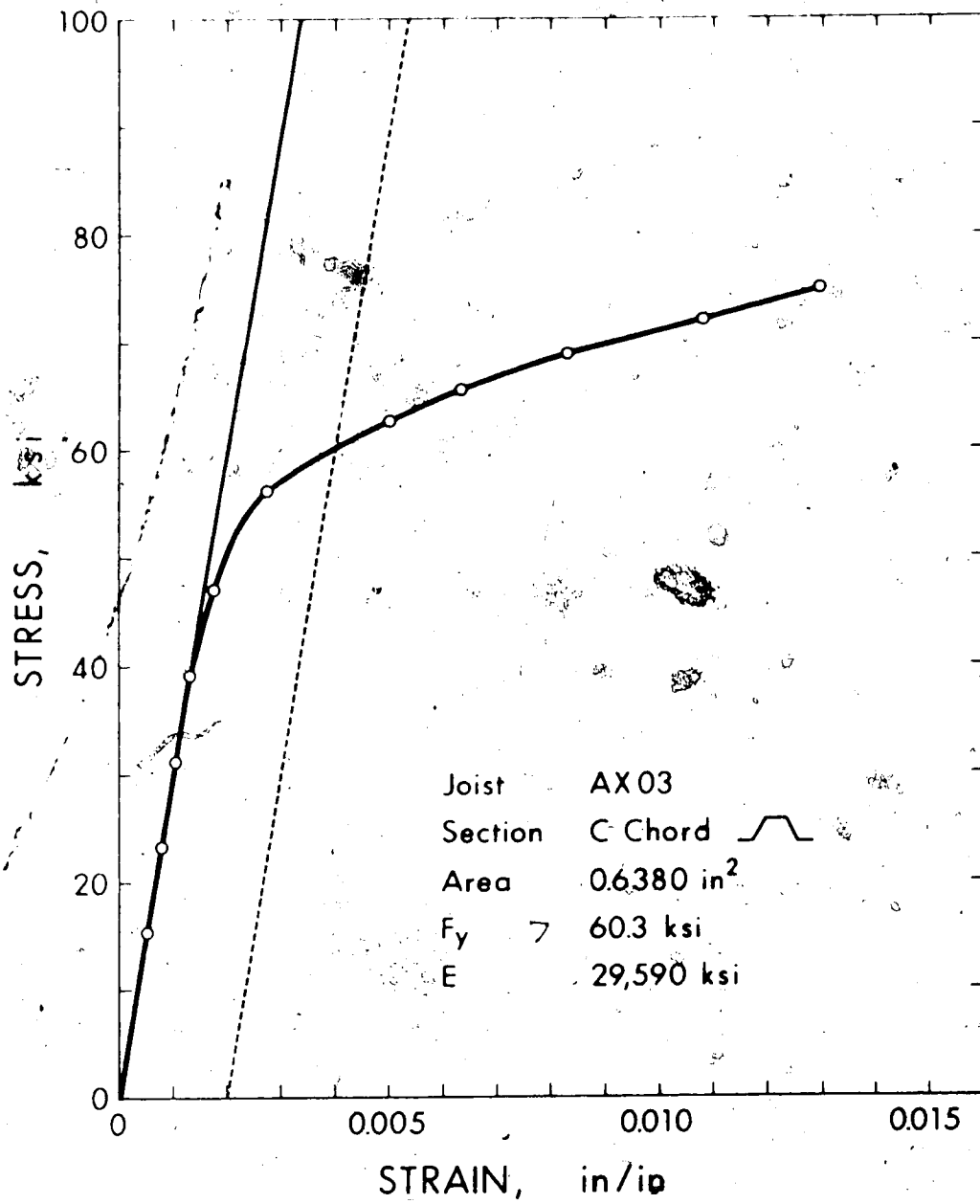


Fig. 4.16 Stress Strain Curve - AX03 & AX04 C Chord

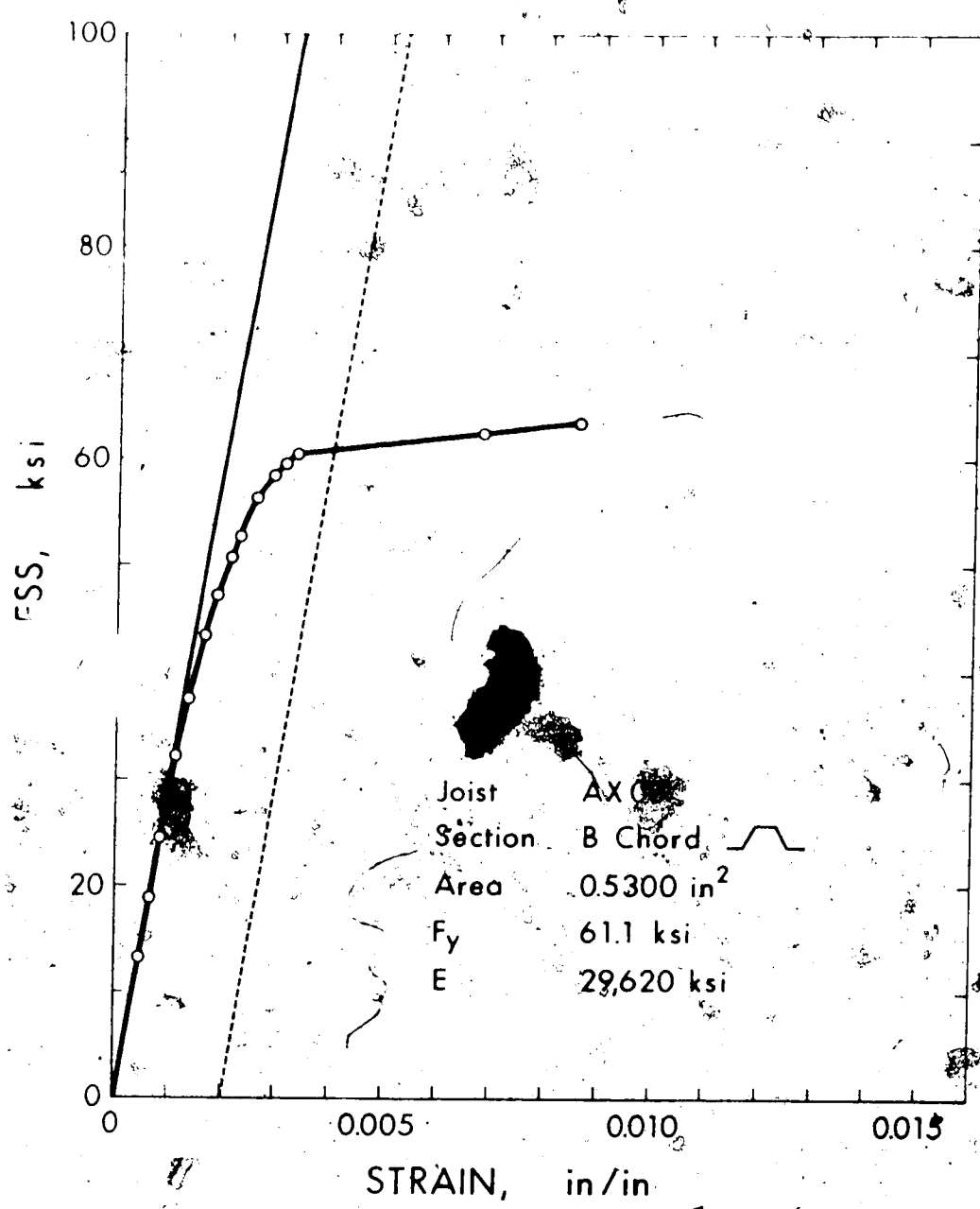


Fig. 4.17 Stress Strain Curve - AX03 & AX04 B Chord

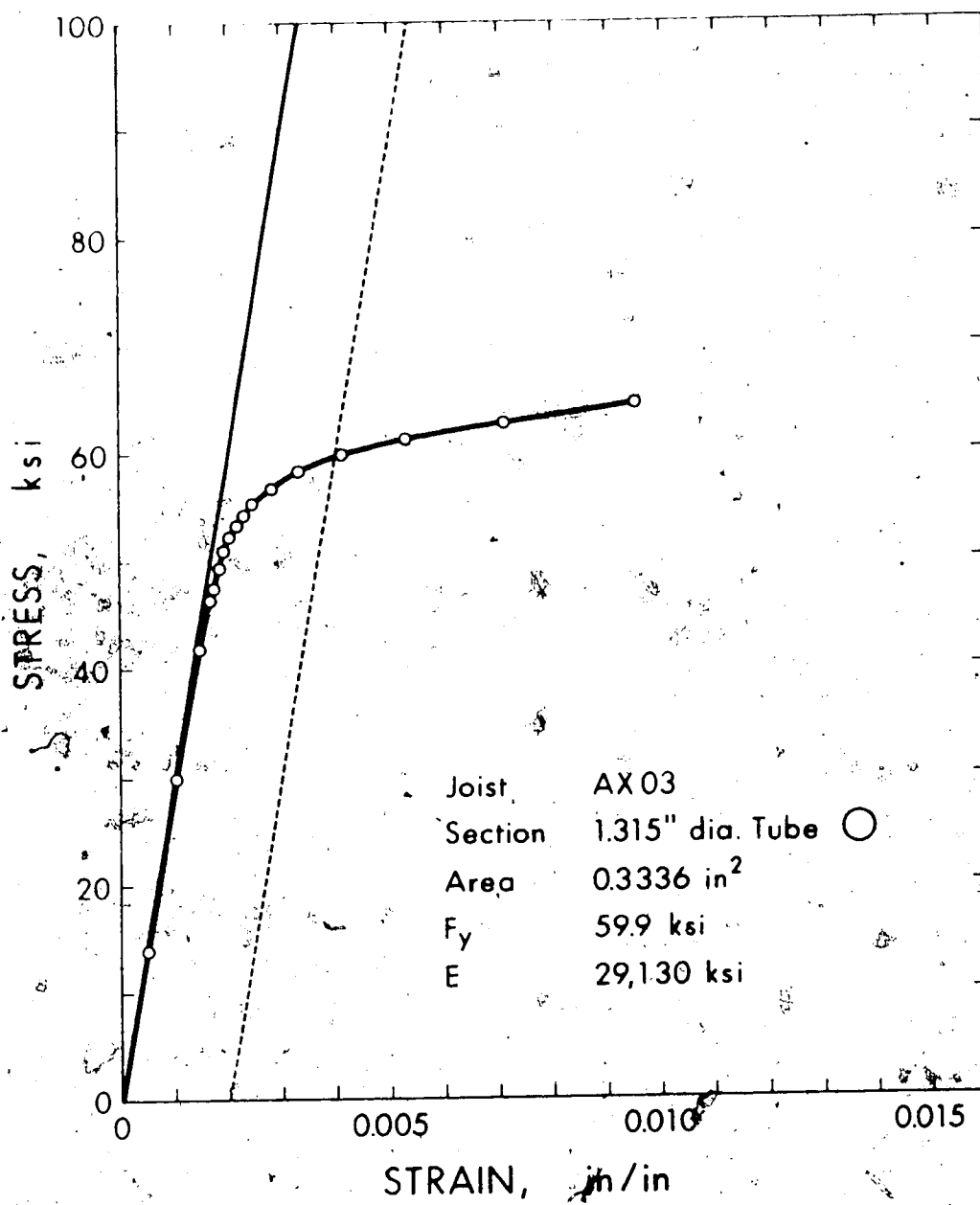


Fig. 4.18 Stress Strain Curve - AX03 & AX04 1.315" Tube

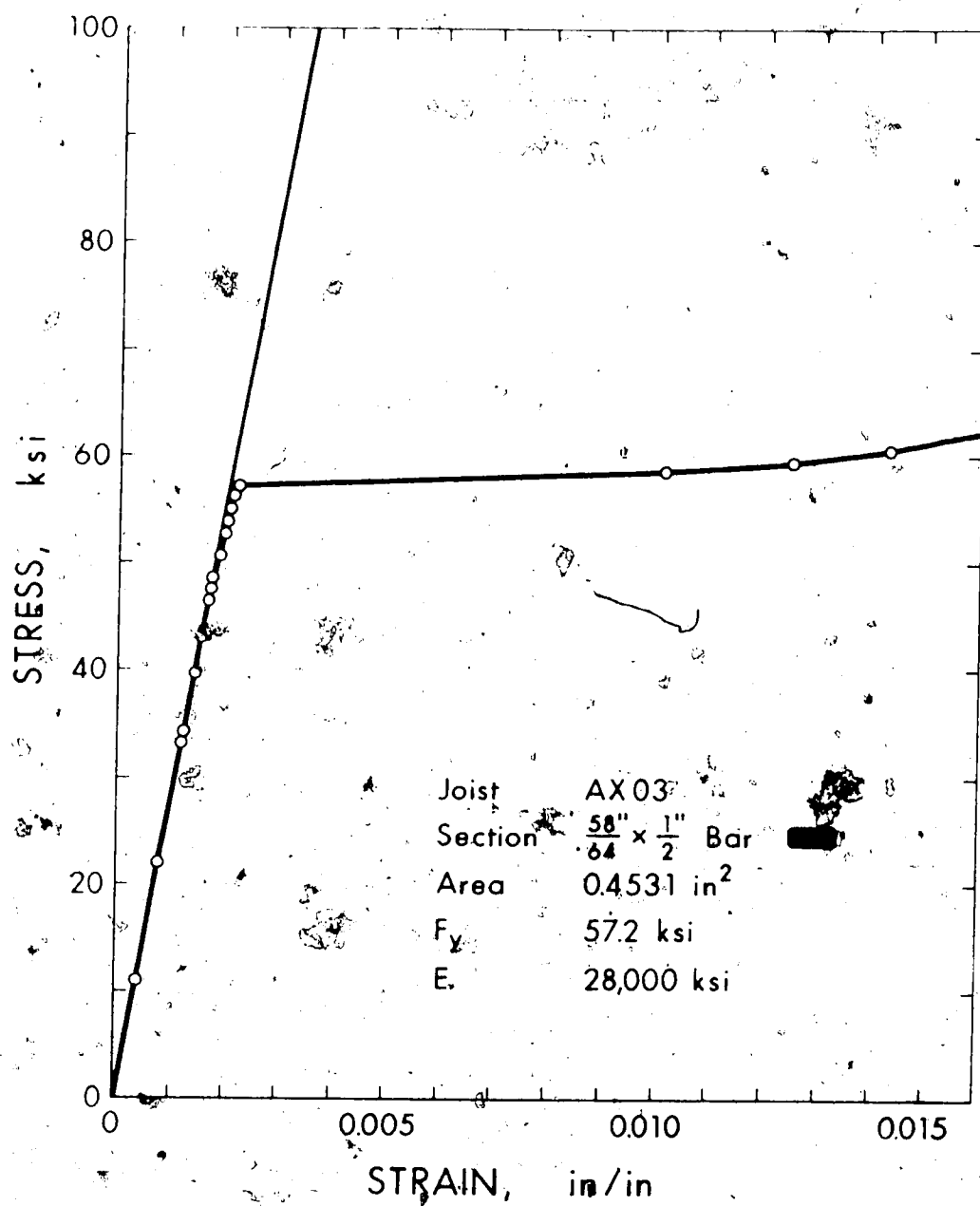


Fig. 4.19 Stress Strain Curve - AX03 & AX04  $\frac{58}{64} \times \frac{1}{2}$  Bar

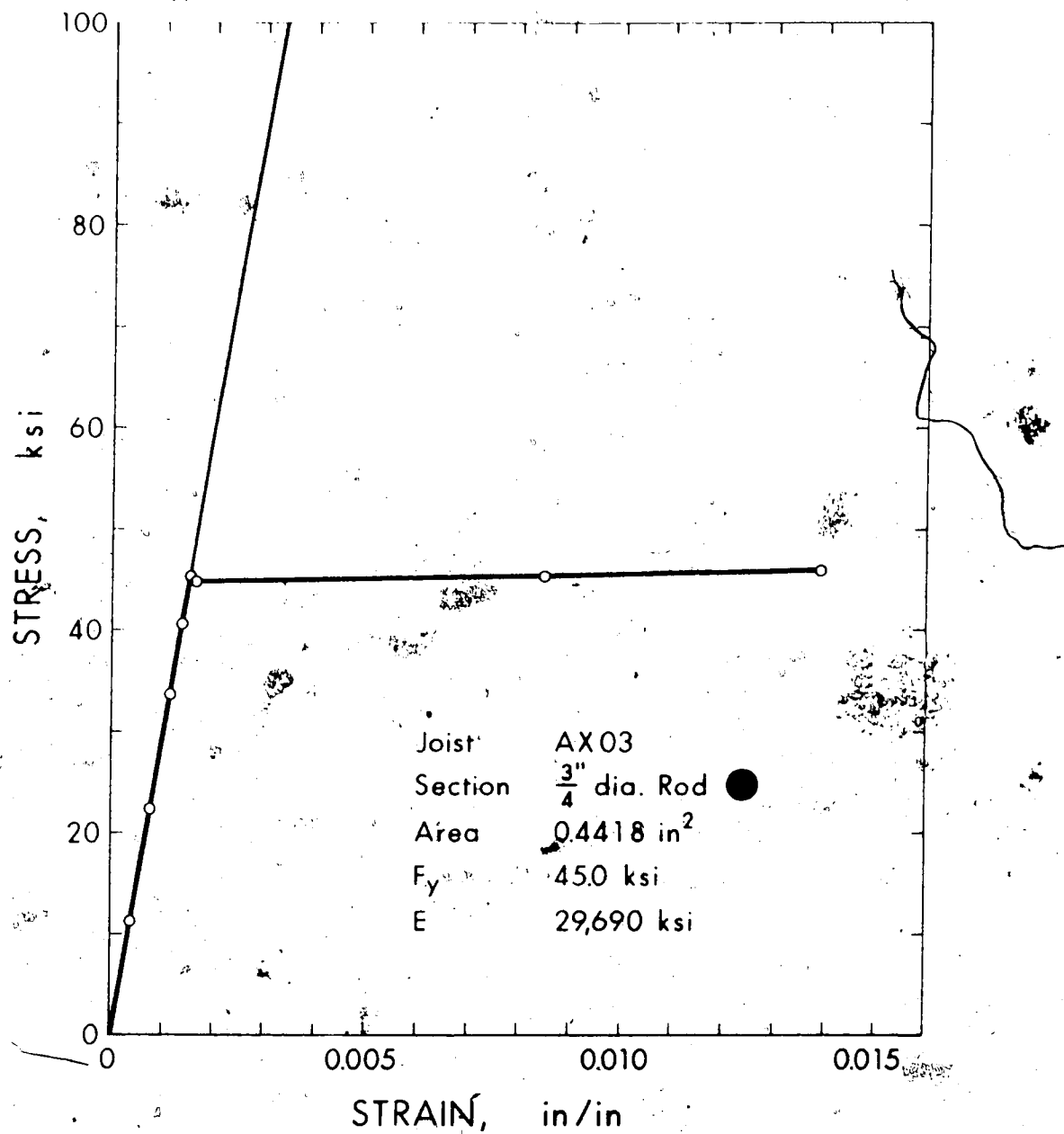


Fig. 4.20 Stress Strain Curve - AX03 & AX04  $\frac{3}{4}$ " Rod

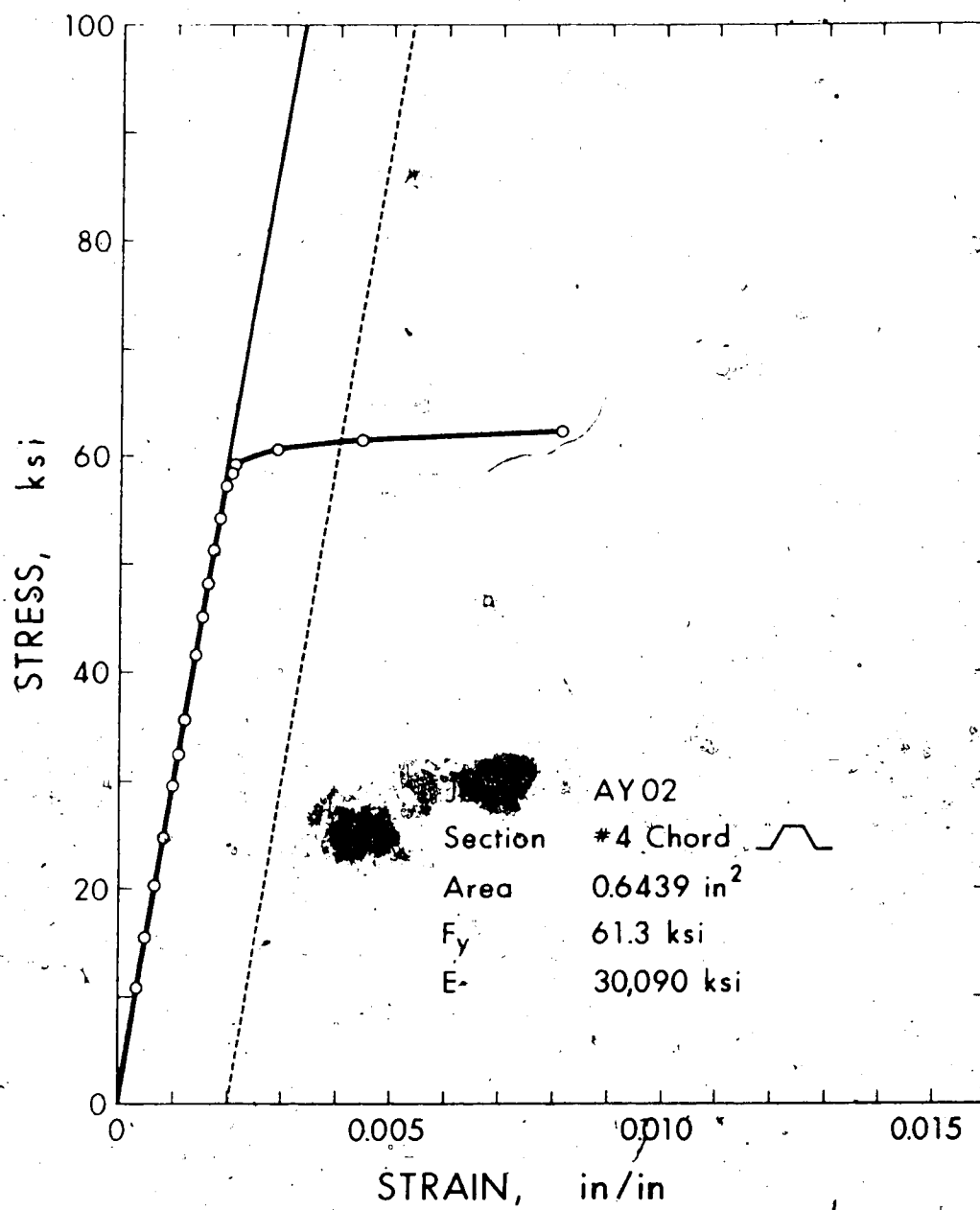


Fig. 4.21 Stress Strain Curve AY01 & AY02 #4 Chord

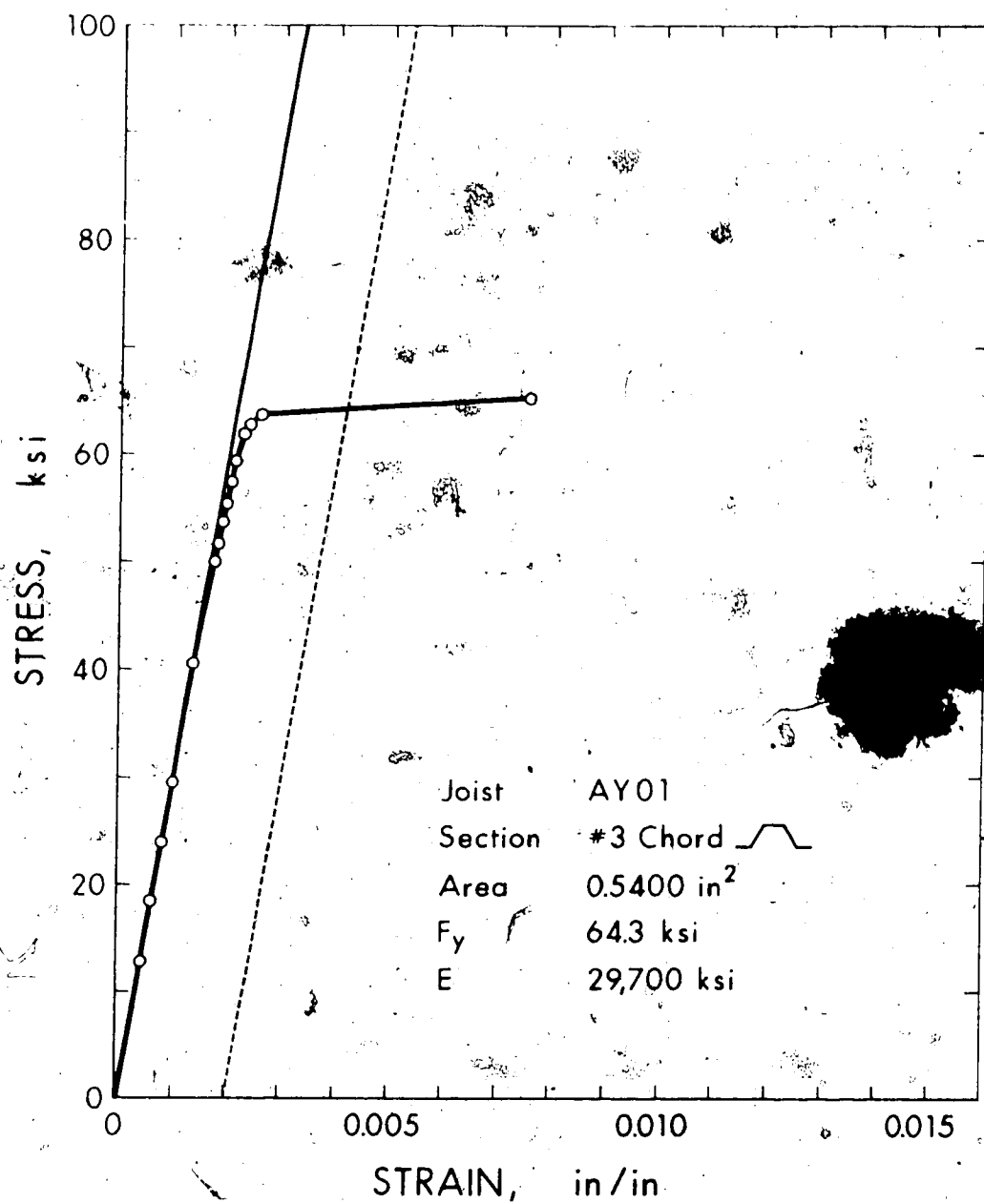


Fig. 4.22 Stress Strain Curve - AY01 & AY02 #3 Chord

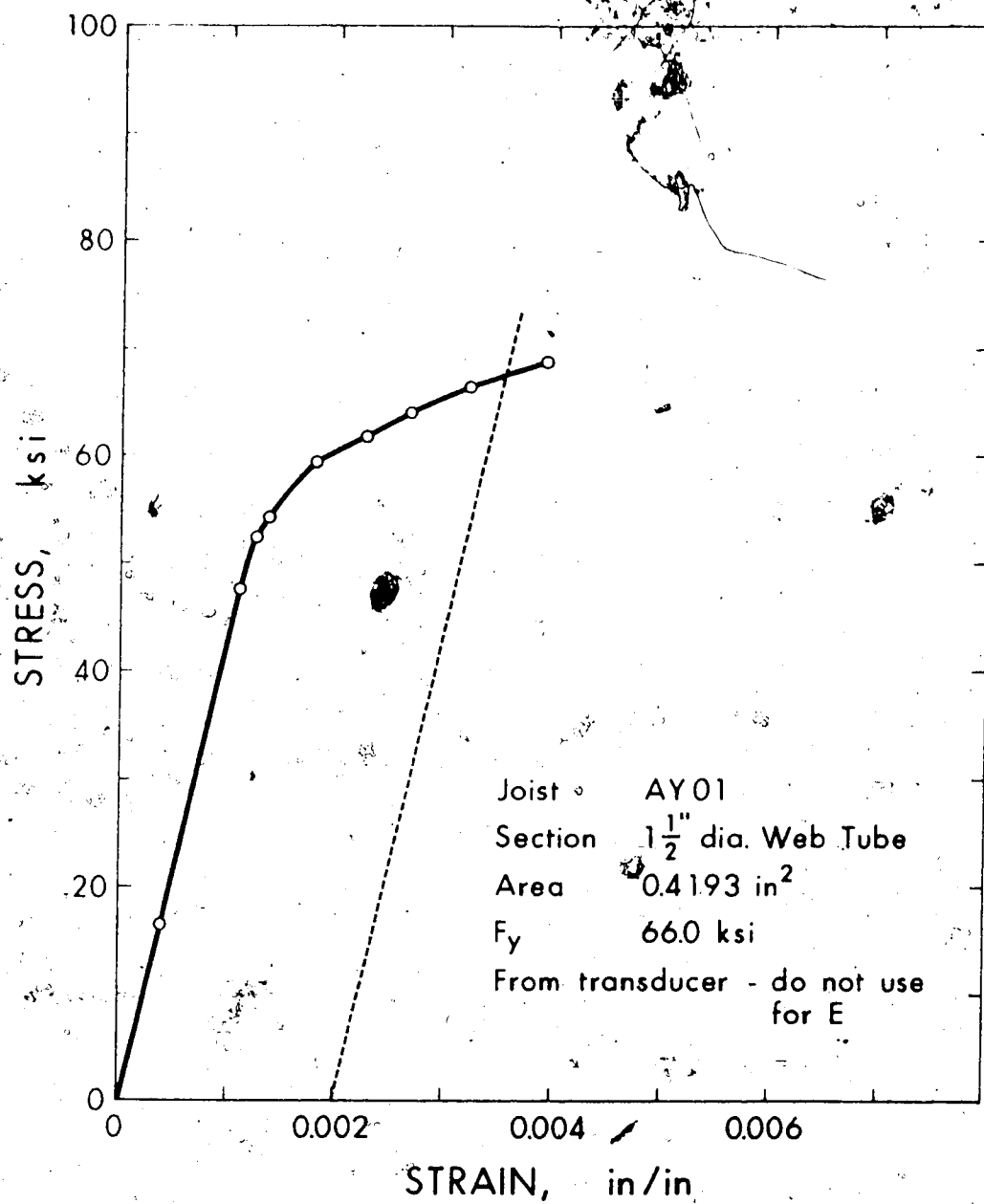


Fig. 4.23 Stress Strain Curve - AY01 & AY02 1 1/2" Tube

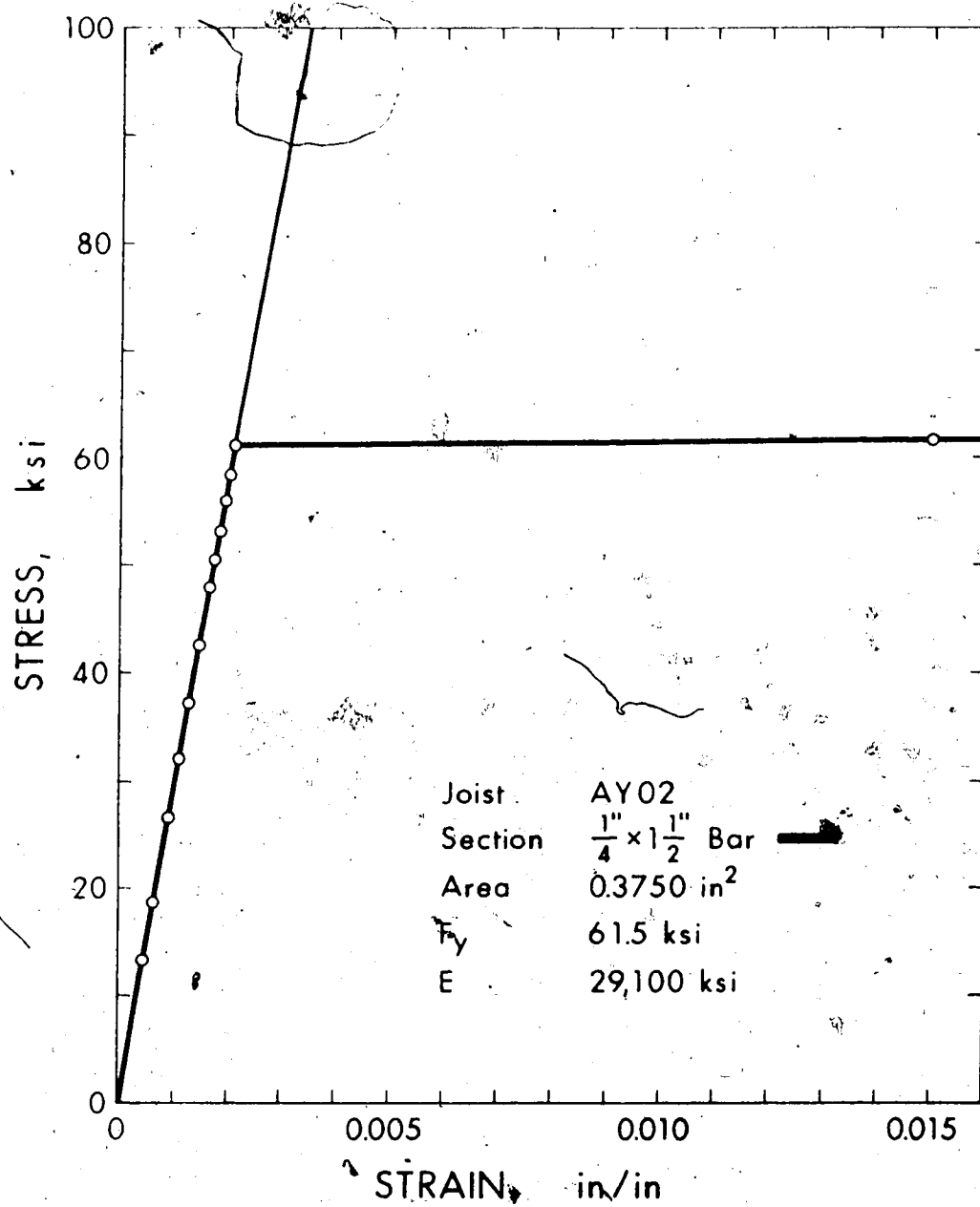


Fig. 4.24 Stress Strain Curve - AY01 & AY02  $\frac{1}{4} \times 1\frac{1}{2}$  Bar

## CHAPTER V

### DISCUSSION OF RESULTS

#### 5.1 Comparison of Measured and Predicted Values

The elastic analyses of the test joists described in Chapter 3 gives all joint displacements, member forces and moments. In the joist tests a few selected joint displacements, the forces in one half of the joist were measured. The results of both are presented in Chapter 4 and are discussed below.

##### 5.1.1 Deflections

The load deflection plots of the test joists are given in Figs. 4.3 to 4.8. From these plots, the planar frame analysis is seen to give the best agreement with measured values although, in all cases, the frame analysis is stiffer than the actual joist response. It is important to note, however, that the predictions of stiffness by the frame analysis are as accurate for the joists with eccentricities (X-type joists) as for joists without significant eccentricities (Y-type joists). Thus the difference between observed and predicted behavior is due to factors ignored by this analysis such as residual stresses due to welding, shear stresses in individual members, initial out-of-straightness of members, and joist camber rather than the inability to model the elastic behavior of the joists with eccentricities.

From Figs. 4.3 to 4.8 it seems reasonable to conclude that if the actual joist geometry, member properties and loading are known, the stiffness of a joist with positive joint eccentricities can be calculated by an elastic analysis by modelling the eccentricities as distinct frame

members. For the joists tested in this study, shear deformations were ignored without significant loss of accuracy.

The predicted joist deflections using the modified beam stiffness procedure as outlined in the CSA Standards were in all cases significantly lower than those observed. This difference can be attributed to two main causes.

The first is the allowance of ten percent to account for axial deformations in the web members. An elastic frame analysis with pin-ended web members was run on a Y-type joist for which the axial stiffness values for web members was made very large, the chord stiffnesses remained unchanged. The midspan deflection was found to decrease by twenty percent compared to the deflection computed using actual member stiffnesses. This would indicate that the midspan deflection in the test joists due to axial deformations in the web members is twice that assumed by the recommendations in the CSA Standards.

The second cause is the reduction of the moment of inertia in the end panels due to the terminating of the bottom chord at the first vertical web member. Due to the geometry chosen for these pilot joists the end panels are 27 percent of the joist span resulting in an over-estimation of the flexural stiffness if the equivalent beam is assumed prismatic.

It is readily seen that for joists with greater span to depth ratios, corresponding to those used in practice, the effects of increased deflection due to the above two causes would be reduced considerably and a better agreement between observed and predicted values using the procedure outlined in the CSA Standards would be achieved. This was found to be so in the tests reported by Olfart and Lenzén (1) and Kennedy

and Rowan (2) in which the test joists had span to depth ratios representative of those used in practice. The agreement between observed and predicted deflections using this method was good.

Fig. 5.1 shows the variation of joist deflections with increasing joint eccentricities as predicted by the elastic analysis. Although the eccentricities do increase the deflections, this increase is not significant until the eccentricities are well above the levels that would be expected in practice. Since the joists in this study were designed to accentuate greatly the effects of eccentricities, it could be expected that for joists with normal span-to-depth ratios, eccentricities would have little effect upon deflections in the elastic range.

While the effect of joint eccentricities on the total joist deflection is small, it appears that there is some increase due to the initiating of yield at lower load levels. This is indicated in the load deflection plots, wherein the difference in agreement of predicted joist deflection with actual deflection is seen to depend upon whether the comparison is made with the initial tangent curve or one of the unloading branches of the load deformation curve. In joists with negligible eccentricities this difference was small.

#### 5.1.2 Axial Forces and Bending Moments

Tables 4.7 to 4.11 show the comparison of measured and calculated stress resultants. For all joists the agreement between calculated and observed axial forces is good. As could be expected, those members carrying larger axial forces tended to have smaller coefficients of variation in the readings, and also show better agreement with calculated values.

A measure of the reliability of the strain readings is the agreement in the value of axial force obtained from the two sets of gauges located at opposite ends on any one member. If the two sets of gauges do not indicate the same force, then one set, or both, have a faulty gauge. For most members, the agreement of the two gauge locations is good.

The agreement of observed bending moments with those predicted by analysis is not as good as the agreement between axial forces. Nevertheless, for joists with significant joint eccentricities such as AX01, AX02 and AX03, the agreement can be considered acceptable. This can be seen from Fig. 4.9 in which the measured bending moment values for joist AX01 are plotted on the bending moment diagram obtained from the elastic frame analysis.

One notable exception in Fig. 4.9 is the shape of the measured moment diagram in the end panel (Member 1T). This deviation from the predicted moment diagram can be explained by the discontinuity as member 1T changed in size as shown in Fig. 3.1. This had the effect of introducing a counter-clockwise moment at the point of discontinuity which affected the strain gauge readings, but was not modelled in the analysis.

The percentage agreement between calculated and observed moments in the AY joists are not nearly so good as in the AX joists, but since these moments are of smaller magnitude these differences are not significant.

It may be concluded that given the joist geometry including joint eccentricities and loading, the resulting axial forces and bending moments can be calculated by a frame analysis.

## 5.2 Failure Modes and Ultimate Strength

The failure loads and the load factors provided by the test joists are summarized in Table 4.12. The load factors are based both on panel point forces at failure and mid span moments at failure, with the latter accounting for the actual spans of the test specimens.

Table 4.12 also summarizes the failure modes. For the joists tested, three distinct modes of failure were observed. These failure modes were influenced by the joint eccentricity, the type of loading and the manufacturing details.

Joists AY01 and AY02 were essentially identical except for the method of loading. Joist AY01 was loaded on the top chord by a two point loading system to simulate a uniform distributed loading of the top chord. Joist AY02 was loaded at the panel points only. Both joists failed by buckling of the top chord in the panel adjacent to midspan, member 5T.

The load at failure for joist AY02 was 2830 lbs/jack and for joist AY01 was 2620 lbs/jack. This difference of 7.4% can be due only to the method of loading since all other factors were as identical as possible. There was also a noticeable difference in the shape of the top chord during the later stages of loading. This is again attributed to the method of loading.

Before loading, in both joists, the top chord was deflected downward between panel points due to welding stresses in fabrication, but the magnitude of these initial displacements was very small (about .02 to .03") with the top chord appearing almost straight to the naked eye. As joist AY02 was loaded, the top chord assumed a single curvature profile. Thus, despite the fact that the welding stresses tended to put

each panel into double curvature, under axial force the top chord changed from its initial profile and buckled in single curvature. This is not in accordance with observations made by Rowan and Kennedy. They concluded that if all welds were on the same side of the neutral axis of the top chord, this being the case here with all welds being at the same level on the underside of the chord, then the top chord would buckle in double curvature. There are two possible reasons for this difference in failure configuration of the top chord. Firstly, due to the nature of the joint, the welding stresses in joist AY02 were very small, and the resulting deformations were too small to affect the buckling of the chord. Secondly, the joists tested by Rowan and Kennedy had a much larger span to depth ratio and so would have had much larger deflections for the same loading. Since compatibility moments are proportional to deflection, and since they also tend to deflect the top chord downward between panel points thereby enhancing the effect of the welding stresses, the combined effects would increase the chances of having the chord buckle in double curvature.

The top chord of AY01 was forced by the loading arrangement to take the shape shown in Fig. 5.4. Thus, while the two point load system imposed bending moments on the top chord which reduced the ultimate capacity of the joist, this was partially offset by the change in buckling shape of the critical member.

Joists AX01, AX02 failed by buckling of the top chord member 3T. This is not the critical top chord member in terms of axial load. The effect of the joint eccentricities was to produce bending moments in the top chord which are a function of the shear force carried by the web members framing into the eccentric joint adjacent to the chord member

in question. For the geometry of both joists, the combination of moment and axial load in member 3T was more critical than that in 5T.

It is unlikely that moments caused by eccentricities could in fact shift the critical top chord member toward the reaction in joists of more normal span to depth ratio. This can be demonstrated by considering specific limits for actual joists. The shortest span listed in the manufacturers catalogue for a joist having the same depth and chord size as used in the test joists is 38 feet. The allowable load for such a joist is 282 lb./ft. Treating the test joist as a simple beam the joint which caused failure had a shear force of 5.06 kips and a moment of 515 in.-kips at the design load of 843 lb./ft. For a span of 38 feet with a design load is 282 lb./ft., the shear force at the location where the moment is 515 in.-kips is 3.24 kips; or conversely the moment at the location where the shear is 5.06 kips is only 37 in.-kips. Thus the combination of high shear force and large eccentric moment which occurred in member 3T is very much restricted to the particular geometry of the test joists.

McDonald (3) and Lenzen (4) came to a similar conclusion by loading a joist with two point loads. The chord members inside the load points carried the highest axial forces, but the web members carried no shear forces. Failure occurred just outside the load point, where both moment and shear were high. Although some joint eccentricity existed in this region, the authors concluded that their loading case was extreme, and that eccentricities would not affect buckling of the top chord under uniform loading.

Joists AX01 and AX02 were both loaded on the top chord to approximate uniform top chord loading. The joist geometries were ident-

ical except that the joint eccentricities for joist AX02 were approximately 30% greater than for AX01. The difference in ultimate load capacity is therefore attributed only to the effects of the different joint eccentricities. This increase in joint eccentricity resulted in only a 5% reduction in ultimate load capacity.

Joists AX03 and AX04 were of similar geometry to AX01 and AX02, respectively, except that the bottom chord in joists AX03 and AX04, instead of being attached to the top chord as was the case for AX01 and AX02, was a separate section. In addition, joists AX03 and AX04 were loaded at the panel points. These differences combined to give a different failure mode. Both AX03 and AX04 failed by the formation of a plastic hinge mechanism at the end joint of the bottom chord.

The failure diagram for this joist is shown in Fig. 5.5. At this point the total shear force in the joist, except for the small portion carried by the top chord which can be neglected, is carried by the eccentric member at the end of the bottom chord. At failure, the sum of all the moments of the forces about point A must be equal to the sum of the resisting moments in the members framing into the joint. Based on determining the plastic moment capacity of each member neglecting the axial force in the member, the agreement between calculated failure moment and the sum of ultimate resistance moments is good.

At failure the end compression diagonal member 3W, in joists AX03 and AX04 had yielded over most of its length under axial load and bending and after failure was completely distorted in lateral buckling. For this reason no material properties could be obtained for this member, and these members were assumed to be identical with member 3W in AX01 and AX02. In computing effects all changes in geometry of the joint as

yielding and rotation took place where ignored. At failure, changes in geometry could have been significant in computing member forces.

As stated earlier joists AX01 and AX03 were identical except for the method of loading and the smaller bottom chord for joist AX03. The same relationship also applies to joists AX02 and AX04. Since the mode of failure of joists AX03 and AX04 was completely different from that of AX01 and AX02 it was not possible to tell whether this difference was due to the method of loading or due to the reduced plastic moment resistance of the bottom chord to prevent formation of a plastic hinge. To answer this question an additional joist AX05 which was not originally envisioned as part of the pilot study was fabricated and tested.

Joist AX05 was as close to the geometry of AX01 as possible but was loaded at the panel points. Thus the differences in behavior of joist AX01 and AX05 would be attributable to the method of loading. Joist AX05 failed in the same mode as joist AX01, that is buckling of the top chord in member 3T. Comparing applied loads at failure the ultimate load capacity of joist AX05 was 7.5% greater than for joist AX01. It is interesting to note that this is essentially identical to the increase in load carrying capacity observed for the Y-type joists when loads were applied at panel points only rather than along the top chord to simulate top chord loading and confirms the findings of Kennedy and Rowan (2).

A joint mechanism type failure would have occurred in joist AY01 at the end of the top chord due to the 2 inch eccentricity of the support. To avoid this, the reaction blocks were moved over to reduce the eccentricity to a negligible amount as described in Sec. 2.2.1. This type of failure mechanism gives a determinable upper bound on the capacity of an eccentric joint; the moment generated by a joint cannot

exceed the sum of the plastic moment capacities of the members framing into that joint.

There was one common characteristic in all the joint tests. At no time was any distress observed in the joints themselves, despite the high shear stresses on them. It is unlikely that in joints with typical span to depth ratios that shear stresses as high as those imposed by the tests would exist. This can be illustrated by again looking at the X-type joints. Fig. 5.6 shows the maximum shear force obtained by treating the joist as a simple beam. Allowable loads and shear forces were calculated as follows:

Let  $P_a$  be the allowable axial force in the top chord

$d$  = depth of joist-ft

$w$  = allowable load - kips/ft

$L$  = span of joist-ft

$$\text{Moment of span} = \frac{wL^2}{8}$$

$$P_a = \frac{wL^2}{8d} \quad w = \frac{8P_a d}{L^2}$$

$$\text{Max. shear} = w \times \frac{L}{2} = \frac{4P_a d}{L}$$

From Fig. 5.6 it can be seen that for the test joists chosen, the short span chosen caused much higher shear stresses than would be encountered in normal spans.

### 5.3 Design Methods for Eccentricity

As mentioned in the literature survey in Chapter 1, a publication by the Steel Company of Canada Ltd., "Hollow Structural Sections" Design Manual for Connections" (9) includes a design method for stresses caused by joint eccentricities. This method includes a simplified

analysis as follows.

The eccentric moment generated at a joint is equal to  $(P_{CR} - P_{CL}) e_1$  where  $P_{CR}$  and  $P_{CL}$  are as defined in the Nomenclature. This moment is distributed equally to the chord members on either side of the joint if the flexural stiffness of the chords on either side are within 50% of each other. The stresses caused by the combined axial forces and eccentric moments are then designed for on the basis of existing interaction formulas of the CSA S16-1969 Clause 17.1.1. It is also pointed out that equal eccentricities at joints under equal forces would cause the chord to buckle in the plane of the truss, with a point of contraflexure half-way between joints. Thus, when checking for stability effects, the allowable compressive stress should be based on an effective length of one-half the panel length. In the formulation of this design procedure, it has been assumed that no transverse loads are applied to the member in question.

There are a number of reasons why this design procedure cannot be used to account for the effects of joint eccentricity in open web steel joists. The design procedure distributes all eccentric moment at a joint into the chord members only. In the joists with significant eccentricities in this study the web members were fully fixed to the chords and contributed to resisting the eccentric moments in proportion to their relative stiffness.

The assumption in the design procedure that there are no transverse loads applied to the chords generally means that the point of contraflexure will be near the midspan of the panel. Since by definition, the compression chord of a steel joist carried transverse loads the buckling shape obtained by assuming a point of contraflexure on eccen-

tricies alone will not apply to the top chord of a joint.

A procedure is given for the design of compression chords in CSA S16-1969, Section 20.9.3 when the panel spacing exceeds 24 inches. This procedure includes a provision for accounting for the interaction between axial force and bending moment in the chord although it is implied that the moments result from the transverse loading of the chord. To investigate the applicability of these interaction formulae for chords of 24 inch length when the moments are caused by both eccentricity and transverse loading, the procedure was applied to the top chord members 3T and 5T for the X-type joists. The yield stress used was obtained from the material tests. The results of these analyses are given in Table 5.1.

Also given in Table 5.1 are the results for web member 3W. Since the provisions of Section 20.9.3 apply only to compression chord members, the interaction formulae from Section 17.1 were used.

The effective lengths used on the above calculations were as suggested in Section 20, that is 0.9 times the panel spacing for chord members and the clear length of the member between chords for the web diagonal. It would appear from the values in Table 5.1 that these interaction formulae are conservative particularly for the web diagonal. This would indicate that before an interaction formulae can be used a more rational means of determining the effective length of members in open web steel joists is required.

The test joists were designed to magnify the effects of joint eccentricity, and the low span-to-depth ratio also magnified the effects of transverse loading between panel points. Whether or not CSA S16-1969 design procedures would give better results for more typical joists is not readily apparent. A more comprehensive study is required to establish

the effects of eccentricities on the effective length of the joist members.

It is noted that the bending moments caused by transverse loading are ignored in current code procedures when the panel length is 24 inches or less. It would not be rational to attempt to account for moments caused by eccentricity in such cases when ignoring the moments due to other causes.

## INTERACTION EQUATION VALUES - AX JOISTS

| JOIST                                       | ax01 | ax02 | ax03 | ax04 | MEMBER |
|---|------|------|------|------|--------|
| $\frac{f_a}{0.60 F_y} + \frac{f_b}{F_b}$    | 1.04 | 1.07 | 1.08 | 1.22 | 3T     |
| $\frac{f_a}{F_a} + \frac{f_b}{F_b}$         | 1.16 | 1.31 | N.A. | N.A. |        |
| $\frac{f_a}{0.60 F_y} + \frac{f_b}{F_b}$    | 1.16 | 1.19 | 0.96 | 1.05 | 5T     |
| $\frac{f_a}{F_a} + \frac{f_b}{F_b}$         | 1.11 | 1.18 | N.A. | N.A. |        |
| $\frac{f_a}{0.60 F_y} + \frac{f_b}{F_b}$    | 1.76 | 2.34 | 2.07 | 2.38 | 3W     |
| $\frac{f_a}{F_a} + \frac{C_{max} F_b}{F_b}$ | 1.80 | 2.18 | 2.08 | 2.34 |        |

TABLE 5.1

YIELD LEVELS AND CROSS SECTIONAL PROPERTIES  
USED AS MEASURED FROM MATERIALS TESTS

K = 0.9 CHORD MEMBERS

KL = CLEAR LENGTH BETWEEN CHORDS FOR WEB MEMBERS

Table 5.1 Interaction Equation Applied to AX Joists

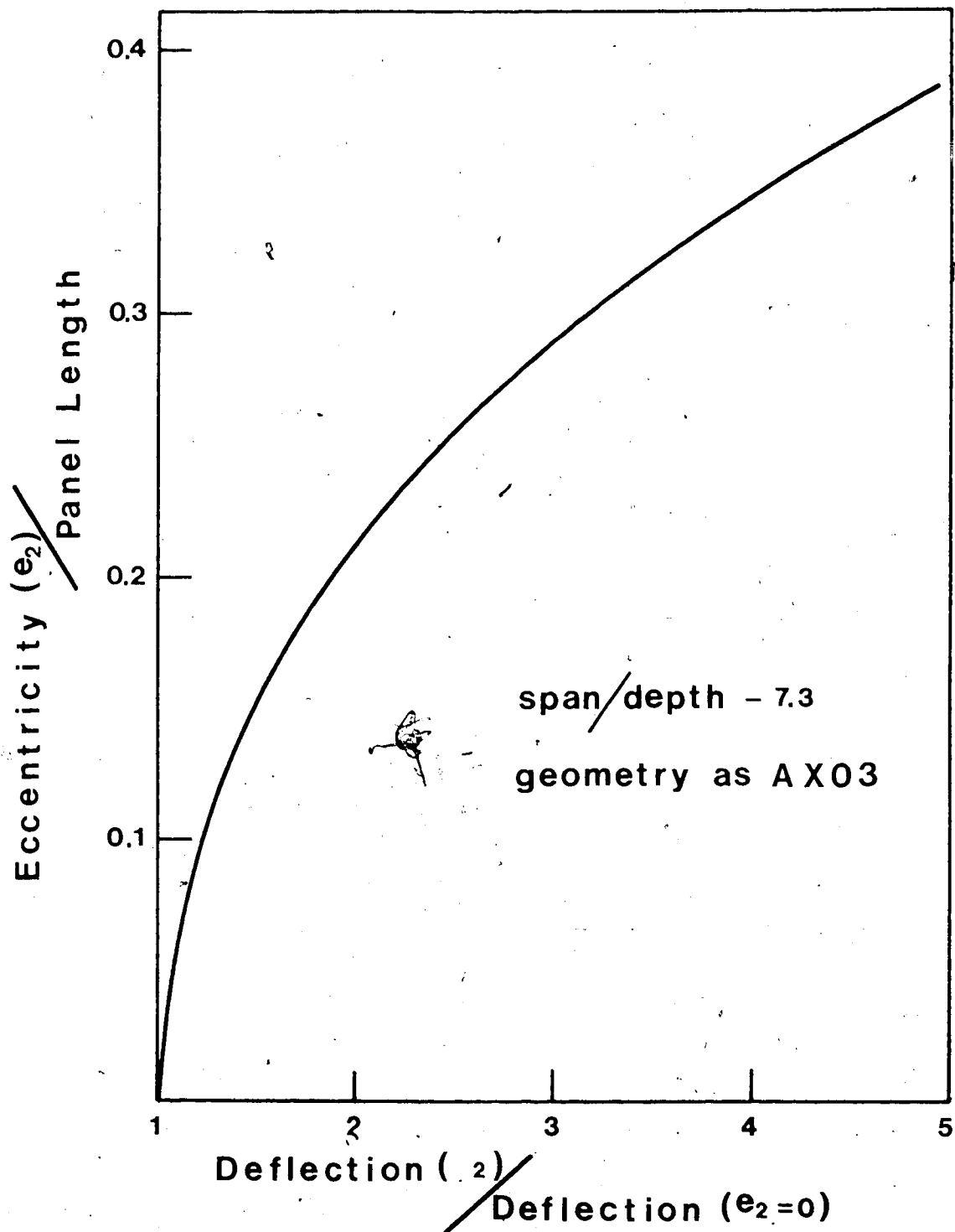


Fig. 5.1 Variation of Joist Deflections with Increasing Eccentricities

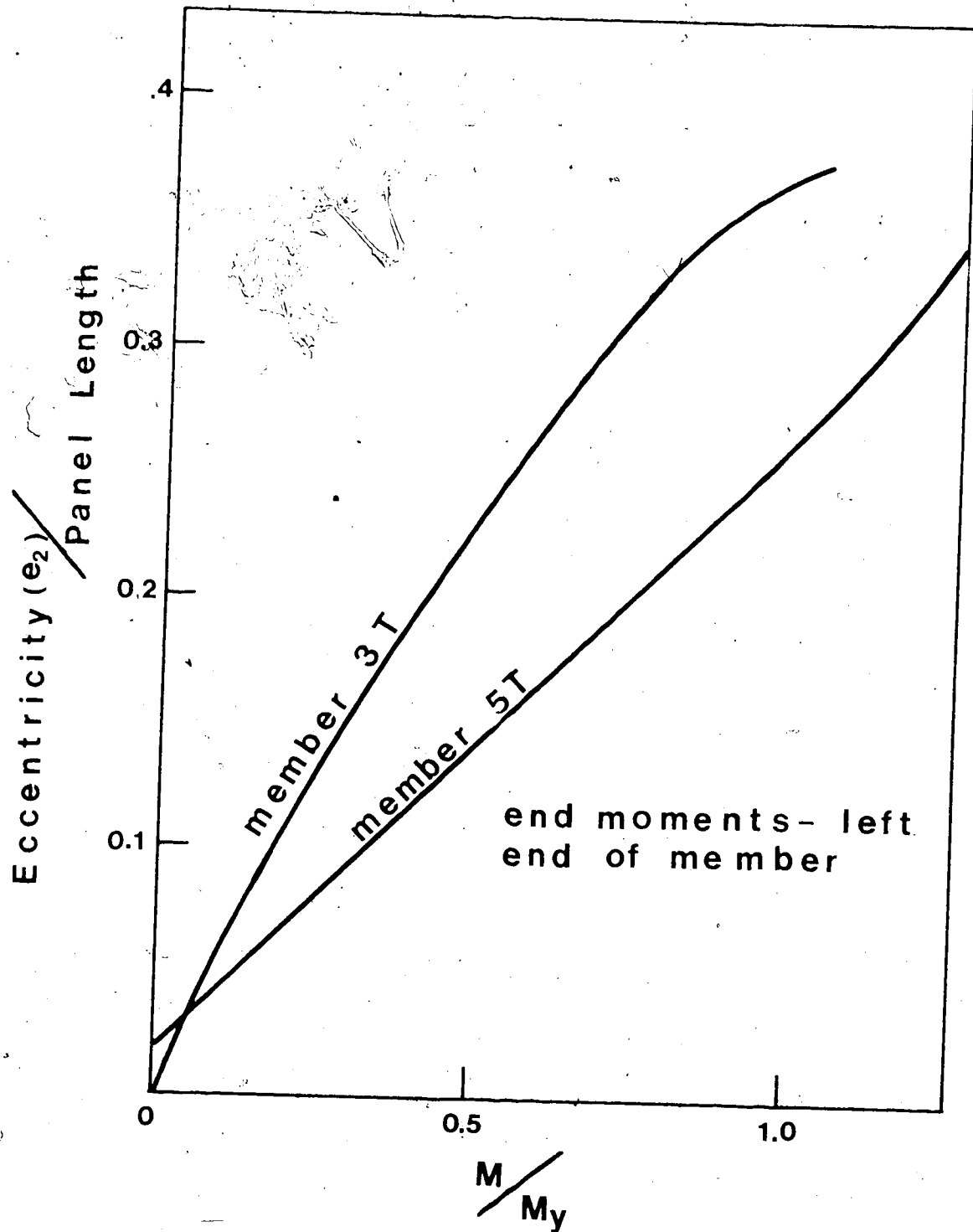


Fig. 5.2 Variation of Chord Bending Moments with Increasing Eccentricities

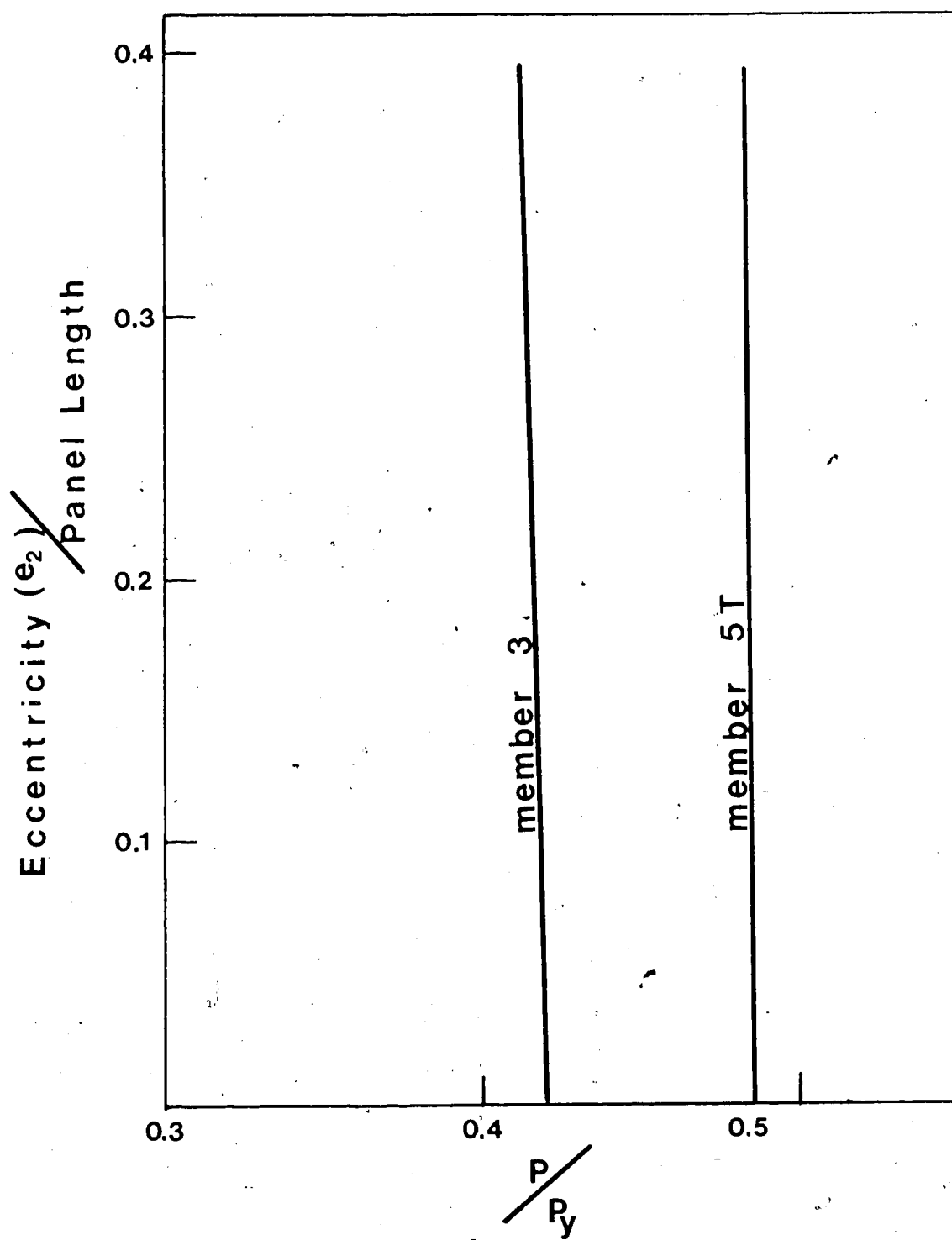
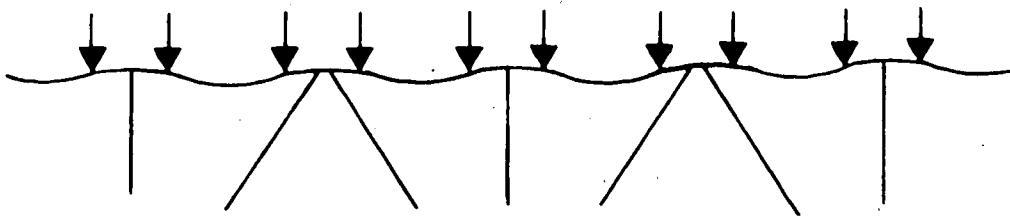


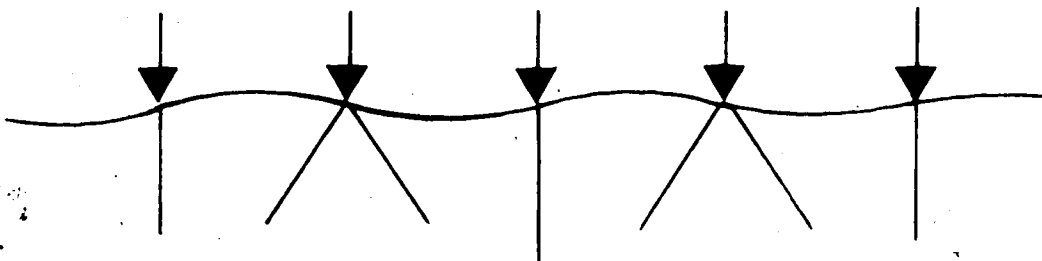
Fig. 5.3 Variation of Chord Axial Forces with Increasing Eccentricities



**Initial Shape AY01 & AY02**



**Buckling Shape AY01**



**Buckling Shape AY02**

**Fig. 5.4 Top Chord Profiles AY Joists**

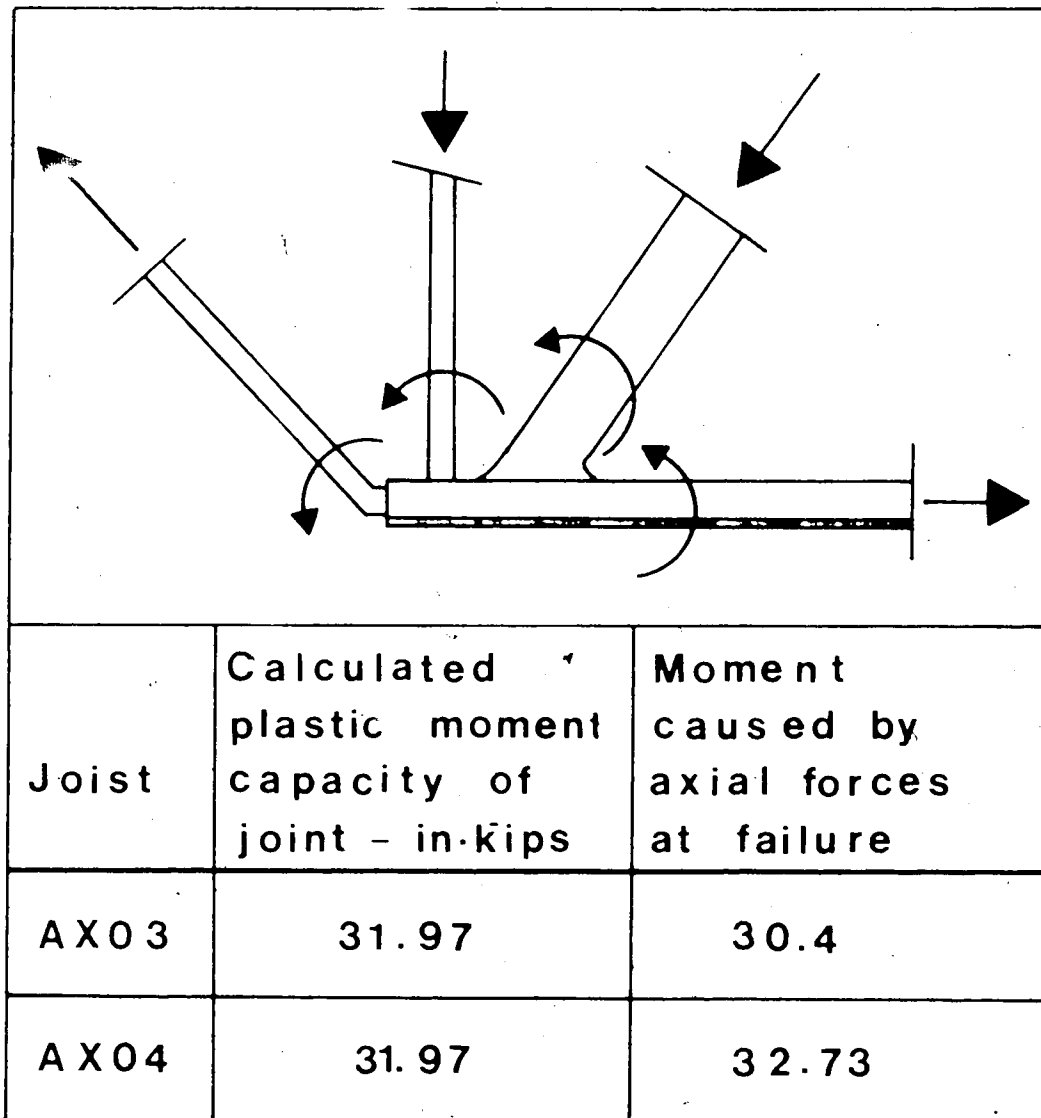


Fig: 5.5: End Panel Mechanism for AX03 and AX04

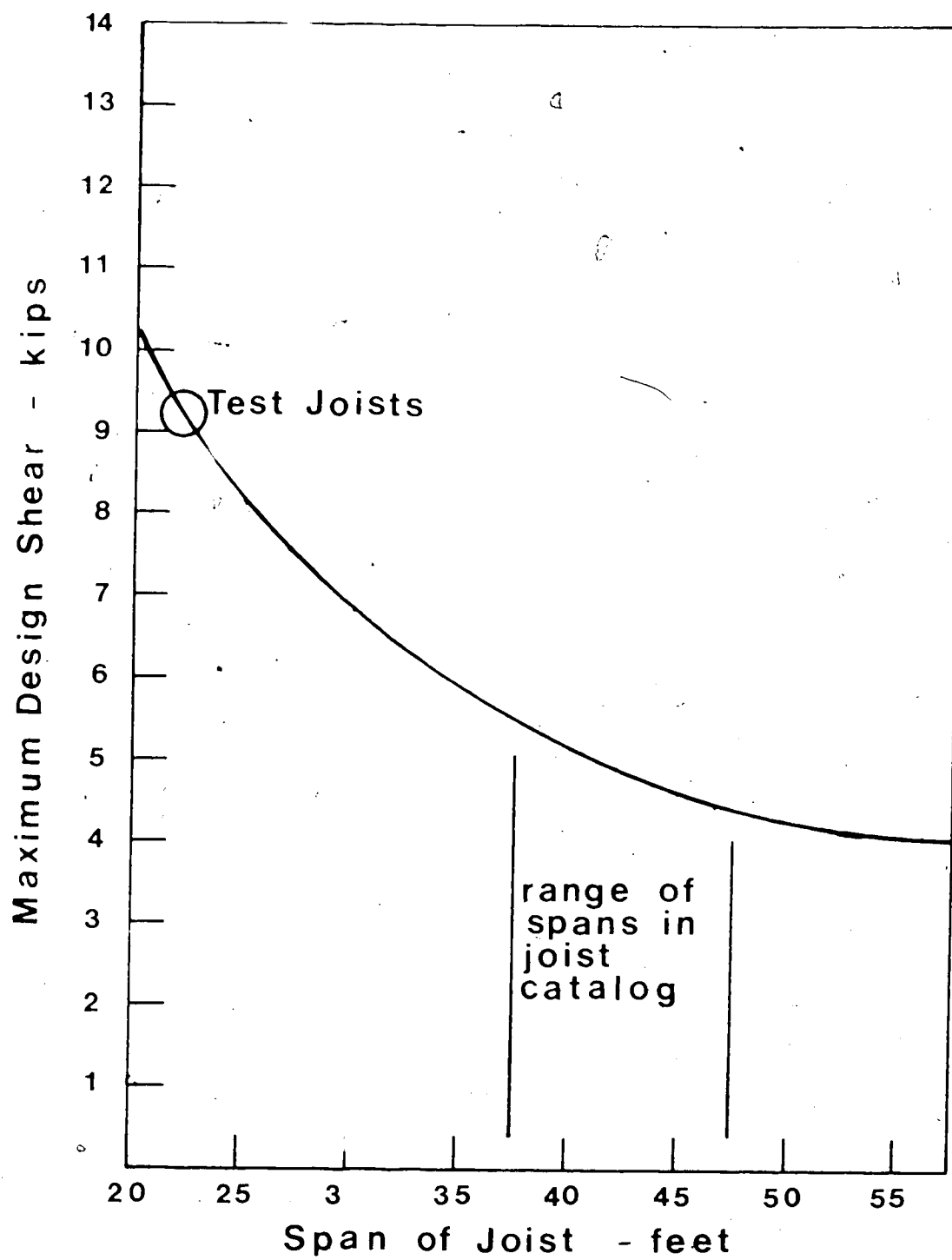


Fig. 5.6 Variation of Shear Force with Joist Span

## CHAPTER VI

## CONCLUSIONS

## 6.1 Conclusions From the Pilot Study

Six open web steel joists were designed to emphasize the effects of eccentricities. The joists were analyzed by an elastic first order frame analysis, and tested to failure. Measurements of axial forces, bending moments, and deflections were taken and compared to the values obtained from analysis. Based on the above work, the following conclusions can be made:

- 1) A satisfactory elastic analysis of a joist with eccentric joints can be obtained by considering the joint eccentricities as short frame members.
- 2) Joint eccentricities have a negligible effect on the axial forces in a joist.
- 3) For the magnitude of joint eccentricities expected in practice the elastic deflections of a joist are increased only negligibly.
- 4) The effect of joint eccentricities is to produce bending moments in the joist members. These moments do not affect the joint capacity, but can affect the axial force capacity of members framing into the eccentric joint.
- 5) In the test joists, the effect of joint eccentricities in decreasing the joist capacity was not as great as the effect of simulating the distribution of the panel point loading uniformly along the top chord.
- 6) At the ends of the joist, where the chords are discontinuous,

the corresponding drop in rotational stiffness coupled with the high shear, makes the joist very susceptible to eccentricities at these joints. The top "bearing" joint is mentioned specifically in the present CSA Standards. This clause should be expanded to include specifically the bottom end joint as well.

## 6.2 Further Research

The pilot study has isolated the major effect of eccentricities as a source of bending moments in joist members. Thus future studies are required to evaluate the axial force capacity of members framing into eccentric joints. This study should also include the effects of top chord loading, initial out-of-straightness of members, and joint details, as these factors have an important effect on effective lengths and buckling strength of joist members. From a qualitative evaluation of the AX test joists, which greatly exceeded the present limits of eccentricity set in the CSA standards, it appears possible that these limits may be relaxed. Due to the restrictive geometry of the test joists, however, further studies and testing are required to confirm this.

## LIST OF REFERENCES

1. Ohmart, R.D. and Lenzen, K.H., "Uniform Load Testing of Open Web Steel Joists". M.Sc. Thesis, University of Kansas, 1961. (Report No. 25, University of Kansas, 1968).
2. Kennedy, D.J.L. and Rowan, W.H.D., "Behavior of Compression Chords of Open Web Steel Joists". Research Report, The University of Toronto, 1963.
3. McDonald, W.S., "Inelastic Behavior of the Compression Chord of Open Web Steel Joists". Ph.D. Thesis, University of Kansas, 1966.
4. Lenzen, K.H., "Design Formulas for the Top Chords of Open-Web Steel Joists". Studies in Engineering Mechanics, Report No. 27, University of Kansas, 1968.
5. Leigh, J.M. and Galambos, T.V., "The Design of Compression Webs in Longspan Steel Joists". Research Report No. 21, Washington University, St. Louis, 1972.
6. Cran, J.A., "Design and Testing of Composite Open Web Steel Joists". Pg. 186-197 of "Proceedings of the First Specialty Conference on Cold-Formed Steel Structures", W.W. Yu, Editor, Department of Civil Engineering, University of Missouri-Rolla, 1971.
7. Hribar, J.A., Laughlin, W.P., "Lateral Stability of Welded Light Trusses". Journal of the Structural Division, Proceedings of the ASCE, ST3, March, 1968.
8. "Hollow Structural Sections, Welded Joint Research Summaries". Technical Report, The Steel Company of Canada, Limited, 1974.
9. "Hollow Structural Sections, Design Manual for Connections". Technical Report, The Steel Company of Canada, Limited, 1971.
10. Eastwood, W., Wood, A.A., "Welded Joints in Tubular Structures Involving Rectangular Sections". pg. 210-216, Ref. 8 above.
11. Beaufait, F.W., et al, "Computer Methods of Structural Analysis", Prentice-Hall, Inc., Englewood Cliffs, N.J., 1970.
12. CSA Standard S16.1-1974, "Steel Structures for Buildings - Limit States Design", Canadian Standards Association, Rexdale, Ontario, 1974.
13. CSA Standard S16-1969, "Steel Structures for Buildings", Canadian Standards Association, Rexdale, Ontario, 1969.

## APPENDIX A

The loading grid in the test bed of the structural laboratory is 2 feet by 2 feet, coinciding with manufacturers' normal panel lengths. Available hydraulic and jacking equipment limited loading points to 10. These considerations, along with planned instrumentation and the desire to test an intermediate span joist resulted in the geometry of test specimens shown in Fig. 3.3.

Table 3.1 shows the section properties for the lighter hat sections for the X joists. The top chord is usually one size larger than bottom chord. Thus the top chord chosen was C.

$$\frac{KL}{r} = \frac{.09 \times 24}{.422} = 51.18 < 90 \text{ (Sec. 20.9.2)}$$

$$F_y = 55 \text{ ksi}$$

$$C_o < \frac{KL}{r} < C_p$$

Thus  $F_a = 0.60 (55) - 0.175 (51.18 - 19) = 27.37 \text{ ksi (Sec. 16.2.2)}$

$$P_a = F_a \times A = 27.37 \times 0.638 = 17.46 \text{ kips}$$

where  $P_a$  is the allowable compressive force in the top chord.

The joist chosen was a 36C, actual depth (out-to-out) is 36.016 inches, with the distance between centroids of chords being 35.035 inches. This geometry was analyzed as a simple truss by a stiffness program. As the model is statically determinate, proper

value of member stiffness were not required. The value of the panel point load required to produce a compressive force of 17.46 kips in member 5T was calculated, from which the allowable uniform load of 0.843 k/ft. for X-type joists was obtained.

Due to differences in the shape of the hat sections used as chords, the equivalent Y joist had a slightly lower uniform load.

Top Chord is #4

$$\frac{KL}{r} = \frac{0.9 \times 24}{0.366} = 59.02 < 90 \text{ (Sec. 20.9.2)}$$

$$F_y = 55 \text{ ksi}$$

$$C_o < \frac{KL}{r} < C_p \quad F_a = 0.60 (55) = 0.75 (59.02 - 19) \\ = 26.00 \text{ ksi} \quad (\text{Sec. 16.2.2})$$

$$P_a = F_a \times A = 26.00 \times .6439 = 16.74 \text{ kips}$$

where  $P_a$  is the allowable compressive force in the top chord.

The same method of calculation as above gave a value of  $w = .800 \text{ k/ft.}$ , which agreed closely to that given on manufacturers shop drawings, which was .794 kips/ft. The value of .794 will be used to establish load factors.

## APPENDIX B

## X-Type Joint - 1.660 Tube

For tube  $I_x = 0.1497 \text{ in.}^4$   $t = 0.100 \text{ in.}$  Circumference = 4.9009 in.

Consider totally flattened configuration

$$I_x = 2 \times \frac{.100 (1/2 \times 4.9009)^3}{12} = 0.2452$$

$$\text{Increase in moment of inertia} = \frac{.2452 - .1497}{.1497} \times 100 = 63.8\%$$

## Y-Type Joint - 1 1/4" Tube

For tube  $I_x = 0.0521 \text{ in.}^4$   $t = 0.083 \text{ in.}$  Circumference = 3.666 in.

Consider totally flattened configuration

$$I_x = \frac{(2 \times .083)^3 \times (1/2 \times 3.666)}{12} = 0.007 \text{ in.}^4$$

Final moment of inertia is 1.3% of initial.